# LUND UNIVERSITY

**Multi-dimensional imaging**

A tool to unravel material properties at the nanoscale

Louis, Boris

2022

[Link to publication](#)

*Total number of authors:*
1

# Multi-dimensional imaging

## A tool to unravel material properties at the nanoscale

KU LEUVEN

# Multi-dimensional imaging

## A tool to unravel material properties at the nanoscale

Boris Louis





JOINT DOCTORAL DISSERTATION

Joint doctoral dissertation for the degree of Doctor of Philosophy (PhD) in Chemistry with specialization in Chemical Physics at the faculty of science at Lund University and the degree of Doctor of Science (PhD) in Chemistry at the faculty of science at KU Leuven, to be publicly defended on the 16th of December 2022 at 9.15 in lecture Hall A, Department of Chemistry, Naturvetarvägen,

14 222 41 Lund

*Faculty opponent*
Prof. Dr. Jürgen Köhler & Prof. Dr. Theo Lasser

| Organization<br>LUND UNIVERSITY | Document name<br>**Doctoral dissertation** |
|---|---|
| Division of Chemical Physics<br>Department of Chemistry<br>P.O. Box 124<br>SE-221 00 Lund, Sweden | Date of issue<br>**2022-11-20** |
| Author(s)<br>Boris Louis | Sponsoring organization |

**Title and subtitle**
**Multi-dimensional imaging: a tool to unravel material properties at the nanoscale**

**Abstract**

Optical microscopy has revolutionized the way we understand our world and has become a crucial tool in a range of disciplines such as biology, physics, chemistry, and material sciences. The development of new microscopy techniques has been capital to its success and wide applicability. A prominent example is the recent development of methods that allow imaging in three dimensions. This has been a breakthrough in biology as scientists realized how important the 3D context is for cells and bacteria. However, in material sciences, the 3D context is not always as important, and thus, it is often more informative to use different parameters such as lifetime $(x,y,\tau)$ or excitation wavelength $(x,y,\lambda)$ as additional "dimensions" to the measurement instead of the classical spatial dimensions. In this thesis, we develop multi-dimensional imaging methods and demonstrate their application in different areas of materials sciences. First, we use multiplane microscopy to do single particle tracking in 3D $(x,y,z,t)$ to provide insight into optical trapping and the assembling of nanoparticles. We show that the inhomogeneous field of the optical trapping laser when tightly focused has a huge influence on the trajectories of the nanoparticles. For instance, it induces the formation of a metastable trapping position and the appearance of helicoidal trajectories. In addition, we show evidence of optical binding outside the irradiated area as the mechanism for the gold nanoparticle assembling under optical trapping. The second method is a correlation-based imaging technique $(x,y,r)$ which was developed to analyse the blinking phenomenon in hybrid halide perovskite film. We show that we can map out the different regions of a film that blink differently. Moreover, by comparing with SEM images, we discovered that these regions correspond to individual grains in the film. This method paves the way to understand non-radiative decay in metal halide Perovskite semiconductors and provides a new type of imaging contrast. Finally, an excitation-emission microscope $(x,y,\lambda exc,\lambda em)$ setup was used to study the structure-property relationships in the conjugated polymer TQ1 by measuring the 2D fluorescence spectra (excitation, emission) of individual molecules. We find that the excitation spectrum of a single chain is broad with a width similar to the corresponding polymer film while the emission spectrum is narrow. This confirms the idea that all the spectroscopic units of the chain absorb while only 1 or a few units contribute to the emission due to efficient intrachain energy transfer. This thesis demonstrates the potential and versatility of multi-dimensional imaging to investigate materials at the nanoscale.

**Key words**
Fluorescence Microscopy, 3D imaging, Multi-dimensional imaging, Single molecule spectroscopy, Correlation imaging, Single particle tracking, Optical trapping, Conjugated polymers, Nanoparticles, Metal Halide Perovskite

Classification system and/or index terms (if any)

| Supplementary bibliographical information | Language<br>English |
|---|---|
| **ISSN** and key title | **ISBN** 978-91-7422-924-0 |

| Recipient's notes | **Number of pages** | Price |
|---|---|---|
| | Security classification | |

I, the undersigned, being the copyright owner of the abstract of the above-mentioned dissertation, hereby grant to all reference sources permission to publish and disseminate the abstract of the above-mentioned dissertation.

Signature

Date 2022-07-11

# Multi-dimensional imaging

## A tool to unravel material properties at the nanoscale

Boris Louis

*To Sacha and Robert, in loving memory*

# Table of Contents

# Abstract

Optical microscopy has revolutionized the way we understand our world and has become a crucial tool in a range of disciplines such as biology, physics, chemistry, and material sciences. The development of new microscopy techniques has been capital to its success and wide applicability. A prominent example is the recent development of methods that allow imaging in three dimensions. This has been a breakthrough in biology as scientists realized how important the 3D context is for cells and bacteria. However, in material sciences, the 3D context is not always as important, and thus, it is often more informative to use different parameters such as lifetime $(x,y,\tau)$ or excitation wavelength $(x,y,\lambda)$ as additional "dimensions" to the measurement instead of the classical spatial dimensions. In this thesis, we develop multi-dimensional imaging methods and demonstrate their application in different areas of materials sciences. First, we use multiplane microscopy to do single particle tracking in 3D $(x,y,z,t)$ to provide insight into optical trapping and the assembling of nanoparticles. We show that the inhomogeneous field of the optical trapping laser when tightly focused has a huge influence on the trajectories of the nanoparticles. For instance, it induces the formation of a metastable trapping position and the appearance of helicoidal trajectories. In addition, we show evidence of optical binding outside the irradiated area as the mechanism for the gold nanoparticle assembling under optical trapping. The second method is a correlation-based imaging technique $(x,y,r)$ which was developed to analyse the blinking phenomenon in hybrid halide perovskite film. We show that we can map out the different regions of a film that blink differently. Moreover, by comparing with SEM images, we discovered that these regions correspond to individual grains in the film. This method paves the way to understand non-radiative decay in metal halide Perovskite semiconductors and provides a new type of imaging contrast. Finally, an excitation-emission microscope $(x,y,\lambda_{exc},\lambda_{em})$ setup was used to study the structure-property relationships in the conjugated polymer TQ1 by measuring the 2D fluorescence spectra (excitation, emission) of individual molecules. We find that the excitation spectrum of a single chain is broad with a width similar to the corresponding polymer film while the emission spectrum is narrow. This confirms the idea that all the spectroscopic units of the chain absorb while only 1 or a few units contribute to the emission due to efficient intrachain energy transfer. This thesis demonstrates the potential and versatility of multi-dimensional imaging to investigate materials at the nanoscale.

# Popular Summary

Since the history of mankind, seeing, observing, and recognizing have been key to our survival and development as a specie. Indeed, seeing the landscape around us has helped us travel around and tame our environment. Observing others' behaviour is one of the first ways humans had to transfer their knowledge. Recognizing predators and/or food that is safe to eat has helped us survive. Hence, it is not surprising that researchers estimate that 80% of our perception is achieved with our eyes.

However, our vision is far from perfect, we cannot see extremely far nor see extremely small objects. In addition, the spectrum of light that we can see is largely limited. It is therefore impossible to fully understand our world relying solely on our vision. This is why a great effort from scientists and engineers was and is still spent on developing technologies to improve upon our vision. Prominent examples of these technologies include the telescope which allows us to see very far away and the microscope which enable us to see very small objects.

The development of new technologies and new methodologies has been capital for the applicability of microscopes and telescopes. One such development enabled these methods to image in multiple dimensions. The most common of these is 3D imaging (x,y,z) which allows viewing an object in all its three spatial dimensions. However, in an experiment, the dimensions can be chosen by the experimenter. For example, one could use the colour of the light or wavelength (x,y,λ) as the third dimension instead of a spatial dimension. This is how telescopes can obtain images of the stars and study their composition at the same time because the colour (spectrum) of the light emitted by the stars is dependent on their composition.

In microscopy, 3D imaging (x,y,z) has had a large impact on biology as scientists realized the importance of the 3D spatial environment for cells and bacteria. However, its application to material sciences had much less impact because the 3D context is usually less important than other properties such as the colour of the light they emit. This is why, in materials sciences, it is often more informative to use other parameters as a third dimension to the measurement. Similar to stars, photovoltaic materials give a lot of information on their properties from the colour of the light they emit.

In this thesis, we demonstrate the development and application of multi-dimensional microscopy techniques in relevant areas of material sciences. First, using 3D

imaging (x,y,z) we studied how small particles assemble with each other when irradiated by a strongly focused laser beam. These assemblies of particles present many different and unexpected behaviours. We show that the inhomogeneity of the laser intensity profile makes the particle travel through it following a helicoidal trajectory. We also show that these small particles can assemble into something resembling a newton cradle system at the nanoscale due to optical binding. Finally, we present another type of small particle assembly which seldomly eject particles at very high speed, like a pistol when rearranging.

Second, we developed a method that calculates the similarity (correlation) between time-dependent signals and then groups these signals accordingly. By looking at the blinking signal of fluorescence in thin films of semiconductors, we were able to map the areas of the film that blink differently. We found that this technique can obtain an image of the microscopic grains.

The last method allows the imaging of single molecules of a fluorescent polymer and their colour (x,y,$\lambda$). Using this technique, we obtain information on the individual sub-unit which are responsible for its fluorescence. We show that all the individual sub-unit contribute to the absorption of light but only one or a few units are responsible for the emission. This is in line with the current understanding of conjugated polymers.

This thesis demonstrates how important the development of new methodologies in multi-dimensional microscopy is for understanding the materials that surround us.

# Acknowledgements

As soon as I started studying Chemistry, I knew I wanted more, and I directly thought of pursuing a PhD. However, I never expected to be in the situation I am, doing a PhD in between two universities. Doing a PhD is of course very challenging, having two universities 1000km apart and two supervisors only make it even more challenging. However, surrounded by the right people, it was a pleasure to take on this challenge. Here, I would like to spend a bit of time thanking the people that made this possible.

Being part of two different labs means that there is twice the amount of people that I need to thank, and I will do my best to thank everyone that helped, from close or from far, scientifically, or socially.

First, I want to thank my co-supervisor, Ivan Scheblykin because, without you, none of this would have been possible. I met you during my Erasmus in Lund where I took your class, this is where I discovered fluorescence microscopy and decided to perform a research stay in your lab. A bit later, you told us to go see the Nobel Prize lecture of W.E. Moerner and Stephan Hell which sparked my interest in single-molecule techniques. After the research stay, you mentioned Johan Hofkens group as a lab where it could be interesting for me to do my master's thesis. And that's pretty much how I arrived here doing a joint PhD between you and Johan's lab. I also want to thank you for the trust you put in me, letting me work on many different topics at the same time with a lot of independence. Despite, the independence, you were always available for discussion and/or help whenever I needed it. I also want to thank you for being also present outside of science, the numerous SMS party, with Ivan "Scheblinking" singing songs in Russian with the guitar, were always really nice and made it feel that the group was so much more than just work. Going for a run together, me initially trying to outrun you and quickly realised it would not be that easy. There is probably so much more like the trip to China, the conference in Russia, in Bayreuth and the many discussions about science or any other topics, once again I thank you for all of it.

Secondly, I want to thank my other co-supervisor, Johan Hofkens. Thank you for proposing to do a joint PhD with Ivan Scheblykin when I was torn between the two labs. It has been an amazing experience and a great opportunity to develop myself as a researcher and a person. I also want to thank you for the trust put in me, a "foreign" student from the far land of Wallonia, allowing me to work on any topic

I wanted to, to develop my skills in optics building setups or programming. I also thank you for providing collaboration opportunities, the one with Prof. Masuhara being the most fruitful I have been part of so far, I finally got to go to Japan in that framework which was a truly amazing experience. Finally, even though you were quite busy you still found time to grab a beer with us once in a while on Friday afternoon which led to very interesting scientific and non-scientific discussions. Thank you very much for everything!

Next, I would like to thank Susana Rocha. Even though officially, you were not my supervisor, you definitely acted like one and took care of most of the supervision while in KU Leuven. For that, I thank you very much and I am so glad that you are now officially my… assessor… (oups). Sorry, I couldn't leave you off the hook with 100% praise. I also want to thank you for the amazing lab environment that you set around us and the organization of group meetings for all PhD students in microscopy so we could get to know each other and each other's project. I also thank you for fostering collaboration and seeing connections between all these different projects. But also, for all the non-scientific parts, the many "coffee break-like" discussion in the upstairs office, at lunch, during the beers on Friday, the BBQs at your place, the conference in Portugal, in Sweden and probably many other occasions. We got along directly with the endless poking, you are a really nice person and I am really glad that I met you. I grew a lot around you as a scientist and as a person, I thank you for all of it.

I would also like to thank Prof. Jürgen Köhler, Prof. Theo Lasser, Prof. Victoria Birkedal, Prof. Elke Debroye, Prof. Peter Samuelsson, Prof. Hiroshi Ujii and Prof. Karl Björesson for reading my PhD thesis and accepting to take part in the defence.

A special thanks go to all the PIs of Chemical Physics Tönu Pullerits, Donatas Zigmantas, Jens Ulrich, Arkady Yartsev. Thank you, a lot, for providing a very pleasant environment to work in and for the interesting discussion at lunch or over fika. Thanks also, for your critical view and feedback on the research presented during the seminar, it was always interesting to hear the discussions that arise from it.

Many thanks to Hiroshi Masuhara, it was a pleasure to collaborate with your lab, thank you for suggesting many interesting topics and experiments. I also want to thank you for the many discussions and feedback on science but also outside. I will always remember when you arrive at the table of the conference in Japan with 2 bottles of saké in your hand with the largest smile, I've seen you have. I wish to be like you when I'm your age. I hope I will get the chance to visit you in Taiwan.

Next, I would like to thank Rafael Camacho. You have guided me from the master's thesis through the first years of my PhD and for that I thank you. During that time you taught me a lot about microscopes, optics and programming, I would simply not be the scientist I am now without you. Of course, our relationship goes beyond science and I'm really happy that I can count you as a friend. A special mention to

Marianne, Lucas and Victor as well, thanks to the family for welcoming me to Göteborg and coming to visit me in Lund, it is always a pleasure to see you all.

I would also like to thank Aboma Merdasa. Thanks for helping me at the start of the PhD with learning the basics of the M1 setup and a bit of image and data analysis. But also, thanks for your presence outside of the lab, it was always nice to hang around with you, seeing you DJ-ing in Malmö, and discussing over a beer. I will always remember how you missed your plane to the US after we left your flat a 3-4 am after some Rhum and Whiskey. Finally, thank you very much for keeping my stuff at your place while I was moving between Belgium and Sweden, it was a much-needed help.

Next, I would like to thank Roger Bresoli-Obach. We started off a little bit on the wrong foot, I think it was quite a bit of pressure for me to have to explain things to you while you were a postdoc. But we ended up having a very nice and productive collaboration with you enjoying the measurement part and me, the image analysis. I am also glad we were getting along outside of work too and I hope to visit you in Barcelona when this PhD is finally over!

Next, I need to thank Sudipta Seth, even though we met quite late in my PhD, I feel like we have known each other for more than that. We got along directly, both scientifically and personally. I am glad to have met you, I think the project we worked on together is still probably the best one I had the opportunity to work on. Thanks a lot for the scientific collaboration and the friendship, I hope to come to visit you in India someday, until then keep up the good mood and *jayanti mangala kali bhadrakali kapalini* !

Next, I would like to thank Kris Janssen and Christian Steuwe, you both helped me a lot during my master's thesis, and taught me a lot of things related to optics and STED microscopy. You were always very patient and explained things very well and for that I thank you. I will always remember Christian coming to my office to get a correction on his French homework. Kris, even though you are impossible to reach now, I was glad to have met you, I just wish we could have a drink or some food once in a while.

I would also like to thank Prof. Kudo Tetsuhiro, Prof. Rafael Delgado, Prof. Marc Melendez, Prof. Juan José Sáenz, Prof. Hajime Ishihara, Chih-Hao and all the members of the COODY-Nano who have provided very useful feedback and research ideas. But also, on a personal level, the meetings in KU Leuven and Kobe were great and I'm really glad I got to meet you all. A special thanks to Prof. Hajime Ishihara for his invitation to Japan, I always dreamt of visiting and I don't think I could have done it early if it was not for your invitation so thank you.

Next, I would like to thank my colleagues from KU Leuven. First, I would like to say that it is always a strange feeling to have to leave for another university and leave everyone behind, after just getting started to know each other. Hence, I wish

I had had more time to get to know each of you better. To Johannes, in the beginning, I thought we were quite different, Flanders vs Wallonia, excel vs MATLAB, word vs latex, a lot of topics to fight for... But actually, we got along very well and I'm really happy we shared an office for many years. Thanks a lot for always being willing to help with experiments or paperwork. I was also glad to work with you and I'm sorry if some of the things did not pan out, like the reptation or the fibre analysis. The conference in Göteborg with the random night finishing a 5 am will remain in my memory for a long time! Wish you the best for your thesis and we'll see each other soon! Guillermo, my fellow joint PhD student, we have surmounted similar situations from the master thesis (having to rebuild an optical system in the middle of it) to the PhD (two supervisors and a LOT of travelling), not even mentioning the hell of paperwork that we were subjected to… I am really happy that I have met you, we understand each other and got along directly, and we are similar in a lot of ways. I really appreciated the time spent with you whether it was scientific discussions, random topics, or outright party time, it was all great. I just wish we had better timing with our joint schedules so we could have seen each other more. I will of course remember the "Trappe night" where we both ended up with a glass in our bag, I thank you again for welcoming me to Madrid, and I know we will keep in touch. To Indra, I am not even sure what to say… In the beginning, I thought we were complete opposites and yet somehow, we ended up getting along very well, always poking at each other when one of us said/did something stupid. Since we did not work much together, I mostly thank you for the good mood you always brought at Lunch, during after-work drinks and parties. I also thank you for the anecdotes you so constantly provide whether it is putting oil in the wrong reservoir in the car or parking on a bus stop, it is always fun to hear. Wait… the latter was with me, oups… I wish you luck in your academic career and I hope we keep in touch! To Quinten, thank you for the discussion on science and other topics we've had during lunch and the many Friday's beers. I'll always remember you coming to Liege just to do almost 300 km on a bike, pretty crazy stuff! Wish you the best for your thesis! To Aline, Marisa and Laurens, we started our PhD more or less at the same time, it was really nice to have you around during the PhD meeting, lunch, the beers on Friday, always there to brighten the mood. Special thanks to Aline for the successful collaboration. To Sergey, you have been my first and only master's student so far, so thank you a lot for enduring me. I know it hasn't always been easy. I also thank you for your scientific collaboration and because I learnt a lot from you.  I enjoyed the time spent together whether related to work or not and of course, I keep in my memory the trip to Japan. To Hongbo, I thank you for the work that we did together, I am really happy with what came out of it even though it seems to struggle to find a journal at the moment. I also thank you for the friendly discussion during lunch and after-works, it is really nice to have you around. To Charlotte and Maria, I haven't known you for a long time and unfortunately, I did not get to see you much as I was mostly working from home, but it was a lot of fun having you around and I keep some very good memories of our shared trip to Göteborg. In particular,

Charlotte getting drunk after 2 ciders and Maria drinking till 5 am on her first conference. To Michiel, I did not share the office with you for that long yet, but I enjoyed it! Thanks a lot for the discussions in the office and during the Friday's beers, it is always nice to have you around. Props for the prank on Susana it was amazing! To Elizabete, it was really nice to get to know you, we mostly saw each other during lunch and on the Friday drinks but I always enjoyed your company. I remember our shared interest in martial arts, maybe once, ill come to train with you! To Pierre and Sam, I did not get to know you very much since I was mostly away when you started and then worked from home on the thesis. Thanks a lot for the discussion at lunch or during after works and parties. A special mention to Sam and his party-modus that seems to be always on.

Next, I would like to thank my colleagues from Lund University. To Marina, I thank you for all the work you did in our collaborations, in particular, for pushing hard on the writing of the papers. It was really nice working with you, and I learnt a lot from you. I also thank you for the time spent outside of work, at the SMS parties etc.. you were always nice to have around.  To Alexander, we did not see each other much because we do not really have the same working schedule, plus I spent a lot of time in Belgium. However, it was really nice to have you around and I think in many ways we have the same mindset and/or interests. Of course, I thank you a lot for all the work you did in the lab, and the automatization of the system. Without that some of the work in this thesis would not have been possible. Thanks a lot for always being willing to lend a hand too! To Bruce and Juanzi, we started our PhDs at the same time, and it was a hell of a ride. I am really happy I got to know you both and I will always remember my visit to China. Thanks a lot for being our guide there, it was really a once-in-a-lifetime experience for me. To Aymen, we did not really work together directly, but I enjoyed a lot the time we spent in the same office. I keep a good memory of going out with you and Sudipta on Fridays, venting about our issues and discussing our futures. Wish you the best to you and your family! To Shraddha and Chen, I am really happy that I got to know you, It was really nice to have you around in the lab, the group meeting and the SMS parties. I just wish I had had more time so I would get to know you better.

To Carine, Eduard, Ann, Greet and Rik I would like to thank you a lot for the help and support you provide for the lab, I think the lab would simply not function without you. I also thank you for every time you have helped me personally and for always being willing to help. A special mention to Carine without whose support the lab would probably collapse. A special thanks to Eduard for providing help and supervision during the installation of the 1064nm laser and for helping with the hardware synchronization of the camera.

Finally, I would like to thank the people that have contributed to this thesis without being part of my work environment, my friends and my family.

To Alicja and Jason, I thank you very much for everything. I enjoyed our time when you came to visit Belgium, our time during my multiple visits to Göteborg, when you visited me in Lund and finally, our somewhat disastrous but super fun recent trip to Poland. Alicja, I am really glad we kept in touch after the Erasmus even though I know it was hard for you since I am not so good at keeping in touch… So thank you for keeping up with me and I am looking forward to our next adventures!

À Guillaume, on se connait depuis nos 7-8 ans, tu as toujours été là pour moi et je pense que je te dois, du moins en partie, la personne que je suis devenu. Un grand merci pour tout. Même si on se voit moins souvent, à cause de la distance qui nous sépare, chaque fois qu'on se voit, j'ai l'impression qu'on s'est vu la veille. Au plaisir de se voir en Suède, en Belgique, en France ou ailleurs à bientôt !

À Lucas, après nos 5 années de Chimie, on a tous les deux enchainés sur un doctorat. Merci d'avoir été présent, que ce soit pour aller boire un verre et "vent" sur la vie de doctorand ou pour des soirées fléchettes/kicker jusqu'à 3h du mat, ça fait toujours plaisir de décompresser, haha. Une mention spéciale pour le catsitting et on se voit bientôt autour d'une bière !

À Martin, même si on s'est un peu éloigné depuis quelques années, notamment à cause de nos travails et rythmes de vie différent, tu as toujours été là. Que ce soit pour aller boire un verre, rendre visite à Guillaume, aller voir des défenses de thèse bien loin de ton sujet de cœur, tu es toujours là et pour cela merci !

A Nicolas Ancion, même si au final tes contributions m'ont plutôt distrait de cette thèse, je te remercie d'avoir été là. Que ce soient les soirées entre potes, les voyages au ski, en Espagne, en Italie ou ailleurs, tu as toujours été là pour me distraire des galères de cette thèse qui semblait ne pas en finir. Bien sûr je n'oublie pas The Good Soap et Oodima qui bien que me distrayant de ma thèse m'ont aussi permis de m'épanouir à travers un projet bien différent de ce que je faisais au boulot. Merci pour tout, Gros bisous à vous 3 et à bientôt autour d'un verre, ou de savons.

À Simon, Quenti, Catherine, Michou, Nicolas, Bronky, Pierre, Marion, Ingrid, Louise, Julie, Croux, Manu, Camille, Jean, Thomas et bien d'autres, merci beaucoup pour le support ces dernières années à travers de verres, de voyages, de concerts, de festivals ou autres activités, je n'aurai pas pu venir à bout de ces années semblant interminables sans vous ! Gros bisous à tous et à nos prochaines aventures.

À Stéphane, même si on a perdu un peu contact depuis l'Erasmus, ça me fait toujours plaisir de te revoir que ce soit autour d'un verre, un resto avec les Chimistes ou autre. Merci beaucoup pour tous ces moments passés ensemble et d'avoir répondu présent pour ma défense.

J'aimerais maintenant remercier ma famille. À Christophe, Annick, Charlotte, Mathys, Sacha, merci pour le soutien durant ces longues années de doctorat et ce, malgré mes absences et mon emploi du temps chargé. Merci aussi de m'avoir procuré un toit pendant mes allers-retours entre la Suède et la Belgique. Et surtout

merci d'avoir fait de moi la personne que je suis aujourd'hui. Sans tout ça je n'aurai pas pu y arriver. À Véronique, Jean, Tatiana et Alexandre merci pour le soutien durant tout le doctorat et merci d'avoir contribué à faire de moi la personne que je suis aujourd'hui. Merci à Tatiana et Guillaume d'être venu me visiter en Suède !

À toi mon amour. Il est 23h50, un dimanche soir, je suis seul devant mon pc à écrire mes remerciements. Normal c'est pour ma thèse, tu me diras… Normal c'est pour l'entreprise… Normal c'est pour… Au final, il y a toujours quelque chose et au bout du compte, tu en auras subis des choses… Des multiples déménagements, en Suède puis en Belgique puis en Suède aux nombreuses heures que je passe à travailler pour les différentes activités dans lesquelles j'ai eu la folle idée de me lancer. Et pendant ce temps-là, tu es là, à mes côtés à essayer de joindre les deux bouts, à essayer de vivre de ton art tout en me soutenant. Merci, merci pour tout. Ta contribution à ce travail est impossible à décrire avec des mots tellement elle a été cruciale. Merci d'avoir été à mes côtés ces (presque) 10 dernières années.  Merci pour le soutien pendant tout le doctorat et particulièrement cette dernière année qui a été encore plus dur pour toi. Merci pour ta gentillesse, ta patience et ta résilience et ton amour. Je t'en serai toujours reconnaissant. Je t'aime plus que tout.

# List of publications

I. **Boris Louis**, Rafael Camacho, Roger Bresolí-Obach, Sergey Abakumov, Johannes Vandaele, Testsuhiro Kudo, Hiroshi Masuhara, Ivan G. Scheblykin, Johan Hofkens, and Susana Rocha: Fast-tracking of single emitters in large volumes with nanometer precision Optics Express Vol. 28, Issue 19, pp. 28656-28671 (2020)

II. **Boris Louis**,[+] Chih-Hao Huang,[+] Rafael Camacho, Ivan G. Scheblykin, Teruki Sugiyama, Tetsuhiro Kudo, Marc Meléndez, Rafael Delgado-Buscalioni, Hiroshi Masuhara[*], Johan Hofkens,[*] Roger Bresolí-Obach[*] 3D incorporation dynamics of dielectric particles to an optical trapping site, Manuscript to be submitted

III. Huang, Chih-Hao.[+], **Louis, Boris**[+], Bresolí-Obach, Roger, Testuhiro Kudo, Rafael Camacho, Ivan G. Scheblykin, Teruki Sugiyama, Johan Hofkens, Hiroshi Masuhara The primeval optical evolving matter by optical binding inside and outside the photon beam. *Nat Commun* **13**, 5325 (2022).

IV. Jia-Syun Lu, Tetsuhiro Kudo*, **Boris Louis**, Roger Bresolí-Obach*, Ivan G. Scheblykin, Johan Hofkens*, and Hiroshi Masuhara* Optical Force-Induced Dynamics of Assembling, Rearrangement, and Three-Dimensional Pistol-like Ejection of Microparticles at the Solution Surface. Phys. Chem. C 2020, 124, 49, 27107–27117

V. **Boris Louis**,[+] Sudipta Seth[+], Johan Hofkens, Yana Vayntzof, Ivan G. Scheblykin Mapping microscale domains and real-time dynamics of photoluminescence quenching traps in halide perovskite Thin Films Manuscript to be submitted.

VI. **Boris Louis**, Alexander Killiaridis, Johan Hofkens, Peter Persson, Ivan G. Scheblykin Excitation spectroscopy of single-conjugated polymer molecules. Manuscript in progress

[+]Authors contributed equally.

# My contribution to the publications

I.      I Participated in the building and calibration of the system with R.C., I designed the experiment with T.K., H.M. R.B, R.C., I.S., J.H. and S.R., I prepared the sample with J.V. and I performed the experiments with R.B. I wrote the software to analyse the data with R.C. and S.A. and performed all the data analysis. I wrote the paper with S.R. and J.H. with input from all co-authors.

II.      I designed the experiments with C.H., R.C., T.S., H.M, R.B. J.H., and I participated in a large part of the measurements with C.H. and R.B. I wrote the analysis software and performed a large part of the analysis with C.H. and R.B. I wrote the manuscript with R.B., C.H., H.M. and J.H. with input from all co-authors.

III.      I designed the experiments with C.H., R.B., T.K. I.S., J.H. and H.M. and I performed part of the measurements with C.H. I wrote the analysis software with R.C. and I performed the analysis with C.H. I wrote the paper with C.H. R.B. and H.M. and J.H. with input from all co-authors.

IV.      I participated in the design of the 3D experiment with R.B. and J.H. I supervised the experiments of J.S. with R.B. I wrote the analysis software and performed the 3D tracking analysis. I wrote the 3D part of the manuscript and helped revise the paper with all co-authors.

V.      I developed the correlation clustering algorithm. I designed the experiments with S.S. and I.S. and performed most of the measurements and data analysis with S.S. Wrote the manuscript with S.S. and I.S. with input from all co-authors.

VI.      I prepared the samples, designed the experiment with I.S. and performed the measurements. I wrote the software to analyse the data and performed the data analysis. I participated in the improvement and calibration of the excitation spectra unit that was made by A.K. with A.K. I wrote the manuscript with I.S. with input from all co-authors.

# Other publications

I. **Louis B**, Caubergh S, Larsson PO, Tian Y, Scheblykin IG. Light and oxygen induce chain scission of conjugated polymers in solution. Phys Chem Chem Phys. 2018;20(3):1829–37.

II. Merdasa A, Kiligaridis A, Rehermann C, Abdi-Jalebi M, Stöber J, **Louis B**, et al. Impact of Excess Lead Iodide on the Recombination Kinetics in Metal Halide Perovskites. ACS Energy Lett. 2019 Jun 14;4(6):1370–8..

III. Gerhard M, **Louis B**, Camacho R, Merdasa A, Li J, Kiligaridis A, et al. Microscopic insight into non-radiative decay in perovskite semiconductors from temperature-dependent luminescence blinking. Nat Commun. 2019 Dec;10(1)

IV. Vandaele J, **Louis B**, Liu K, Camacho R, Kouwer PHJ, Rocha S. Structural characterization of fibrous synthetic hydrogels using fluorescence microscopy. Soft Matter. 2020 May;16(17):4210–9.

V. Gerhard M, **Louis B**, Frantsuzov PA, Li J, Kiligaridis A, Hofkens J, et al. Heterogeneities and Emissive Defects in MAPbI3 Perovskite Revealed by Spectrally Resolved Luminescence Blinking. Adv Opt Mater. 2021 Sep;9(18)

VI. Grześ G, Wolski K, Uchacz T, Bała J, **Louis B**, Scheblykin IG, et al. Ladder-like Polymer Brushes Containing Conjugated Poly(Propylenedioxythiophene) Chains. Int J Mol Sci. 2022 May;23(11):5886–5886.

VII. Acke A, Van Belle S, **Louis B**, Vitale R, Rocha S, Voet T, et al. Expansion microscopy allows high resolution single cell analysis of epigenetic readers. Nucleic Acids Res. 2022 Sep 23;50(17):e100–e100.

VIII. Hongbo Yuan, Kaizheng Liu, Mar Cóndor, Jorge Barrasa-Fano, **Boris Louis**, Johannes Vandaele, Paula de Almeida, Quinten Coucke, Wen Chen, Egbert Oosterwijk, Hans Van Oosterwyck, Paul H. J. Kouwer and Susana Rocha Synthetic fibrous hydrogels as a platform to decipher cell-matrix mechanoreciprocity. *Manuscript submitted to PNAS*

IX. Tetsuhiro Kudo, **Boris Louis**, Hikaru Sotome, Jim Jui-Kai Chen, Syoji Ito, Hiroshi Miyasaka, Hiroshi Masuhara, Johan Hofkens, Roger Bresolí-Obach Gaining control on optical force by stimulated-emission resonance effect. *Manuscript in preparation.*

# Abbreviations

3LA – 3 particles linear assembly

CC – Concentric circular

CP – Conjugated Polymers

|CN| - Average Correlation to Neighbour

DG – Diffraction Grating

ET – Energy Transfer

EM – CCD Electron Multiplying Charge Coupled Device

HCP – Hexagonal Close Packing

MP(s) – MicroParticle(s)

MSD – Mean Squared Displacement

NA – Numerical Aperture

NP(s) – Nanoparticle(s)

PCoClust – Pseudo-Correlation Clustering

PL – PhotoLuminescence

PSF – Point Spread Function

PMMA – Poly(Methyl MethAcrylate)

PS - PolyStyrene

r – Pearson Correlation coefficient

sCMOS – Scientific Complementary Metal-Oxide Semiconductor

SEM – Scanning Electron Microscopy

SMEES – Single Molecule Excitation Emission Spectroscopy

SMS – Single Molecule Spectroscopy

SPT – Single Particle Tracking

TQ1 – Poly[Thiophene-bis(3octyloxyphenyl)-quinoxaline]

# Chapter 1
# Introduction

Since the history of mankind, seeing, observing, and recognizing have been key to our survival and development as a specie. Seeing the landscape around us has helped us tame our environment. Observing others' behaviour is one of the first ways humans had to transfer their knowledge. Recognizing predators and/or food that is safe to eat has helped us survive. Hence it is not surprising that the majority of our perception is achieved with our eyes, making vision our most important sense.[1,2]

Yet, our vision is far from perfect, we cannot see extremely far nor see very small objects. In addition, the spectrum of light that we perceive is largely limited. It is therefore impossible to fully understand our world relying solely on our vision. Moreover, our sight is easy to deceive as context, background and motion can heavily affect the way we perceive the colour, size and shape of an object.[3–6] An example of misinterpretation of our sight due to a difference in the background is illustrated by a simple Munkres illusion in Figure 1.1. Two vertical grey rectangles are displayed with black (left) or white(right) stripes crossing them. While the left
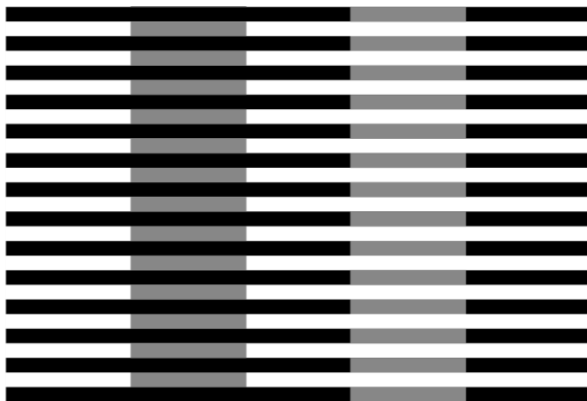


**Figure 1.1 Simple Munker's optical illusion: The two grey bands have exactly the same colour. However, our eyes perceive them differently because of the different background and neighbourhood. Indeed, on the left band, the grey band is overlaid with black stripes making it appear darker while on the right, it is overlaid with white stripes making it appear lighter.**

grey rectangle appears darker, they are in fact the same colour, the stripes are tricking our eyes into seeing them in different shades due to their different environment. Another example of deception of our eyes is eyewitnesses who have long been considered one of the most reliable kinds of testimony while they are often responsible for false accusations.[7] Finally, with the rise of photoshop, deep learning and deep fakes, being able to trust what we see, might not be possible anymore.

Considering the importance of vision as well as its flaws, it is not surprising that a significant portion of engineering and scientific work has been spent developing devices and methods to improve and extend our vision. The most prominent examples are the telescope which allows observing objects that are very far away and the microscope which enables the observation of small objects. This thesis focuses on microscopes.

One of the earliest known examples of a microscope was attributed to Hans and Zacharias Janssen, at the turn of the 16th century. However, it was only designed and used for scientific purposes in the 17th century by Antony Van Leeuwenhoek. The main components were then light and two lenses: the objective, and the eyepiece. Figure 1.2 below presents the basic principle of a standard light microscope. The objective generates an intermediate image that is enlarged (image 1). The eyepiece magnifies the image generated by the objective and projects it so that it can be observed by the eye. The resulting image (image 2) is a perfect copy of the object but magnified and inverted. The extent of the magnification depends on the characteristics of the lenses.
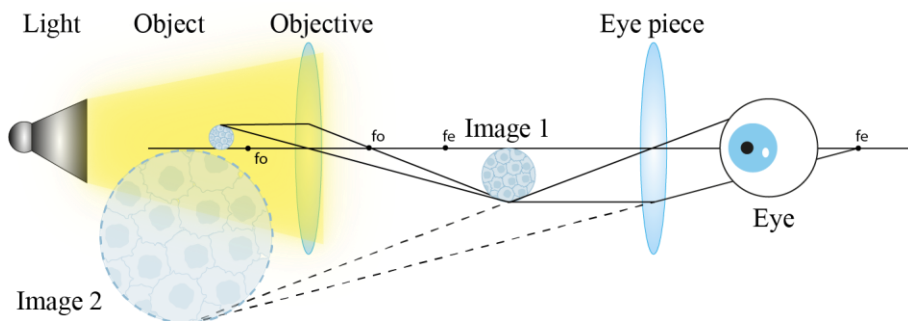


**Figure 1.2: Schematic of a standard light microscope: The light illuminates the sample; the transmitted light is collected by the objective which generate a magnified image of the object. The eye piece generates an enlarged image which can be observed by the eye.**

Ever since it was invented, the microscope has enabled discoveries in most fields of science but, more particularly, in biology and material sciences. Despite this immense step, the first microscopes were limited having relatively low contrast and

a poor resolution. It took years of optics and methodology development to arrive at the current state of the art where single molecules can be readily observed on a microscope. Indeed, about thirty years ago, W.E. Moerner and M. Orrit reported the detection of single molecules, the latter using fluorescence.[8–10] Fluorescence is the spontaneous emission of light after the absorption of photons (see Chapter 2 for more details). The ability to observe individual molecules and/or a small part of a sample allows us to see beyond the ensemble average. This turned out to be crucial because individual molecules were found to behave quite differently from one another, even when belonging to the same material.

This discovery had an extremely large impact and fluorescence microscopes are now a very common tool in the labs. W.E. Moerner was awarded 1/3 of the Nobel prize in Chemistry in 2014 for his contribution to the single-molecule microscopy field. The rest of the Nobel prize was shared for new imaging methodologies allowing to obtain resolutions below the theoretical physical limit (diffraction limit, see Chapter 2). The revolution of fluorescence microscopy has led to where we are today, where labs are readily able to resolve a few nm structures on a microscope.

Despite the developments, there is still a shared issue with vision, microscopy, and telescopes: they all present a two-dimensional view of an inherently three-dimensional world. Figure 1.3 shows a simple example of the limitation and misinterpretation that imaging in two-dimension of a three-dimensional object can yield. With a single image plane, one may conclude that the object is a disk, while in fact, it is a cone. In more complex systems, such misinterpretation can lead to the wrong conclusions.
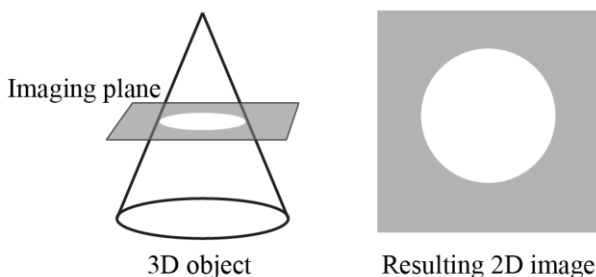


**Figure 1.3: 2D vs 3D: Illustration of how imaging a two-dimensional cross-section of a 3D object can lead to wrong interpretation of the shape of the object. For example, from that two-dimensional image we cannot distinguish between a round based pyramid, a cylinder, and a sphere.**

Consequently, in parallel to the development of single-molecule microscopy and super-resolution, microscopy evolved toward multi-dimensionality and many methods now allow imaging in three dimensions.

While Biology highly benefits from three-dimensional imaging because the 3D context is often crucial to understanding the structure and function of living organisms. These benefits are less obvious in materials sciences where the 3D context is not always relevant. In these systems, it is often more informative to use different parameters such as lifetime $(x,y,\tau)$ or excitation wavelength $(x,y,\lambda)$ as additional "dimensions" to the measurement instead of the classical spatial dimensions. Hence, in this thesis, we refer to multi-dimensional imaging as any method that performs imaging in at least two dimensions while measuring other parameters such as time, excitation wavelength, emission spectra, time correlation… As we will see in this thesis, by diversifying the type of additional dimensions used, we can craft methods that are suited to explore different areas of materials sciences.

The research presented in this thesis concentrate on the development and applications of multi-dimensional fluorescence microscopy methods to relevant areas of materials sciences. Papers I & II present the development of a multiplane microscope and a fast-tracking algorithm which allows the investigation of nanoparticles dynamics as they come to an optical trap in three dimensions $(x,y,z)$. We demonstrate the formation of a metastable trapping position and the appearance of helicoidal trajectories which could not have been uncovered with fast 3D imaging. Paper III investigate the early formation of an optically formed assembly of gold nanoparticles using optical trapping. We demonstrate for the first time optical binding outside of the focus as the underlying mechanism for the formation and growth of these assemblies. Paper IV uses multiplane microscopy to study the 3D pistol-like ejection from a polystyrene nanoparticle assembly. Paper V presents the development and applications of a temporal correlation imaging method $(x,y,r)$ that separates the areas of a metal halide perovskite semiconductor film that blink differently. By comparing with electron microscopy, we show that the areas found by the algorithm perfectly match individual grains in the film. Paper VI uses single molecule excitation emission imaging to study spectroscopic units of TQ1 conjugated polymers. The results obtained are in agreement with the idea that all the spectroscopic units contribute to the absorption but only a small subset of them is responsible for the emission.

# References

1.  Ripley DL, Politzer T. Vision Disturbance after TBI. NRE. 2010 Nov 19;27(3):215–6.

2.  Hutmacher F. Why Is There So Much More Research on Vision Than on Any Other Sensory Modality? Front Psychol. 2019 Oct 4;10:2246.

3.  Monnier P, Shevell SK. Large shifts in color appearance from patterned chromatic backgrounds. Nat Neurosci. 2003 Aug;6(8):801–2.

4.  Gandhi T, Kalia A, Ganesh S, Sinha P. Immediate susceptibility to visual illusions after sight onset. Current Biology. 2015 May;25(9):R358–9.

5.  Hong SW, Kang MS. Motion Alters Color Appearance. Sci Rep. 2016 Dec;6(1):36272.

6.  Sinha P, Crucilla S, Gandhi T, Rose D, Singh A, Ganesh S, et al. Mechanisms underlying simultaneous brightness contrast: Early and innate. Vision Research. 2020 Aug;173:41–9.

7.  Albright TD. Why eyewitnesses fail. Proc Natl Acad Sci USA. 2017 Jul 25;114(30):7758–64.

8.  Moerner WE, Kador L. Optical detection and spectroscopy of single molecules in a solid. Phys Rev Lett. 1989 May 22;62(21):2535–8.

9.  Ambrose WP, Moerner WE. Fluorescence spectroscopy and spectral diffusion of single impurity molecules in a crystal. Nature. 1991 Jan;349(6306):225–7.

10. Orrit M, Bernard J. Single pentacene molecules detected by fluorescence excitation in a $p$ -terphenyl crystal. Phys Rev Lett. 1990 Nov 19;65(21):2716–9.

# Chapter 2:
# Theoretical background

## 2.1 Fluorescence

The basics of absorption and emission of light are often described using Jablonski diagrams (see Figure 2.1), where the energy levels of the molecules are depicted. There are three types of energy levels, electronic, vibrational, and rotational. Vibrational levels are found between two electronic levels (S0, S1) as shown in Figure 2.1 and rotational levels are found between two vibrational levels (not shown). Every molecule can absorb light provided that the energy of the light has adequate energy, that is, it corresponds to the difference in energy between two of its energy levels. Fluorescence (F) is an electronic transition, hence, it occurs between two electronic levels, from S1 to S0 and induces the emission of a photon (light). [1]



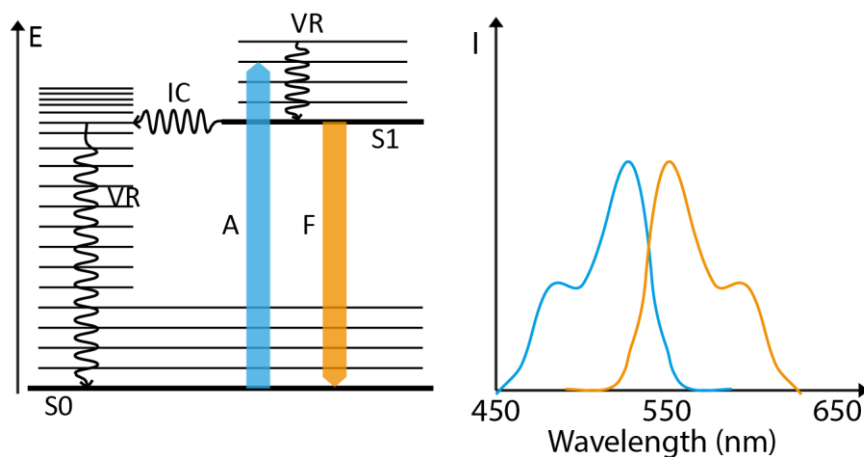**Figure 2.1: Simplified Jablonski diagram and absorption emission spectra. The Jablonski diagram presents the different events that can occur during light matter interaction. A is absorption, F is fluorescence, VR is vibrational relaxation, IC is internal conversion, E is energy, S0 and S1 are the electronic ground state and excited state respectively. B) Schematic of a typical absorption and fluorescence spectra in the visible**

After absorption of a photon, an electron of the molecule is promoted from S0 (ground state) to S1 (excited state), with a certain vibrational state. Vibrational states relax significantly faster than electronic states, hence, vibrational relaxation (VR) first occurs to the vibrational ground state of S1 then S1 relaxes to S0 within some nanoseconds. The excess energy from the electron is dissipated via the emission of a photon, which is the fluorescence emission. Since a certain amount of energy is lost during the vibrational relaxation, the energy of the photon emitted is lower than the initially absorbed photon.

Figure 2.1b shows a schematic of a typical absorption and emission spectrum for a fluorescent molecule. The molecules that are responsible for absorption/emission in the visible are often referred to as chromophores. Since different chromophores absorb and emit at different wavelengths, by selecting the excitation wavelength, selective excitation of a specific chromophore is possible.[1]

## 2.2 Fluorescence microscopy

Fluorescence microscopy is highly similar to the standard light microscope that is briefly described in Chapter 1 in that it also uses a light source and two lenses. The main difference is that it employs a laser to excite the molecules and that the signal observed is the fluorescence light instead of the transmitted light. A very simple fluorescence microscope is shown in Figure 2.2.[2]

Briefly, the excitation laser source is collimated by the objective resulting in a wide excitation spot onto the sample. This mode of excitation is called wide-field illumination. The illumination pattern on the sample often displays a Gaussian-like shape. The light is absorbed by the sample which in turn emits fluorescence. The fluorescence signal is collected by the objective and directed toward the tube lens that will generate the final image onto the camera. The camera records the images which are then saved on the computer. On the way toward the detector, a dichroic mirror reflects the laser without reflecting the fluorescence signal and additional filters can be placed to remove unwanted signals.

The ability to selectively excite some chromophores but not others give fluorescence microscopy a high selectivity. Using filters that block specific parts of the light spectrum, selective detection is also possible. Moreover, fluorescence is a zero-background signal giving fluorescence images a very high contrast.

In addition, chemistry has now reached a point where we can craft chromophores and tune their absorption and emission properties. These molecules can then be selectively attached to fluorescently labelling biological structure or materials.[3–5] Fluorescent labels allows us to image more or less anything regardless of whether

the object or structure of interest is fluorescent or not, making fluorescence imaging a very versatile imaging tool.
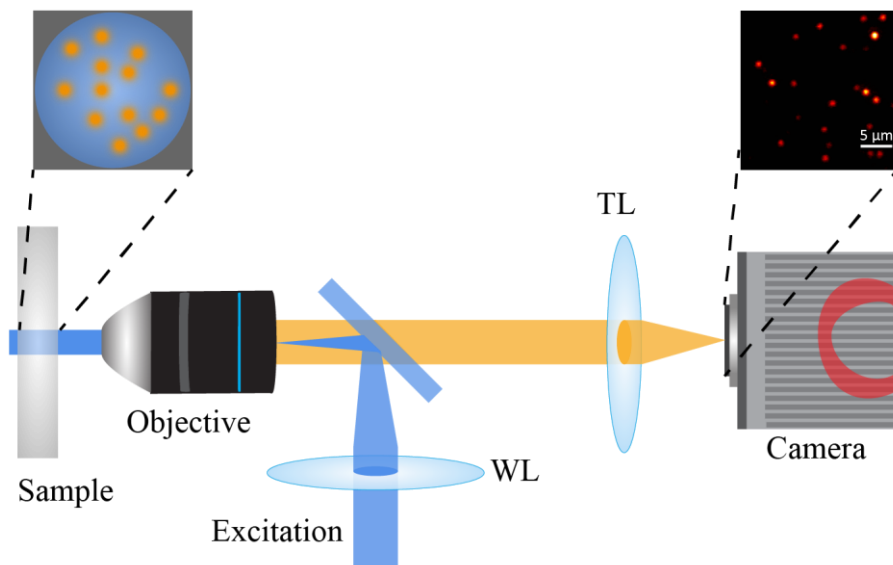


**Figure 2.2: Widefield Fluorescence Microscope: The excitation laser is focused by the widefield lens (WL) on the back aperture of the objective leading to wide-field illumination. The fluorescence emitted by the sample is collected by the objective and collimated toward the tube lens. On the way, the laser reflections/scattering and unwanted signal are filtered out using a dichroic mirror and additional filters. The image is reconstructed on a camera via the tube lens.**

While strong emission in the visible is relatively uncommon in unlabelled biological samples, in material sciences, many materials of interest have their absorption and emission spectrum in the visible. Indeed, a lot of these materials belong to the category of semiconductors and are studied for their photo-physical properties for potential applications in optoelectronics, photovoltaics or LEDs. In this case, labelling is no longer an option as studying the light emitted by the sample gives us more information about its properties and thus its potential for real-world applications.

## Resolution in Microscopy

The resolution of a microscope determines the smallest feature that it can resolve. To study micrometre and nanometre structures, it is crucial to understand what factors influence the resolution. It depends on the wavelength of the light and the parameters of the objective used. When light passes through an aperture (the

objective lens in this case) diffraction occurs resulting in a diffraction pattern. Since the aperture is circular, the diffraction pattern is an airy disk which is characterized by a bright region at the centre with concentric rings around. As a consequence, even a point source, when imaged through a lens, will yield a significantly broader, airy disk pattern. If two of these patterns are too close to each other, they will overlap and it will no longer be possible to distinguish them individually, limiting the quality of the imaging. Figure 2.3 shows how the diffraction limit impacts the imaging where the airy pattern is simplified into a 2D Gaussian. Due to the significant broadening of the signal, (a ➜ b), the hexagonal structure depicted in c) is completely lost in d).
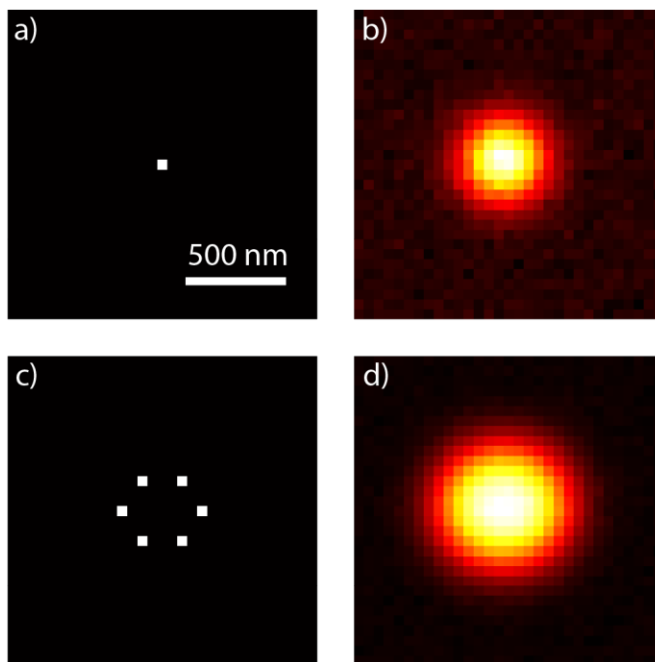


**Figure 2.3: Practical implication of the diffraction limit: a) Intensity of a single molecule emitter illuminating a single pixel on the detector if there was no diffraction limit b) Simulated signal recorded by the camera due to the diffraction limit (here simplified as a Gaussian with FWHM = 300nm . c-d) demonstrate how the diffraction limit impact the resolution of simple structure, the hexagon is completely lost in the broadened signals.**

The first formal definition of the resolution was given by Abbé in 1873 (eq.2.1), followed by Rayleigh, Sparrow, and Houston.[6–9]

$$d = \frac{\lambda}{2\,NA} \qquad \text{(Eq. 2.1)}$$

Where d is the resolution, λ is the wavelength of the light, and NA is the numerical aperture of the objective which characterizes the proportion of light that the objective can capture. The resolution limit is typically between 200-500 nm in standard imaging conditions (NA = 1, 400 < λ < 800).

## Fluorescence Blinking

Fluorescence blinking or flickering is a phenomenon first observed in semiconductor nanocrystals and later in single molecules. It is characterized by a time-dependent fluorescence intensity, usually manifested by two levels, a bright state "ON" and a dark state "OFF" (see Figure 2.4).[10–14]
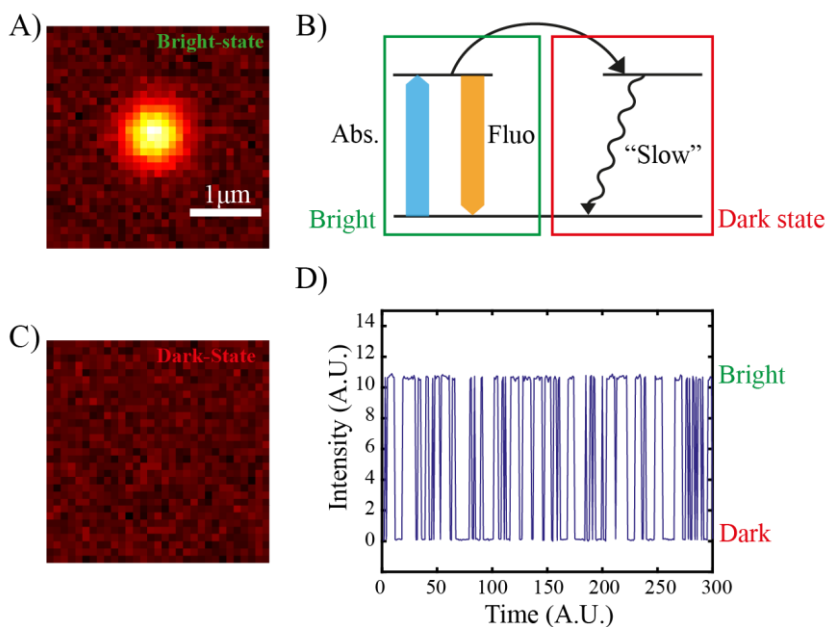


**Figure 2.4: Fluorescence Blinking: Illustration of a fluorescent molecule in emissive states ("ON") and in non-emissive states or dark state ("OFF"). The fluctuations of intensity over shows two clear levels, one of which is around 0 after background subtraction.**

The blinking phenomenon is attributed to the system going into a dark state from which it cannot emit (Figure 2.4 b) and in which it remains for a significant amount of time, typically a few tenths of milliseconds. The nature behind this dark state is beyond the scope of the thesis and depends largely on the nature of the system studied.

The ability of single molecules to turn ON and OFF turned out to be a crucial phenomenon to circumvent the diffraction limit in microscopy (see the dedicated section).

## Tracking of single particles

Besides obtaining images of a labelled structure, an important use of fluorescence microscopy is the possibility to track particles and molecules. The idea is to follow a molecule or a particle in a movie over time by recording its position for each frame. Then, by studying its motion, one can obtain information about the diffusion, the viscosity but also on the type of motion (freely diffusing, confined or active transport) which can give information on the function of the molecules and/or the properties of the system it is embedded in .[15–22]

To track objects through time, the object first needs to be detected on each frame, a good detection algorithm for single-molecule is found here.[23] Once all the desired objects are identified, their position needs to be determined accurately. This is typically done by fitting a mathematical function to the fluorescence signal. The Gaussian function (Eq. 2.2) is the most commonly used due to its high accuracy and simplicity.[24,25] An example of such fit is given in Figure 2.5A where the data is presented in colour and the corresponding fit in white.

$$f(x,y) = A \exp\left(-\left(\frac{(x-x_0)}{2\sigma^2} + \frac{(y-y_0)}{2\sigma^2}\right)\right) \qquad \text{(Eq. 2.2)}$$

The great advantage of using a mathematical function is that one can obtain the centre position of the object with a sub-pixel precision that would normally not be allowed by the diffraction limit. This will be discussed in more detail in the next section.

Once a set of positions is obtained at each time frame, the traces need to be reconstructed by connecting the positions that belong to the same particle. This is likely the trickiest part of particle tracking as misassignment can result in erroneous data. Many approaches exist and their performances depend largely on the system studied (interacting, non-interacting, large motions,). The simplest approach minimizes the square displacement over all particles between each frame.[17,24,26–28]

Once we obtained the traces for all particles detected, we can finally extract the interesting quantity such as the diffusion coefficient and viscosity. To do so, the mean squared displacement (MSD) is usually computed.[17,29–31] The equation for MSD and the relationship to diffusion and viscosity are given below:

$$MSD(\tau) = \langle(x(t) - x(t-\tau))^2\rangle + \langle(y(t) - y(t-\tau))^2\rangle \\ + \langle(z(t) - z(t-\tau))^2\rangle \qquad \text{(Eq. 2.3)}$$

$$MSD(\tau) = 2nD_n\tau \qquad \text{(Eq. 2.4)}$$

$$D = \frac{k_B T}{6\pi\eta r_0} \qquad \text{(Eq. 2. 5)}$$

Where x(t), y(t), z(t) are the coordinates of the particle at time t. $\tau$ is the delay between the time points compared. n is the dimensionality, n=3 in the case where x,y and z are considered. D is the diffusion coefficient. $k_b$ is the Boltzmann constant. T is the temperature, $\eta$ is the viscosity and $r_0$ is the hydrodynamic radius of the particle.

The main categories of motion are schematically represented in Fig.2.5B. The type of motion is determined by the dependence of the MSD on the time interval. A linear dependence is linked to random Brownian diffusion, a sub-linear regime is considered a confined motion, and a super-linear regime is typically due to active transport.
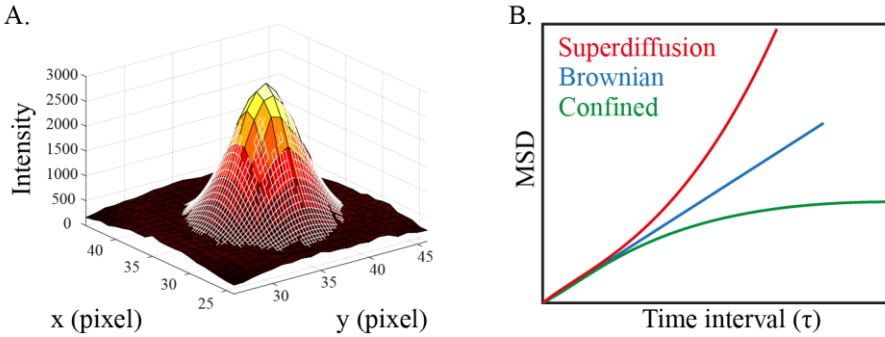


**Figure 2.5: Particle Tracking. A) Example of two-dimensional intensity profile of a single particle fitted by a 2D Gaussian (fit in white). B) The Brownian diffusion is given by a linear relationship between the MSD and the time interval. When the particle has some directionality (red curve), either by a flow or an active transport mechanism, it enters a super diffusion regime yielding a power law. When the motion is confined (green curve) the MSD will tend to an asymptotic value.**

## Circumventing the diffraction limit

Recently, scientists have been able to circumvent the infamous diffraction limit. Some of the main actors in these developments were even awarded the Nobel Prize in Chemistry in 2014. These methods are now often referred to as super-resolution methods. A succinct description is given in this thesis, the interested reader is referred to the following reviews[32–36] to have a more detailed overview of these impressive techniques.

Most super-resolution methods use the ability of chromophores to be turned "ON" and "OFF". Some molecules are photo-switchable, that is, they can be changed from an emitting state to a non-emitting state by using different excitation wavelengths. However, most chromophores exhibit blinking and photo-bleaching as an "ON/OFF" mechanism. These methods exploit these "ON/OFF" mechanisms to control the density of chromophores that are emitting at any given time to avoid the overlapping of airy disk patterns. If the patterns do not overlap the centre of the molecules can be accurately localized by fitting a mathematical function exactly as explained in the particle tracking section.[37] Hence, by separating the chromophores in time their positions can be known with high accuracy allowing the reconstruction of a super-resolved image. The basic idea behind localization-based super-resolution methods is illustrated in Figure.2.6, using the previous hexagon example from Figure 2.3. Note that a large number of images is required to obtain optimal results.[25,38,39] Many methods used this approach, and they mostly differ by the way the density of emitting chromophores is controlled. In PALM[40,41], photobleaching is the mechanism that allows separation of the chromophores in time, STORM[39,42] uses stochastic blinking for this and PAINT[43] uses attaching-detaching of the chromophores. Finally, SOFI[44–46] uses the correlated blinking over time to distinguish chromophores via high-order correlation analysis based on cumulant and thus does not require Gaussian fitting.

$$\sigma = \frac{\sigma_{PSF}}{\sqrt{N_p}} \qquad \text{(Eq. 2.6)}$$

It is worth noting that these methods only require a standard wide-field microscope with a minimal adaption of experimental conditions since image analysis is the core of these methods making them widely applicable and relatively cheap to use.

Other super-resolution methods use optics and/or spectroscopic ruse to circumvent the diffraction limit. Examples include 4PI microscopy which uses two objectives to increase the numerical aperture.[47–49] Stimulated emission depletion (STED) uses an additional doughnut-shaped laser to quench fluorescence outside of the doughnut centre via stimulated emission, effectively reducing the excitation volume to up to a few tenths of nanometres. [50,51] Structured illumination microscopy (SIM) uses spatially structure excitation to shift high-frequency components in the Fourier space such that they appear in the observable range of the optical system. Images with many different patterns are then required to reconstruct a super-resolved image (typically factor 2 compared to the diffraction limit). [52–54] Finally, the highest optical resolution techniques are MINFLUX[55–57] which uses the laser intensity profile and smart software to localize the particle and cryogenic localization which uses cryogenic temperature to increase the stability and photon emitted of the emitter leading to outstanding resolutions.[58–60] Both yield resolutions close to 1 nm.
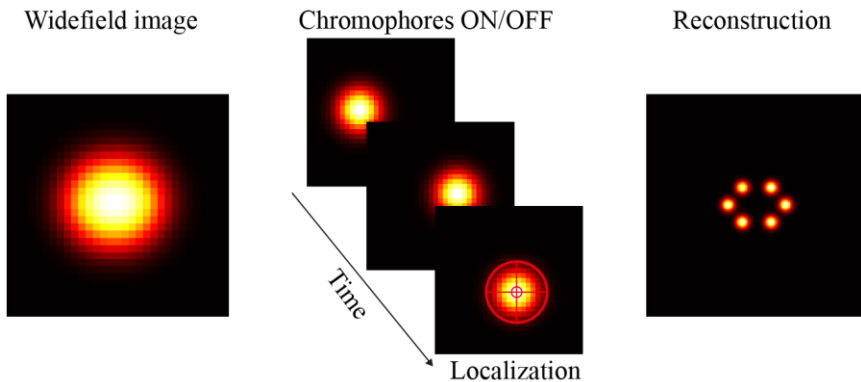
**Figure 2.6: Localization microscopy: The time-average widefield image of the hexagon structure presented in Fig. 2.3 is super-resolved by separating in time the emission of each individual emitter using the stochastic blinking. When the emitter is isolated on the image, it can be localized with high precision. The localization precision is then used to recreate the image using the precision as the new width for the diffraction limited pattern**

# 2.3 Multi-dimensional microscopy

Multi-dimensional microscopy is mostly understood as three-dimensional imaging (x,y,z,(t)). In this thesis, the term is used in the widest sense of the term whereby the two first dimensions are (x,y) coordinates (imaging) and the additional dimension(s) can be anything such as the axial direction (z), time (t), lifetime ($\tau$), excitation wavelength ($\lambda_{exc}$), emission wavelength ($\lambda_{em}$), correlation of intensity through time (r) and any combination. Figure 2.7 shows a simple representation of what a typical data set looks like. Hence, when the additional dimensions are not the axial direction or time, the idea is typically to map a certain property of the sample to the image location and sample structure.

With this broader definition in mind, one may realize that, even if they were not branded as such, most of the super-resolution methods are multi-dimensional. Indeed, the increase in resolution always comes from an increased dimensionality in the data that is processed. Localization-based methods use time and on/off dynamic as additional dimensions to resolve individual chromophores, STED uses stimulated emission and lifetime to increase resolution, SOFI uses time and correlation, etc...

Throughout this thesis, I refer to three-dimensional imaging for (x,y,z,(t)) and spectroscopic imaging when the additional dimensions are different from the axial position.
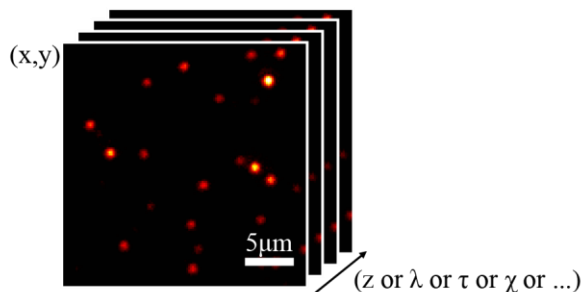


**Figure 2.7: Multi-dimensional imaging data. The key component here is that two-dimension needs to be an image of the sample, typically (x,y), while the additional dimensions can be either spatial (z) or temporal (t) or different parameters such as lifetime ($\tau$), wavelength ($\lambda$) or correlation ($\chi$)**

## Three-dimensional imaging

Three-dimensional imaging has been mostly driven by biology and biochemistry applications where the 3D spatial context is often crucial to understanding the structure of interest as well as their functions. [61–63]

Initially, most of the 3D imaging was done using a scanning confocal microscope. Since the out-of-plane light is blocked by design, taking images at different z-position allows the acquisition of a 3D image.[64–67] However, the imaging procedure is quite slow due to the scanning, making it complicated to study live samples and or perform particle tracking. Consequently, different strategies have emerged to solve the problem of acquisition speed in 3D microscopy. There are 3 main types of approaches, 1) modifications to the excitation beam 2) encoding of axial position in 2D 3) Simultaneous acquisition of axial planes using specific optics.

Among modifications to the excitation beam, there is multi-focal two-photon microscopy which uses a rotating micro-lens disk to generate multiple foci thereby reducing the scanning time[68]. Light sheet microscopy is another method which uses a sheet of light spread parallel to the x-y plane as excitation that is scanned across the axial direction. This yields a wide-field type acquisition in x-y with the z-sectioning of a confocal microscope taking advantage of both techniques and reducing significantly the acquisition time.[34,67,69,70] Light sheet microscopy has had

a very large impact on biology and is the tool of choice for large-volume 3D imaging.

Another approach to 3D imaging is the encoding of the axial position in the shape of the point-spread function (PSF) which is called PSF engineering. The PSF is the response of the optical system to a point source. This method uses optical elements (phase plates) to modify the shape of the PSF in such a way that its shape depends on its position with respect to the focal plane thereby encoding the axial position in the shape of the PSF. After careful calibration of the dependence of the shape on the z-position, a 3D image can be reconstructed from the individual position of the emitters. The principle is shown in Figure 2.8 B where astigmatism is used to induce a z-dependent ellipticity.[42] Different z-dependent patterns have been developed to cover different axial ranges such as the double helix[71–73] and the tetrapod[74]. The main issue is that the size of these patterns can impede the density of emitter one can observe simultaneously since the overlap between patterns can affect the reading of the position drastically.[75,76]
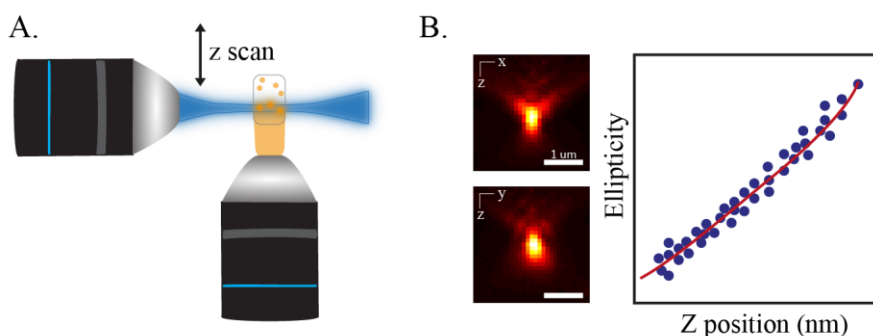


**Figure 2.8: 3D microscopy: A) Schematic of an example of possible configuration for a light sheet microscope. The sheet of light is scanned along z through the sample while a second objective is used to collect the fluorescence. B) PSF engineering principle, here a asymmetrical lens is used creating a change in ellipticity by broadening the PSF along X or Y depending if the particle is below or above the focus. By Calibrating the ellipticity change as a function of z position, an accurate z position can be retrieved.**

Finally, Multi-plane microscopy involves the use of an optical element (e.g. beam splitter, prism) to split the detected light in multiple paths with different optical lengths between the tube lens and the camera. Since it is the method of choice in this thesis, we will dive into more details.

To understand how it works, we must examine a little closer, how a microscope generates an image. Figure 2.9 shows a simplified microscope. If an object is placed

at the focal plane of the objective (or imaging plane), the image will be recreated by the tube lens at its focal plane, where the detector is typically placed (solid black line). In a wide-field microscope, the emission is also collected from out-of-focus planes which can be viewed by moving the detector back and forth (see Figure 2.9) Multiplane microscopy makes use of this feature but, instead of moving the detector, it tunes the distance between the tube lens and the detector using some optical schemes.
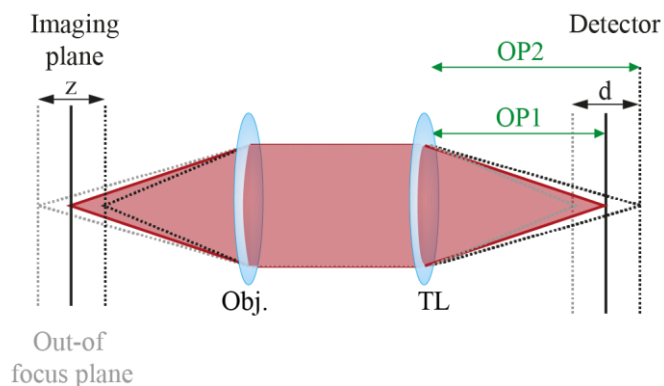


**Figure 2.9: Basic sketch of a microscope. The image plane (solid black line) which is the plane at present at the focal plane of the objective is reproduced at the focal plane of the tube lens with a magnification factor depending on the optics. The dotted line represents the out of focus plane which can be imaged either by moving the sample/objective relative to each other or by moving the tube lens/detector relative to each other**

One simple way of achieving this is by placing a beam splitter between the tube lens and the detector (see Figure 2.10). In that way, one can create two optical paths, OP1 and OP2, of different lengths resulting in two images at different focal depths in the sample. In Figure 2.10 OP1 focuses on the red solid line on the detector while OP2 focuses on the Gray dotted line which represents light from an out-of-focus plane. This is the fundamental principle behind biplane microscopy, the first multi-plane imaging method.[72,77,78]

However, two planes are not enough datapoint in z to make a true 3D image this is why biplane microscopy was mostly used for 3D tracking and localization. Hence, various strategies have been developed to increase the number of planes that could be imaged simultaneously. By increasing the number of beam splitters and a more intricate arrangement of mirrors, four planes detected on 4 cameras could be obtained[79], later improved by Prof. Lasser's group to 8 planes detected on only two camera detectors.[80] With the help of a prism, they later published a similar feat with significantly simpler optical alignment.[81] In Parallel, Prof. Abrahamsson's group

used a chromatic correction grating and a prism to obtain 9 and later, 25 planes simultaneously. [82–86]
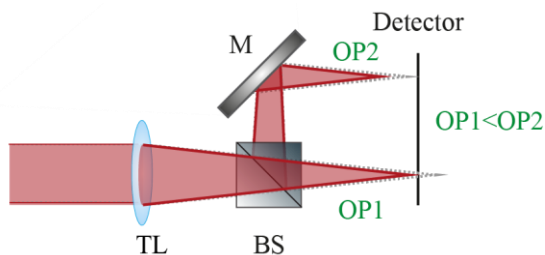


**Figure 2.10: Sketch of a biplane detection system. A beam-splitter (BS) is placed after the tube lens, splitting the signal into 2 different paths having 50% of the initial light. Using a mirror (M), the second path can be redirected to the detector. By tuning the distance between the mirror and the beam splitter, one can tune the distance between the two axial planes imaged in the sample.**

One of the drawbacks is that the division of the signal by the number of channels can limit the application of the technique. For the system studied in this thesis, this was not a problem and multiplane microscopy was used in papers I-IV.

## Spectroscopic imaging

In material sciences, standard 3D microscopy is not as impactful as for biological samples because spectroscopy is often more relevant than the 3D context. Hence, more intricate measurement is needed where the additional dimensions are often spectroscopic such as the lifetime and the emission spectrum. Spectroscopic imaging is, in principle, an even broader range of tools than 3D imaging. This is because it is up to the user/scientist to choose what parameters are relevant to map with the imaging and develop the optical system that allows for the measurements. Therefore, we will focus on the most common categories and the ones that are the most relevant to this thesis.

Fluorescence lifetime imaging $(x,y,\tau)$ or FLIM is a confocal microscopy method, that uses pulsed excitation and a single-photon counter which allows for measuring the arrival time of photons. From the arrival time distribution, the fluorescence radiative lifetime can be extracted. [87,88] While it has been used in biology, mostly paired with energy transfer (FRET), it is also very useful when the materials emit on their own (organic, inorganic or hybrid semiconductor). Indeed, in that case, the lifetime directly reports on the local properties of the material observed. In conjugated polymer, it has been used in polymer blend with strong phase separation allowing an additional contrast[89,90] and in hybrid halide perovskite, it can be used to

judge the quality and or local degradation state[91] and lifetime-encoded security tag.[92]

Spectral imaging (x,y,λ) can be performed on both confocal and widefield and usually uses a diffraction grating to split the emission light collected from the sample into its different wavelength components $(x,y,\lambda_{em})$.[93–95] Another alternative is to scan the excitation wavelength and have the fluorescence intensity report on the amount that was absorbed $(x,y,\lambda_{exc})$.[93,96–98] Of course both can also be performed at the same time yielding a 4D dataset $(x,y, \lambda_{exc,} \lambda_{em})$. Spectral imaging will be explored in more detail in chapter IV. Once again, for materials that absorb and emit in the visible such as the one used in LED or photovoltaic technologies, such methods are highly useful. For instance, it allows for discovering that single conjugated polymer molecules had highly different spectral features than the bulk and that it depended on the conformation of the chain.[99–102]

Lastly, correlation imaging (x,y,r), uses the time correlation of the pixel intensity as an additional dimension in the measurement. One of the main measures of correlation is the Pearson correlation coefficient which measures the strength of the relationship between two variables (see Eq. 2.7).

$$r = \frac{\sum(x_i - \bar{x})(y_i - \bar{y})}{\sqrt{\sum(x_i - \bar{x})^2 \sum(y_i - \bar{y})^2}} \qquad \text{(Eq. 2.7)}$$

While image correlation spectroscopy is the most known imaging method that uses correlation, it usually analyses the correlation of the intensity on the entire image or a large region of it and as such cannot perform a pixel-by-pixel mapping. [103,104] Here, we consider correlation imaging a method that can map how the correlation between pixels and their neighbours changes spatially. SOFI, however, is a correlation imaging method where the correlation helps to build a super-resolved and high-contrast image[44,45]. Paper V, presents a new correlation imaging technique which allows for studying local fluorescence blinking in semiconductor films.

## 2.4 Optical Trapping

Discovered by Ashkin in 1986, optical trapping is a technique that allows controlling the position of objects by using a tightly focused laser beam (high NA objective required). [105–108] He shared the Nobel Prize in physics in 2018 for his work on optical trapping. Figure 2.11 illustrates the basic principle as well as the forces at play. The two main forces to be considered are the gradient force which pushes the particle toward the centre of the focus in all directions and the scattering force which pushes the particle along the direction of the laser light. For a particle to be stably trapped, the gradient force needs to be higher than the scattering force.

Since its invention, optical trapping has been used in various research fields for manipulating micro and nanoscale objects such as nanoparticles, live cells, proteins, DNA, or small molecules.[106,109–113] It has also been successfully used to trigger crystallization in amino acids [114,115], lysozymes[116] or even lead halide perovskite.[117]
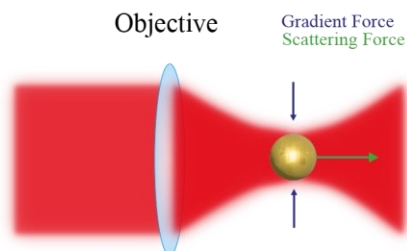


**Figure 2.11: Optical trapping: A laser is tightly focused on a gold particle. The gradient force pushes the particle toward the centre of the beam in all directions. The scattering force which is due to the transmission of the photon momentum to the particle, pushes the particle along the optical axis. When the gradient force is stronger than the scattering force, the particle is stably trapped at the centre of the laser focus.**

## 2.5 Image analysis in microscopy

The attentive reader will have already noticed how important image analysis is to the field of microscopy. Indeed, we have already mentioned methods such as particle tracking, localization, and correlation analysis (SOFI) which without the need to modify heavily the experimental setup allow to gather significantly more information out of the same measurement.

Since image analysis is such an important part of microscopy and considering that this thesis presents some image analysis contribution, let us review some of the basics of image analysis and how it can help to extract information from the imaging data.

To understand image analysis, we need to understand what an image is from the data point of view. It is simply a collection of pixels with intensity values forming a matrix of numbers. It is up to the experimenter to interpret these collections of intensity value into usable scientific data. In some cases, it can be done by simple eye inspection, but quantification is always a better approach to get the information out of the image as it removes some of the bias.

## Pre-processing

While quantifying the images sounds like a great idea, in practice, there is often the need to perform pre-processing of the data to ensure the quantification is as good as possible, particularly when the images are multi-dimensional.

For instance, for measurement over time, it is quite often necessary to perform a drift correction. This is because the longer the measurement, the higher the probability that the sample moves which must be considered. This is particularly true when attempting high-resolution measurement since even a 50-100 nm drift can significantly impact the quality of the result. Most methods involve either cross-correlation[118], tracking of a fixed tracer[42,119], or the localization data themselves to correct for the drift[120]. In this thesis, both the correlation-based approach and the localization approach are used.

In the case of spectroscopic imaging, it is often needed to perform background subtraction to ensure the correct spectrum is extracted. The ideal case is to subtract the background in the vicinity of the treated object.

## Image segmentation

One of the simple approaches to extracting information from an image is segmentation. The idea is to divide the image into its different constituents: objects of interest and background. To do so, the image is simplified into a binary image (0's and 1's) where the pixels of the image are labelled as 1 or 0 based on certain criteria. Depending on the complexity of the data there are many different methods which can be based on intensity, colour, texture, …[121]

In standard microscopy, the criterion is often intensity for which the most common approach is thresholding[122–124]. Many more approaches exist but they are beyond the scope of the thesis, the interested reader is directed to the book chapter by Prof. Carolina Wählby which gives a thorough overview of the different segmentation methods[121].

An illustration of the segmentation of a nuclear membrane is shown in Figure 2.9. In this case, the segmentation also allows the differentiation of the inside of the nucleus from the outside. The size of the segmented area can also be measured and its shape analyze.

In spectroscopic imaging, segmentation can also be used, for instance, by segmenting the parts that have similar behaviours in the third dimension (e.g. emission, excitation, correlation in time…). The correlation-based analysis presented in Paper V is a time-correlation-based segmentation technique.
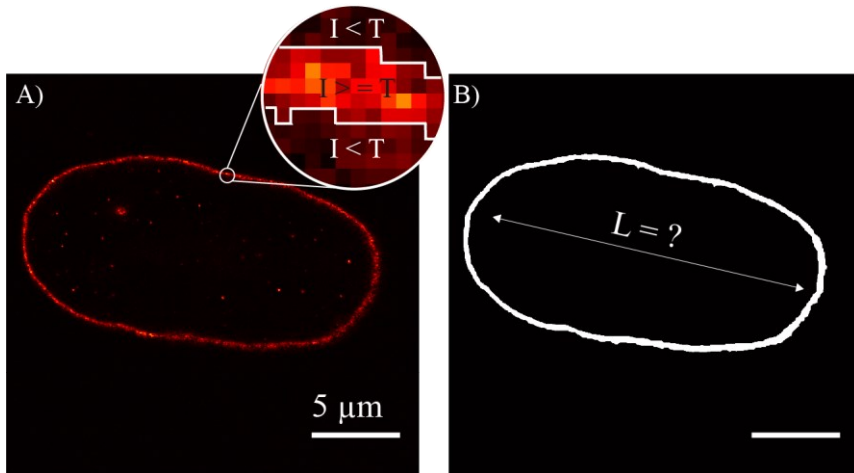
**Figure 2.9 Segmentation: A) Image of the lamina fluorescently labelled. Otsu thresholding was performed which leads to labelling the pixel as 0 or 1 depending on whether the local intensity value is below or above the determined threshold, as shown in the inset. B) Resulting binary image after removal of the small object.**

## Three-dimensional image processing

When processing images that have multiple dimensions, new issues that arise. One of them is the size of the data which starts to be significant and can induce memory and speed issues during the analysis. For example, a 512x512x1000 matrix in MATLAB will be about 2 Gb. Hence, with some of the methods described above, several Gb data are regularly encountered. Hence, care should be taken when loading the data to avoid any memory issues and optimize the analysis speed. Finally, while having more dimensions always gives more information, extracting meaningful data taking into consideration the multi-dimensional context can prove challenging.

An example is three-dimensional single-particle tracking (3D SPT) which becomes very slow using 3D fitting in multiplane microscopy due to the number of parameters to be fitted. [84,125] Paper I demonstrates an alternative approach based on a phasor [126] which allows for fast determination of the 3D position of single particles in multiplane microscopy.

# References

1. Lakowicz JR, editor. Introduction to Fluorescence. In: Principles of Fluorescence Spectroscopy [Internet]. Boston, MA: Springer US; 2006 [cited 2022 Sep 1]. p. 1–26. Available from: http://link.springer.com/10.1007/978-0-387-46312-4_1

2. Lichtman JW, Conchello JA. Fluorescence microscopy. Nat Methods. 2005 Dec;2(12):910–9.

3. Fili N, Toseland CP. Fluorescence and Labelling: How to Choose and What to Do. In: Toseland CP, Fili N, editors. Fluorescent Methods for Molecular Motors [Internet]. Basel: Springer Basel; 2014 [cited 2022 Sep 1]. p. 1–24. (Experientia Supplementum; vol. 105). Available from: http://link.springer.com/10.1007/978-3-0348-0856-9_1

4. Sahoo H. Fluorescent labeling techniques in biomolecules: a flashback. RSC Adv. 2012;2(18):7017–29.

5. Gonçalves MST. Fluorescent Labeling of Biomolecules with Organic Probes. Chem Rev. 2009 Jan 14;109(1):190–212.

6. Rayleigh. XXXI. *Investigations in optics, with special reference to the spectroscope*. Lond Edinb Dublin Philos Mag J Sci. 1879 Oct;8(49):261–74.

7. Sparrow CM. On Spectroscopic Resolving Power. Astrophys J. 1916 Sep;44:76.

8. Houston WV. A Compound Interferometer for Fine Structure Work. Phys Rev. 1927 Mar 1;29(3):478–84.

9. Murphy DB. Fundamentals of light microscopy and electronic imaging. New York: Wiley-Liss; 2001. 368 p.

10. Cook RJ, Kimble HJ. Possibility of Direct Observation of Quantum Jumps. Phys Rev Lett. 1985 Mar 11;54(10):1023–6.

11. Nirmal M, Dabbousi BO, Bawendi MG, Macklin JJ, Trautman JK, Harris TD, et al. Fluorescence intermittency in single cadmium selenide nanocrystals. Nature. 1996 Oct;383(6603):802–4.

12. Efros AlL, Rosen M. Random Telegraph Signal in the Photoluminescence Intensity of a Single Quantum Dot. Phys Rev Lett. 1997;78(6):1110–3.

13. Moerner WE, Orrit M. Illuminating Single Molecules in Condensed Matter. Science. 1999 Mar 12;283(5408):1670–6.

14. Dickson RM, Cubitt AB, Tsien RY, Moerner WE. On/off blinking and switching behaviour of single molecules of green fluorescent protein. Nature. 1997 Jul;388(6640):355–8.

15. Anderson CM, Georgiou GN, Morrison IE, Stevenson GV, Cherry RJ. Tracking of cell surface receptors by fluorescence digital imaging microscopy using a charge-coupled device camera. Low-density lipoprotein and influenza virus receptor mobility at 4 degrees C. J Cell Sci. 1992 Feb 1;101(2):415–25.

16. Kusumi A, Sako Y, Yamamoto M. Confined lateral diffusion of membrane receptors as studied by single particle tracking (nanovid microscopy). Effects of calcium-induced differentiation in cultured epithelial cells. Biophys J. 1993 Nov;65(5):2021–40.

17. Crocker JC, Grier DG. Methods of Digital Video Microscopy for Colloidal Studies. J Colloid Interface Sci. 1996;179(1):298–310.

18. Sheetz MP, Turney S, Qian H, Elson EL. Nanometre-level analysis demonstrates that lipid flow does not drive membrane glycoprotein movements. Nature. 1989 Jul;340(6231):284–8.

19. Levine AJ, Lubensky TC. One- and Two-Particle Microrheology. Phys Rev Lett. 2000 Aug 21;85(8):1774–7.

20. Chen DT, Weeks ER, Crocker JC, Islam MF, Verma R, Gruber J, et al. Rheological Microscopy: Local Mechanical Properties from Microrheology. Phys Rev Lett. 2003 Mar 14;90(10):108301.

21. Lee GM, Ishihara A, Jacobson KA. Direct observation of brownian motion of lipids in a membrane. Proc Natl Acad Sci. 1991 Jul 15;88(14):6274–8.

22. de Brabander M, Nuydens R, Ishihara A, Holifield B, Jacobson K, Geerts H. Lateral diffusion and retrograde movements of individual cell surface components on single motile cells observed with Nanovid microscopy. J Cell Biol. 1991 Jan 1;112(1):111–24.

23. Sergé A, Bertaux N, Rigneault H, Marguet D. Dynamic multiple-target tracing to probe spatiotemporal cartography of cell membranes. Nat Methods. 2008 Aug;5(8):687–94.

24. Cheezum MK, Walker WF, Guilford WH. Quantitative Comparison of Algorithms for Tracking Single Fluorescent Particles. Biophys J. 2001 Oct;81(4):2378–88.

25. Deschout H, Cella Zanacchi F, Mlodzianoski M, Diaspro A, Bewersdorf J, Hess ST, et al. Precisely and accurately localizing single emitters in fluorescence microscopy. Nat Methods. 2014 Mar;11(3):253–66.

26. Boltyanskiy R, Merrill JW, Dufresne ER. Tracking particles with large displacements using energy minimization. Soft Matter. 2017 Mar 15;13(11):2201–6.

27. Chenouard N, Smal I, de Chaumont F, Maška M, Sbalzarini IF, Gong Y, et al. Objective comparison of particle tracking methods. Nat Methods. 2014 Mar;11(3):281–9.

28. Anthony S, Zhang L, Granick S. Methods to Track Single-Molecule Trajectories. Langmuir. 2006 Jun;22(12):5266–72.

29. Howse JR, Jones RAL, Ryan AJ, Gough T, Vafabakhsh R, Golestanian R. Self-Motile Colloidal Particles: From Directed Propulsion to Random Walk. Phys Rev Lett. 2007 Jul 27;99(4):048102.

30. Dunderdale G, Ebbens S, Fairclough P, Howse J. Importance of Particle Tracking and Calculating the Mean-Squared Displacement in Distinguishing Nanopropulsion from Other Processes. Langmuir. 2012 Jul 31;28(30):10997–1006.

31. Michalet X. Mean square displacement analysis of single-particle trajectories with localization error: Brownian motion in an isotropic medium. Phys Rev E. 2010 Oct 20;82(4):041914.

32. von Diezmann L, Shechtman Y, Moerner WE. Three-Dimensional Localization of Single Molecules for Super-Resolution Imaging and Single-Particle Tracking. Chem Rev. 2017 Jun 14;117(11):7244–75.

33. Möckl L, Moerner WE. Super-resolution Microscopy with Single Molecules in Biology and Beyond–Essentials, Current Trends, and Future Challenges. J Am Chem Soc. 2020 Oct 21;142(42):17828–44.

34. Gustavsson AK, Petrov PN, Moerner WE. Light sheet approaches for improved precision in 3D localization-based super-resolution imaging in mammalian cells [Invited]. Opt Express. 2018 May 14;26(10):13122.

35. Vangindertael J, Camacho R, Sempels W, Mizuno H, Dedecker P, Janssen KPF. An introduction to optical super-resolution microscopy for the adventurous biologist. Methods Appl Fluoresc. 2018 Mar 16;6(2):022003.

36. Hell SW. Far-Field Optical Nanoscopy. Science. 2007 May;316(5828):1153–8.

37. Patterson G, Davidson M, Manley S, Lippincott-Schwartz J. Superresolution Imaging using Single-Molecule Localization. Annu Rev Phys Chem. 2010 Mar 1;61(1):345–67.

38. Ober RJ, Ram S, Ward ES. Localization accuracy in single-molecule microscopy. Biophys J. 2004 Feb;86(2):1185–200.

39. Rust MJ, Bates M, Zhuang X. Sub-diffraction-limit imaging by stochastic optical reconstruction microscopy (STORM). Nat Methods. 2006 Oct;3(10):793–5.

40. Betzig E, Patterson GH, Sougrat R, Lindwasser OW, Olenych S, Bonifacino JS, et al. Imaging intracellular fluorescent proteins at nanometer resolution. Science. 2006 Sep 15;313(5793):1642–5.

41. Hess ST, Girirajan TPK, Mason MD. Ultra-high resolution imaging by fluorescence photoactivation localization microscopy. Biophys J. 2006 Dec 1;91(11):4258–72.

42. Huang B, Wang W, Bates M, Zhuang X. Three-dimensional super-resolution imaging by stochastic optical reconstruction microscopy. Science. 2008 Feb 8;319(5864):810–3.

43. Dai M. DNA-PAINT Super-Resolution Imaging for Nucleic Acid Nanostructures. In: Ke Y, Wang P, editors. 3D DNA Nanostructure [Internet]. New York, NY: Springer New York; 2017 [cited 2022 Oct 5]. p. 185–202. (Methods in Molecular Biology; vol. 1500). Available from: http://link.springer.com/10.1007/978-1-4939-6454-3_13

44. Dertinger T, Colyer R, Iyer G, Weiss S, Enderlein J. Fast, background-free, 3D super-resolution optical fluctuation imaging (SOFI). Proc Natl Acad Sci U A. 2009 Dec 29;106(52):22287–92.

45. Dertinger T, Colyer R, Vogel R, Enderlein J, Weiss S. Achieving increased resolution and more pixels with Superresolution Optical Fluctuation Imaging (SOFI). Opt Express. 2010 Aug 30;18(18):18875–85.

46. Dertinger T, Xu J, Naini OF, Vogel R, Weiss S. SOFI-based 3D superresolution sectioning with a widefield microscope. Opt Nanoscopy. 2012 Dec 1;1(2):2.

47. Bahlmann K, Jakobs S, Hell SW. 4Pi-confocal microscopy of live cells. Ultramicroscopy. 2001 Apr;87(3):155–64.

48. Hell SW, Lindek S, Cremer C, Stelzer EHK. Confocal microscopy with an increased detection aperture: type-B 4Pi confocal microscopy. Opt Lett. 1994 Feb 1;19(3):222.

49. Egner A, Jakobs S, Hell SW. Fast 100-nm resolution three-dimensional microscope reveals structural plasticity of mitochondria in live yeast. Proc Natl Acad Sci. 2002 Mar 19;99(6):3370–5.

50. Hell SW, Wichmann J. Breaking the diffraction resolution limit by stimulated emission: stimulated-emission-depletion fluorescence microscopy. Opt Lett. 1994;19(11):780.

51. Farahani JN, Schibler MJ, Bentolila LA. Stimulated Emission Depletion (STED) Microscopy: from Theory to Practice. Microsc Sci Technol Appl Educ. 2010;2(4):1539–47.

52. Gustafsson MGL. Surpassing the lateral resolution limit by a factor of two using structured illumination microscopy. SHORT COMMUNICATION. J Microsc. 2000;198(2):82–7.

53. Saxena M, Eluru G, Gorthi SS. Structured illumination microscopy. Adv Opt Photonics. 2015 Jun 30;7(2):241.

54. Heintzmann R, Huser T. Super-Resolution Structured Illumination Microscopy. Chem Rev. 2017 Dec 13;117(23):13890–908.

55. Balzarotti F, Eilers Y, Gwosch KC, Gynnå AH, Westphal V, Stefani FD, et al. Nanometer resolution imaging and tracking of fluorescent molecules with minimal photon fluxes. Science. 2017 Feb 10;355(6325):606–12.

56. Gwosch KC, Pape JK, Balzarotti F, Hoess P, Ellenberg J, Ries J, et al. MINFLUX nanoscopy delivers 3D multicolor nanometer resolution in cells. Nat Methods. 2020 Feb;17(2):217–24.

57.  Pape JK, Stephan T, Balzarotti F, Büchner R, Lange F, Riedel D, et al. Multicolor 3D MINFLUX nanoscopy of mitochondrial MICOS proteins. Proc Natl Acad Sci. 2020 Aug 25;117(34):20607–14.

58.  Dahlberg PD, Saurabh S, Sartor AM, Wang J, Mitchell PG, Chiu W, et al. Cryogenic single-molecule fluorescence annotations for electron tomography reveal in situ organization of key proteins in *Caulobacter*. Proc Natl Acad Sci. 2020 Jun 23;117(25):13937–44.

59.  Dahlberg PD, Moerner WE. Cryogenic Super-Resolution Fluorescence and Electron Microscopy Correlated at the Nanoscale. Annu Rev Phys Chem. 2021 Apr 20;72(1):253–78.

60.  Mazal H, Wieser FF, Sandoghdar V. Deciphering a hexameric protein complex with Angstrom optical resolution. eLife. 2022 May 26;11:e76308.

61.  Fischer RS, Wu Y, Kanchanawong P, Shroff H, Waterman CM. Microscopy in 3D: a biologist's toolbox. Trends Cell Biol. 2011 Dec;21(12):682–91.

62.  Schneckenburger H, Richter V. Challenges in 3D Live Cell Imaging. Photonics. 2021 Jul 13;8(7):275.

63.  Agard DA, Hiraoka Y, Shaw P, Sedat JW. Chapter 13 Fluorescence Microscopy in Three Dimensions. In: Methods in Cell Biology [Internet]. Elsevier; 1989 [cited 2022 Oct 3]. p. 353–77. Available from: https://linkinghub.elsevier.com/retrieve/pii/S0091679X08609863

64.  Carrington WA, Lynch RM, Moore EDW, Isenberg G, Fogarty KE, Fay FS. Superresolution Three-Dimensional Images of Fluorescence in Cells with Minimal Light Exposure. Science. 1995 Jun 9;268(5216):1483–7.

65.  Piston DW, Masters BR, Webb WW. Three-dimensionally resolved NAD(P)H cellular metabolic redox imaging of the in situ cornea with two-photon excitation laser scanning microscopy. J Microsc. 1995 Apr;178(1):20–7.

66.  Shotton D, White N. Confocal scanning microscopy: three-dimensional biological imaging. Trends Biochem Sci. 1989 Nov;14(11):435–9.

67.  Voie AH, Burns DH, Spelman FA. Orthogonal-plane fluorescence optical sectioning: three-dimensional imaging of macroscopic biological specimens. J Microsc. 1993 Jun;170(Pt 3):229–36.

68.  Straub M, Hell SW. Multifocal multiphoton microscopy: A fast and efficient tool for 3-D fluorescence imaging. Bioimaging. 1998 Dec;6(4):177–85.

69. Chen BC, Legant WR, Wang K, Shao L, Milkie DE, Davidson MW, et al. Lattice light-sheet microscopy: imaging molecules to embryos at high spatiotemporal resolution. Science. 2014 Oct 24;346(6208):1257998.

70. Lu CH, Tang WC, Liu YT, Chang SW, Wu FCM, Chen CY, et al. Lightsheet localization microscopy enables fast, large-scale, and three-dimensional super-resolution imaging. Commun Biol. 2019 Dec;2(1):177.

71. Pavani SRP, Thompson MA, Biteen JS, Lord SJ, Liu N, Twieg RJ, et al. Three-dimensional, single-molecule fluorescence imaging beyond the diffraction limit by using a double-helix point spread function. Proc Natl Acad Sci U A. 2009 Mar 3;106(9):2995–9.

72. Badieirostami M, Lew MD, Thompson MA, Moerner WE. Three-dimensional localization precision of the double-helix point spread function versus astigmatism and biplane. Appl Phys Lett. 2010 Oct 18;97(16):161103.

73. Thompson MA, Lew MD, Badieirostami M, Moerner WE. Localizing and Tracking Single Nanoscale Emitters in Three Dimensions with High Spatiotemporal Resolution Using a Double-Helix Point Spread Function. Nano Lett. 2010 Jan 13;10(1):211–8.

74. Shechtman Y, Weiss LE, Backer AS, Sahl SJ, Moerner WE. Precise Three-Dimensional Scan-Free Multiple-Particle Tracking over Large Axial Ranges with Tetrapod Point Spread Functions. Nano Lett. 2015 Jun 10;15(6):4194–9.

75. Möckl L, Roy AR, Moerner WE. Deep learning in single-molecule microscopy: fundamentals, caveats, and recent developments [Invited]. Biomed Opt Express. 2020 Mar 1;11(3):1633.

76. Nehme E, Freedman D, Gordon R, Ferdman B, Weiss LE, Alalouf O, et al. DeepSTORM3D: dense 3D localization microscopy and PSF design by deep learning. Nat Methods [Internet]. 2020 Jun [cited 2020 Jun 16]; Available from: http://www.nature.com/articles/s41592-020-0853-5

77. Juette MF, Gould TJ, Lessard MD, Mlodzianoski MJ, Nagpure BS, Bennett BT, et al. Three-dimensional sub-100 nm resolution fluorescence microscopy of thick samples. Nat Methods. 2008 Jun;5(6):527–9.

78. Ram S, Prabhat P, Chao J, Ward ES, Ober RJ. High accuracy 3D quantum dot tracking with multifocal plane microscopy for the study of fast intracellular dynamics in live cells. Biophys J. 2008 Dec 15;95(12):6025–43.

79. Ram S, Kim D, Ober RJ, Ward ES. 3D Single Molecule Tracking with Multifocal Plane Microscopy Reveals Rapid Intercellular Transferrin Transport at Epithelial Cell Barriers. Biophys J. 2012 Oct;103(7):1594–603.

80. Geissbuehler S, Sharipov A, Godinat A, Bocchio NL, Sandoz PA, Huss A, et al. Live-cell multiplane three-dimensional super-resolution optical fluctuation imaging. Nat Commun. 2014 Dec 18;5:5830.

81. Descloux A, Grußmayer KS, Bostan E, Lukes T, Bouwens A, Sharipov A, et al. Combined multi-plane phase retrieval and super-resolution optical fluctuation imaging for 4D cell microscopy. Nat Photonics. 2018 Mar;12(3):165–72.

82. Abrahamsson S, McQuilken M, Mehta SB, Verma A, Larsch J, Ilic R, et al. MultiFocus Polarization Microscope (MF-PolScope) for 3D polarization imaging of up to 25 focal planes simultaneously. Opt Express. 2015 Mar 23;23(6):7734.

83. Abrahamsson S, Chen J, Hajj B, Stallinga S, Katsov AY, Wisniewski J, et al. Fast multicolor 3D imaging using aberration-corrected multifocus microscopy. Nat Methods. 2013 Jan;10(1):60–3.

84. Hajj B, Wisniewski J, El Beheiry M, Chen J, Revyakin A, Wu C, et al. Whole-cell, multicolor superresolution imaging using volumetric multifocus microscopy. Proc Natl Acad Sci U A. 2014 Dec 9;111(49):17480–5.

85. Oudjedi L, Fiche JB, Abrahamsson S, Mazenq L, Lecestre A, Calmon PF, et al. Astigmatic multifocus microscopy enables deep 3D super-resolved imaging. Biomed Opt Express. 2016 Jun;7(6):2163.

86. Hirata Miyasaki E, Pettersson GM, Zaw K, John DD, Thibeault B, Lynch B, et al. 25 plane multifocus microscopy for fast and live 3D imaging (Conference Presentation). In: Luo Q, Ding J, Fu L, editors. Neural Imaging and Sensing 2020 [Internet]. San Francisco, United States: SPIE; 2020 [cited 2020 Aug 17]. p. 1. Available from: https://www.spiedigitallibrary.org/conference-proceedings-of-spie/11226/2550979/25-plane-multifocus-microscopy-for-fast-and-live-3D-imaging/10.1117/12.2550979.full

87. Gerritsen HC, Asselbergs MAH, Agronskaia AV, Van Sark WGJHM. Fluorescence lifetime imaging in scanning microscopes: acquisition speed, photon economy and lifetime resolution: FAST FLUORESCENCE LIFETIME IMAGING. J Microsc. 2002 Jun 14;206(3):218–24.

88. Krishnan RV, Masuda A, Centonze VE, Herman B. Quantitative imaging of protein–protein interactions by multiphoton fluorescence lifetime imaging microscopy using a streak camera. J Biomed Opt. 2003;8(3):362.

89. Cadby A, Dean R, Fox AM, Jones RAL, Lidzey DG. Mapping the Fluorescence Decay Lifetime of a Conjugated Polymer in a Phase-Separated Blend Using a Scanning Near-Field Optical Microscope. Nano Lett. 2005 Nov 1;5(11):2232–7.

90. Cadby AJ, Dean R, Elliott C, Jones RAL, Fox AM, Lidzey DG. Imaging the Fluorescence Decay Lifetime of a Conjugated-Polymer Blend By Using a Scanning Near-Field Optical Microscope. Adv Mater. 2007 Jan 8;19(1):107–11.

91. Sheng R, Wen X, Huang S, Hao X, Chen S, Jiang Y, et al. Photoluminescence characterisations of a dynamic aging process of organic–inorganic $CH_3NH_3PbBr_3$ perovskite. Nanoscale. 2016;8(4):1926–31.

92. Yakunin S, Chaaban J, Benin BM, Cherniukh I, Bernasconi C, Landuyt A, et al. Radiative lifetime-encoded unicolour security tags using perovskite nanocrystals. Nat Commun. 2021 Dec;12(1):981.

93. Owen DM, Auksorius E, Manning HB, Talbot CB, de Beule PAA, Dunsby C, et al. Excitation-resolved hyperspectral fluorescence lifetime imaging using a UV-extended supercontinuum source. Opt Lett. 2007 Dec 1;32(23):3408.

94. Frank JH, Elder AD, Swartling J, Venkitaraman AR, Jeyasekharan AD, Kaminski CF. A white light confocal microscope for spectrally resolved multidimensional imaging. J Microsc. 2007 Sep;227(3):203–15.

95. Zhang Z, Kenny SJ, Hauser M, Li W, Xu K. Ultrahigh-throughput single-molecule spectroscopy and spectrally resolved super-resolution microscopy. Nat Methods. 2015 Oct;12(10):935–8.

96. Favreau PF, Hernandez C, Heaster T, Alvarez DF, Rich TC, Prabhat P, et al. Excitation-scanning hyperspectral imaging microscope. J Biomed Opt. 2014 Apr 11;19(4):046010.

97. Chen K, Yan R, Xiang L, Xu K. Excitation spectral microscopy for highly multiplexed fluorescence imaging and quantitative biosensing. Light Sci Appl. 2021 Dec;10(1):97.

98. Löhner A, Ashraf K, Cogdell RJ, Köhler J. Fluorescence-excitation and Emission Spectroscopy on Single FMO Complexes. Sci Rep. 2016 Oct;6(1):31875.

99. Hu D, Yu J, Barbara PF. Single-molecule spectroscopy of the conjugated polymer MEH-PPV. J Am Chem Soc. 1999;121(29):6936–7.

100. Yu Z, Barbara PF. Low-temperature single-molecule spectroscopy of MEH-PPV conjugated polymer molecules. J Phys Chem B. 2004;108(31):11321–6.

101. Mirzov O. Single-molecule imaging and spectroscopy of the π-conjugated polymer MEH-PPV. 2006;

102. Huser T, Yan M, Rothberg LJ. Single chain spectroscopy of conformational dependence of conjugated polymer photophysics. Proc Natl Acad Sci. 2000 Oct 10;97(21):11187–91.

103. Nohe A, Petersen NO. Image Correlation Spectroscopy. Sci STKE [Internet]. 2007 Dec 18 [cited 2022 Oct 4];2007(417). Available from: https://www.science.org/doi/10.1126/stke.4172007pl7

104. Wiseman PW. Image Correlation Spectroscopy: Principles and Applications. Cold Spring Harb Protoc. 2015 Apr;2015(4):pdb.top086124.

105. Ashkin A. Acceleration and Trapping of Particles by Radiation Pressure. Phys Rev Lett. 1970 Jan 26;24(4):156–9.

106. Ashkin A, Dziedzic JM, Bjorkholm JE, Chu S. Observation of a single-beam gradient force optical trap for dielectric particles. Opt Lett. 1986 May 1;11(5):288.

107. Ashkin A, Dziedzic JM, Yamane T. Optical trapping and manipulation of single cells using infrared laser beams. Nature. 1987 Dec;330(6150):769–71.

108. Ashkin A. Optical trapping and manipulation of neutral particles using lasers. Proc Natl Acad Sci. 1997 May 13;94(10):4853–60.

109. Bustamante C, Smith SB, Liphardt J, Smith D. Single-molecule studies of DNA mechanics. Curr Opin Struct Biol. 2000;10(3):279–85.

110. Bustamante C, Bryant Z, Smith SB. Ten years of tension: single-molecule DNA mechanics. Nature. 2003;421(January):423–7.

111. Ashkin A, Dziedzic JM. Optical Trapping and Manipulation of Viruses and Bacteria. Science. 1987 Mar 20;235(4795):1517–20.

112. Grier DG. A revolution in optical manipulation. Nature. 2003 Aug;424(6950):810–6.

113. Gao D, Ding W, Nieto-Vesperinas M, Ding X, Rahman M, Zhang T, et al. Optical manipulation from the microscale to the nanoscale: fundamentals, advances and prospects. Light Sci Appl. 2017 Sep;6(9):e17039–e17039.

114. Sugiyama T, Adachi T, Masuhara H. Crystallization of Glycine by Photon Pressure of a Focused CW Laser Beam. Chem Lett. 2007 Dec 5;36(12):1480–1.

115. Yuyama KI, Sugiyama T, Masuhara H. Laser Trapping and Crystallization Dynamics of l-Phenylalanine at Solution Surface. J Phys Chem Lett. 2013 Aug 1;4(15):2436–40.

116. Yuyama K ichi, Chang KD, Tu JR, Masuhara H, Sugiyama T. Rapid localized crystallization of lysozyme by laser trapping. Phys Chem Chem Phys. 2018;20(9):6034–9.

117. Yuyama K ichi, Islam MJ, Takahashi K, Nakamura T, Biju V. Crystallization of Methylammonium Lead Halide Perovskites by Optical Trapping. Angew Chem Int Ed. 2018 Oct 8;57(41):13424–8.

118. Parslow A, Cardona A, Bryson-Richardson RJ. Sample Drift Correction Following 4D Confocal Time-lapse Imaging. J Vis Exp. 2014 Apr 12;(86):51086.

119. Grover G, Mohrman W, Piestun R. Real-time adaptive drift correction for super-resolution localization microscopy. Opt Express. 2015 Sep 7;23(18):23887.

120. Mlodzianoski MJ, Schreiner JM, Callahan SP, Smolková K, Dlasková A, Šantorová J, et al. Sample drift correction in 3D fluorescence photoactivation localization microscopy. Opt Express. 2011 Aug 1;19(16):15009.

121. Wählby C. Image Segmentation, Processing and Analysis in Microscopy and Life Science. In: Zazzu V, Ferraro MB, Guarracino MR, editors. Mathematical Models in Biology [Internet]. Cham: Springer International Publishing; 2015 [cited 2022 Oct 9]. p. 1–16. Available from: http://link.springer.com/10.1007/978-3-319-23497-7_1

122. Otsu N. A Threshold Selection Method from Gray-Level Histograms. IEEE Trans Syst Man Cybern. 1979 Jan;9(1):62–6.

123. Sahoo PK, Soltani S, Wong AKC. A survey of thresholding techniques. Comput Vis Graph Image Process. 1988 Feb;41(2):233–60.

124. Sankur B. Survey over image thresholding techniques and quantitative performance evaluation. J Electron Imaging. 2004 Jan 1;13(1):146.

125. Kirshner H, Aguet F, Sage D, Unser M. 3-D PSF fitting for fluorescence microscopy: implementation and localization application. J Microsc. 2013 Jan;249(1):13–25.

126. Martens KJA, Bader AN, Baas S, Rieger B, Hohlbein J. Phasor based single-molecule localization microscopy in 3D (pSMLM-3D): An algorithm for MHz localization rates using standard CPUs. J Chem Phys. 2018 Mar 28;148(12):123311.

# Chapter 3:
# Materials & Scientific direction

In this Chapter, I give an overview of the different materials that were studied using multi-dimensional imaging. I also give a brief review of why the category of material is interesting and where is this thesis positioned in the state of the art. The three material types that were studied in this thesis are nanoparticles, conjugated polymers, and metal halide perovskite.

## 3.1 Nanoparticles

Nanoparticles are particles that are in the nanometre range, meaning that at least one of their dimensions is in the 1-100 nm range (Figure 3.1), even though it is sometimes used for larger particles.[1,2] As of today, nanoparticles come in a large spectrum of possible shapes (spherical, cubes, rods…), sizes and compositions (metals, inorganics, organics, composite…), all of which influence their application and properties.[3–6] Needless to say, this extremely wide variety of nanoparticles makes their scope and applications equally wide and beyond the scope of this thesis. Nevertheless, let us review some of the main fields of applications of nanoparticles before moving onto the scientific direction taken in this thesis.

Nanoparticles are already very present in our daily lives and will likely be more and more common.[7] They can be found in cosmetics such as sunscreen, toothpaste, shampoo and others where they are used as pigments, thickeners, UV absorbers (e.g. $TiO_2$) or anti-bacterial agents (Ag, Au) [7,8]. They can also be found in food and their packaging where they are used as food additives, carriers for smart delivery of nutrients, antimicrobial agents or fillers to improve the strength and durability of the packaging.[7,9] In paints they serve as pigment and/or thickener and are present in many other applications.[7,10,11] Finally, nanoparticles are also found in our environment due to dust storms, volcanic eruptions, forest fires and ashes (natural sources) and in diesel and engine exhaust, cigarette smoke and building demolition (man-made).[1,7]

In sciences, nanoparticles have been attractive for their application in catalysis due to a high surface-to-volume ratio.[12–14] They also have a wide scope of applications

in biology and medicine from labelling[15,16] and label-free imaging [17] to drug delivery systems[3,4,15,18,19] and photothermal therapies.[15,20] The advantage here is that they can be functionalized to have targeting capabilities and thus deliver the drug, the contrast or the heat precisely where it is needed thereby reducing potential side effects.[16–20] Finally, nanoparticles have also attracted significant attention from physicists for their size-dependent properties[21] such as surface plasmon resonance.[22–24]

In this thesis, we study different types of nanoparticles using multiplane microscopy and optical trapping. This work was initiated in close collaboration with Prof. Hiroshi Masuhara (NCTU, Taiwan). Among other topics, his group studied the crystallization of molecules using an optical trap at an air/water interface.[25–28] Notably, they observed that the crystal formed could extend tens of micrometres beyond the laser focus. To understand this phenomenon better, they trapped nanoparticles at different interfaces (Figure 3.1B) as a model system because individual amino acids cannot be distinguished under the microscope in such high concentrations.

His group observed that nanoparticles of different materials, sizes and shapes form large assemblies when optically trapped at an interface (see Figure 3.1 C).[29–32] The assemblies show quite complex shapes, are highly dynamic and extend far away from the focal point of the trapping laser, not unlike the crystallization of the molecules. However, from a 2D picture, it is impossible to fully understand what is happening as these assemblies and their dynamics are clearly and three-dimensional. This is why we developed the multiplane microscope with an optical trap to study these assemblies of nanoparticles trapped at an interface in 3D using single-particle tracking.
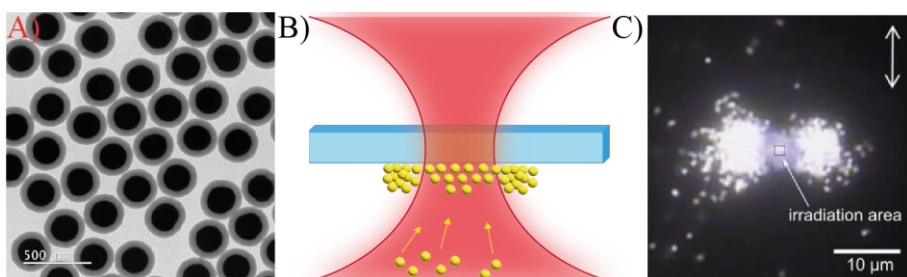


**Figure 3.1: Nanoparticles, optical trapping, and assembly: A) SEM image of nanoparticle composite with a gold core and a Silica shell B) Schematic of the optical trapping of nanoparticles at a water/glass interface, illustrating the assembly formation. C) 2D Dark field image of a gold nanoparticle assembly obtained by Prof. Masuhara's group**

Given the complexity of the tracking in such assemblies, the work was divided into different parts. The first was dedicated to understanding the formation of the assembly and thus it required an understanding of how particles arrive at the trap.

For this, we used 200 nm fluorescently labelled polystyrene nanoparticles as a model to understand the incoming of the particles to the trap and the influence of different parameters (laser power and polarization, particle size…). This was the focus of Paper I in which the combination of multiplane and optical trapping is developed and Paper II in which the dynamic of the incoming nanoparticle to the optical trap was studied in detail.

The second part was the initial stages and dynamics of the assembly formation with only a few particles to understand its formation and growth. This has been the focus of Paper III in which optical binding was shown to have a major impact on the formation of these assemblies.

Lastly, to investigate the dynamic of the full-size assembly, a small number of fluorescently doped gold nanoparticles was incorporated into the assembly which can be easily tracked due to their low concentration. This part of the research is still ongoing and is not part of this thesis.

# 3.2 Organo-metal Halide Perovskite

Organo-metal halide perovskites are a type of semiconductor which forms an ABX3 Perovskite crystal structure. There are many variants, but the main components are typically A= an organic molecule (typically methylammonium), B = a metal centre (typically lead), and X = a halogen (Br, I, Cl). The structure for $MAPbI_3$ is schematically shown in Figure 3.2A. Firstly reported in 1978,[33] it is however only from 2012-2013 that these materials have attracted attention due to their rapidly increasing efficiency as active material in photovoltaic solar cells. [34–38] It is now in a place where it can rival silicon solar cells, by recently reaching 26.1% solar-cell efficiency.[39] A PL image of a film used for a high-efficiency solar cell is shown in Figure 3.2B.

One of the main features of interest, outside the raw efficiency, is the ease of preparation and the low-cost, solution process methods which allowed a lot of laboratories to jump on the topic with minimal synthesis expertise.[35,37] Surprisingly, this simple solution process synthesis still yields high charge mobility material and often high fluorescence yield which has been attributed to its defect tolerance.[40–43]

Nevertheless, the fact that the quantum yield is still far from unity and depends on temperature indicates the presence of non-radiative channels. The presence of fluorescence blinking also supports this idea.[43–48] Consequently, many approaches to reduce these non-radiative channels such as surface passivation[49–51] or light soaking[52,53] have been studied. However, without a clear understanding of the mechanisms behind these non-radiative channels, it can be complicated to rationally designed methods to reduce them, let alone to remove them.
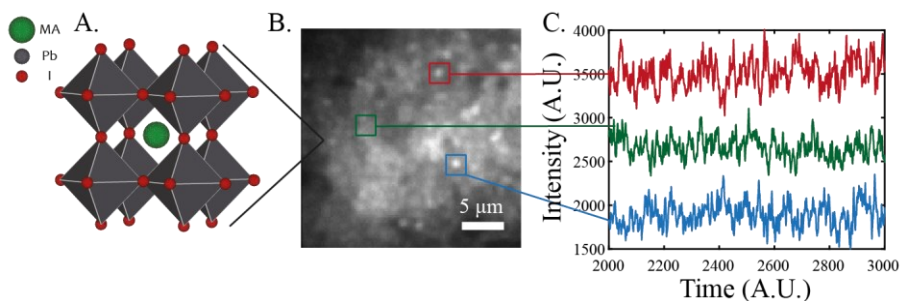
**Figure 3.2: Methyl ammonium lead iodide blinking in film.** MAPbI$_3$ crystal structure which composed the film shown in the PL image. PL image from which blinking traces have been extracted from. This film was synthesized in the same way as for high efficiency solar cell. Intensity traces showing blinking in MAPbI$_3$ films. With the absence of structure on the PL image it is quite challenging to select the area to analyze.

The non-radiative channel that has captured our attention, is fluorescence blinking due to the efficiency with which it affects the quantum yield. Moreover, it is ubiquitous to metal halide perovskite materials where it has been found in almost every system from quantum dots and nanocrystals to micro-crystals and films. The current explanation for blinking in larger systems such as micro-crystal is the "super-trap" model in which a single trap is responsible for the quenching. When a "super-trap" is active, most of the fluorescence is quenched and the charges recombined non-radiatively. [54–59]

Despite the omnipresence of blinking in perovskite material, all blinking studies focus on isolated nano or micro-sized crystals. However, without equivalent studies in film or devices, it is impossible to confirm whether the observation made in these systems are still valid. Hence, we cannot conclude whether blinking has an impact on device performance or not. The connection between individual grain blinking and device performances is unknown and can only be speculated on.

The main reason why such a study has not been performed yet is likely due to the challenge that analysing blinking in a film, or any largely connected blinking entities, represents. Indeed, when the object is isolated, a simple detection[60] can be performed and the fluctuating intensity of the blinking entity is easily extracted. When all the entities are connected and their sizes and positions are unknown, it becomes complicated to select the fluctuating area to be analysed both in terms of size and position (Figure 3.2 B, C). This is of course in part due to the diffraction limit and the fact that the density of emitting sites is too high for most super-resolution to be applied.

Paper V presents the development and application of a correlation-based approach which allows for the analysis of fluctuating intensity by dividing the image into

highly correlated regions. The method is presented in detail in Chapter IV and is applied to blinking in perovskite films in Paper V.

# 3.3 Conjugated Polymers

Polymers more commonly known as plastic, are large molecules with a periodical structure formed by the repetition of a structural unit called a monomer. They are usually unidimensional chains, however, different chains can be also cross-linked and, recently, pure 2D polymers looking like molecular sheets were synthesized.[61,62]

Polymers' properties are determined not only by their structural units but also by their conformation and environment, offering great possibilities for tuning/controlling their properties. Indeed, one can make polymers transparent or coloured, conductive, insulating and even fluorescent. A great variety of electronic properties in combination with solution processability and interesting mechanical properties (flexibility, high strength, and lightweight), make polymers a ubiquitous class of materials. Indeed, from the food industry (e.g. packaging) to electronics (e.g. photovoltaics, LED), engineering (automotive) and even medical applications (e.g. carriers for drug delivery), polymers are found in virtually every aspect of our modern life.[61–66]

Conjugated polymers have a backbone that is made of an alternation of double and single bonds (see Figure. 3.3 A). This type of chemical structure allows electrons to delocalize along the chain leading to semi-conducting properties and usually fluorescence. These polymers are mostly used in photovoltaic, LED and optoelectronic technologies.[67] Their performances in those applications are governed by their photo-physics. Understanding the photo-physics of these materials is therefore of paramount importance to unravel the structure-function relationship.

Despite the technological progress and years of research, the understanding of conjugated polymers' photophysics is far from complete. It is known that intra- and interchain interactions govern the properties.[68–75] A prominent and recent example is that by sole optimization of chain morphology, polymer-only-based solar cells have achieved efficiencies of 9.5%.[76] However, the exact role of these interactions is only known approximately for a few model polymers which are usually not used directly in optoelectronics. One of the main problems is that every chain has a unique conformation resulting in unique, chain-dependent properties, which are obscured by population averaging in traditional spectroscopy. Figure 3.3C shows a true colour image of MEH-PPV demonstrating a wide range of emission colours. In addition, the control on polymer synthesis is far from perfect, which leads to a wide distribution of chain length inside a sample (poly-dispersity, PDI) and chemical

defects, obscuring even further the link between the structure and the properties in bulk experiments.[77–79]

For instance, conjugation in conjugated polymer does not actually extend throughout the whole chain but rather resides in sub-units, usually referred to as spectroscopic units (illustrated in figure 3.3 B). Therefore, the conjugated polymer emission spectrum does not change significantly beyond 10-20 monomeric units depending on the polymer. This is because the chain is very dynamic and presents a lot of defects such as kinks and angles between different part of the chain which often makes the polymer behaves as if the conjugation was only 10~15 units. This is often referred to as the conjugation length of the polymer. It is accepted that a conjugated polymer chain behaves like multiple absorbing molecules (multi-chromophoric system), where each spectroscopic unit is a single chromophore. Hence, at the single-molecule level, the spectroscopic properties are highly dependent on the conformation of the chain as this will have a direct impact on the length of the spectroscopic unit and thus on the spectroscopy of the molecules.[69–71,80–84]
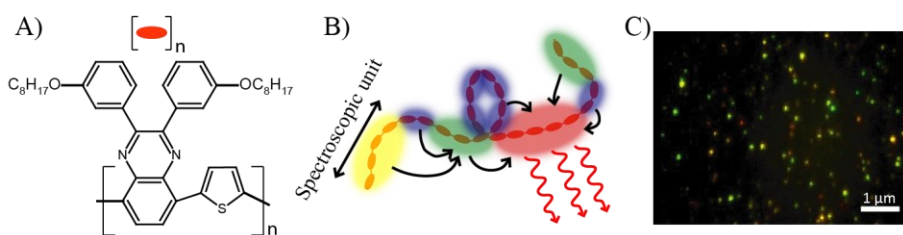


**Figure: 3.3 Conjugated polymers. A) TQ1 conjugated polymer chemical structure B) a chain divided in spectroscopic units of various length leading to various emissions (colors are just chosen to show that shorter units will emit more blue and longer more red) C) an image of single-molecule sample of a conjugated polymer showing different emissions**

When the light is absorbed by these spectroscopic units, their proximity makes it possible to transfer energy to each other via energy transfer. Energy transfer occurs from a higher energy unit (shorter spectroscopic unit, lower conjugation) to a lower energy one (longer spectroscopic unit). Hence, most of the energy ends up funnelling to the spectroscopic unit(s) with the lowest energy. This results in individual polymer chains often exhibiting relatively narrow emission spectra, similar to single chromophores.[85] Therefore, it is easy to understand that a lot of information is lost when studying only the emission spectra since everything happens as if there were a single or a few units instead of the entire chain. On the other hand, if it was readily measurable, the absorption spectra of a single-conjugated polymer chain would directly inform us about the distribution of spectroscopic units and thus allow for studying the relationship between the conformation and the spectroscopy.

The excitation spectrum which can be measured at the single-molecule level yields highly similar information to absorption. Therefore, we decided to use single-molecule excitation spectroscopy (SMES) and excitation-emission spectroscopy (SMEES) to investigate the relationship between the conformation of the chain and the distribution of spectroscopic units on TQ1 conjugated polymers. Chapter IV details the practical aspect of these methods while the results are compiled in Paper VI.

# References

1. Jeevanandam J, Barhoum A, Chan YS, Dufresne A, Danquah MK. Review on nanoparticles and nanostructured materials: history, sources, toxicity and regulations. Beilstein J Nanotechnol. 2018 Apr 3;9:1050–74.

2. Khan I, Saeed K, Khan I. Nanoparticles: Properties, applications and toxicities. Arab J Chem. 2019 Nov;12(7):908–31.

3. Caldorera-Moore M, Guimard N, Shi L, Roy K. Designer nanoparticles: incorporating size, shape and triggered release into nanoscale drug carriers. Expert Opin Drug Deliv. 2010 Apr;7(4):479–95.

4. Liu Y, Tan J, Thomas A, Ou-Yang D, Muzykantov VR. The shape of things to come: importance of design in nanotechnology for drug delivery. Ther Deliv. 2012 Feb;3(2):181–94.

5. Kinnear C, Moore TL, Rodriguez-Lorenzo L, Rothen-Rutishauser B, Petri-Fink A. Form Follows Function: Nanoparticle Shape and Its Implications for Nanomedicine. Chem Rev. 2017 Sep 13;117(17):11476–521.

6. Zahmatkesh I, Sheremet M, Yang L, Heris SZ, Sharifpur M, Meyer JP, et al. Effect of nanoparticle shape on the performance of thermal systems utilizing nanofluids: A critical review. J Mol Liq. 2021 Jan 1;321:114430.

7. Gupta R, Xie H. Nanoparticles in Daily Life: Applications, Toxicity and Regulations. J Environ Pathol Toxicol Oncol Off Organ Int Soc Environ Toxicol Cancer. 2018;37(3):209–30.

8. Raj S, Jose S, Sumod US, Sabitha M. Nanotechnology in cosmetics: Opportunities and challenges. J Pharm Bioallied Sci. 2012 Jul;4(3):186–93.

9. Singh T, Shukla S, Kumar P, Wahla V, Bajpai VK, Rather IA. Application of Nanotechnology in Food Science: Perception and Overview. Front Microbiol. 2017 Aug 7;8:1501.

10. Smulders S, Luyts K, Brabants G, Landuyt KV, Kirschhock C, Smolders E, et al. Toxicity of nanoparticles embedded in paints compared with pristine nanoparticles in mice. Toxicol Sci Off J Soc Toxicol. 2014 Sep;141(1):132–40.

11. Wu Q, Miao W shou, Zhang Y du, Gao H jun, Hui D. Mechanical properties of nanomaterials: A review. Nanotechnol Rev. 2020 Mar 24;9(1):259–73.

12. Xia Y, Yang H, Campbell CT. Nanoparticles for Catalysis. Acc Chem Res. 2013 Aug 20;46(8):1671–2.

13. Narayan N, Meiyazhagan A, Vajtai R. Metal Nanoparticles as Green Catalysts. Mater Basel Switz. 2019 Nov 2;12(21):E3602.

14. Gao C, Lyu F, Yin Y. Encapsulated Metal Nanoparticles for Catalysis. Chem Rev. 2021 Jan 27;121(2):834–81.

15. Salata O. Applications of nanoparticles in biology and medecine. J Nanobiotechnology. 2004;2(1):3.

16. Bhirde A, Xie J, Swierczewska M, Chen X. Nanoparticles for cell labeling. Nanoscale. 2011 Jan;3(1):142–53.

17. Reynders H, Van Zundert I, Silva R, Carlier B, Deschaume O, Bartic C, et al. Label-Free Iron Oxide Nanoparticles as Multimodal Contrast Agents in Cells Using Multi-Photon and Magnetic Resonance Imaging. Int J Nanomedicine. 2021 Dec;Volume 16:8375–89.

18. Fortuni B, Inose T, Ricci M, Fujita Y, Van Zundert I, Masuhara A, et al. Polymeric Engineering of Nanoparticles for Highly Efficient Multifunctional Drug Delivery Systems. Sci Rep. 2019 Dec;9(1):2666.

19. Van Zundert I, Bravo M, Deschaume O, Cybulski P, Bartic C, Hofkens J, et al. Versatile and Robust Method for Antibody Conjugation to Nanoparticles with High Targeting Efficiency. Pharmaceutics. 2021 Dec 14;13(12):2153.

20. Jaque D, Martínez Maestro L, del Rosal B, Haro-Gonzalez P, Benayas A, Plaza JL, et al. Nanoparticles for photothermal therapies. Nanoscale. 2014;6(16):9494–530.

21. Halperin WP. Quantum size effects in metal particles. Rev Mod Phys. 1986 Jul 1;58(3):533–606.

22. Metiu H. Surface enhanced spectroscopy. Prog Surf Sci. 1984 Jan;17(3–4):153–320.

23. Moskovits M. Surface-enhanced spectroscopy. Rev Mod Phys. 1985 Jul 1;57(3):783–826.

24. Ghosh SK, Pal T. Interparticle Coupling Effect on the Surface Plasmon Resonance of Gold Nanoparticles: From Theory to Applications. Chem Rev. 2007 Nov 1;107(11):4797–862.

25. Sugiyama T, Adachi T, Masuhara H. Crystallization of Glycine by Photon Pressure of a Focused CW Laser Beam. Chem Lett. 2007 Dec 5;36(12):1480–1.

26. Sugiyama T, Yuyama KI, Masuhara H. Laser trapping chemistry: from polymer assembly to amino acid crystallization. Acc Chem Res. 2012 Nov 20;45(11):1946–54.

27. Yuyama KI, Sugiyama T, Masuhara H. Laser Trapping and Crystallization Dynamics of l-Phenylalanine at Solution Surface. J Phys Chem Lett. 2013 Aug 1;4(15):2436–40.

28. Yuyama K ichi, Chang KD, Tu JR, Masuhara H, Sugiyama T. Rapid localized crystallization of lysozyme by laser trapping. Phys Chem Chem Phys. 2018;20(9):6034–9.

29. Wang SF, Kudo T, Yuyama K ichi, Sugiyama T, Masuhara H. Optically Evolved Assembly Formation in Laser Trapping of Polystyrene Nanoparticles at Solution Surface. Langmuir. 2016 Nov 29;32(47):12488–96.

30. Kudo T, Yang SJ, Masuhara H. A Single Large Assembly with Dynamically Fluctuating Swarms of Gold Nanoparticles Formed by Trapping Laser. Nano Lett. 2018 Sep 12;18(9):5846–53.

31. Wu CL, Wang SF, Kudo T, Yuyama K ichi, Sugiyama T, Masuhara H. Anomalously Large Assembly Formation of Polystyrene Nanoparticles by Optical Trapping at the Solution Surface. Langmuir. 2020 Dec 1;36(47):14234–42.

32. Kamit A, Tseng C, Kudo T, Sugiyama T, Hofkens J, Bresolí-Obach R, et al. Unraveling the three-dimensional morphology and dynamics of the optically evolving polystyrene nanoparticle assembly using dual-objective lens microscopy. J Chin Chem Soc. 2022 Jan;69(1):120–32.

33. Weber D. CH$_3$NH$_3$PbX$_3$, ein Pb(II)-System mit kubischer Perowskitstruktur / CH$_3$NH$_3$PbX$_3$, a Pb(II)-System with Cubic Perovskite Structure. Z Für Naturforschung B. 1978 Dec 1;33(12):1443–5.

34. Kim HS, Lee CR, Im JH, Lee KB, Moehl T, Marchioro A, et al. Lead Iodide Perovskite Sensitized All-Solid-State Submicron Thin Film Mesoscopic Solar Cell with Efficiency Exceeding 9%. Sci Rep. 2012 Dec;2(1):591.

35. Snaith HJ. Perovskites: The Emergence of a New Era for Low-Cost, High-Efficiency Solar Cells. J Phys Chem Lett. 2013 Nov 7;4(21):3623–30.

36. Kim HS, Im SH, Park NG. Organolead Halide Perovskite: New Horizons in Solar Cell Research. J Phys Chem C. 2014 Mar 20;118(11):5615–25.

37. Green MA, Ho-Baillie A, Snaith HJ. The emergence of perovskite solar cells. Nat Photonics. 2014 Jul;8(7):506–14.

38. Stranks SD, Snaith HJ. Metal-halide perovskites for photovoltaic and light-emitting devices. Nat Nanotechnol. 2015 May;10(5):391–402.

39. Min H, Lee DY, Kim J, Kim G, Lee KS, Kim J, et al. Perovskite solar cells with atomically coherent interlayers on SnO2 electrodes. Nature. 2021 Oct 21;598(7881):444–50.

40. Stranks SD, Eperon GE, Grancini G, Menelaou C, Alcocer MJP, Leijtens T, et al. Electron-Hole Diffusion Lengths Exceeding 1 Micrometer in an Organometal Trihalide Perovskite Absorber. Science. 2013 Oct 18;342(6156):341–4.

41. Buin A, Pietsch P, Xu J, Voznyy O, Ip AH, Comin R, et al. Materials Processing Routes to Trap-Free Halide Perovskites. Nano Lett. 2014 Nov 12;14(11):6281–6.

42. Huang H, Bodnarchuk MI, Kershaw SV, Kovalenko MV, Rogach AL. Lead Halide Perovskite Nanocrystals in the Research Spotlight: Stability and Defect Tolerance. ACS Energy Lett. 2017 Sep 8;2(9):2071–83.

43. Gerhard M, Louis B, Camacho R, Merdasa A, Li J, Kiligaridis A, et al. Microscopic insight into non-radiative decay in perovskite semiconductors from temperature-dependent luminescence blinking. Nat Commun. 2019 Dec;10(1).

44. Richter JM, Abdi-Jalebi M, Sadhanala A, Tabachnyk M, Rivett JPH, Pazos-Outón LM, et al. Enhancing photoluminescence yields in lead halide perovskites by photon recycling and light out-coupling. Nat Commun. 2016 Dec;7(1):13941.

45. Sutter-Fella CM, Li Y, Amani M, Ager JW, Toma FM, Yablonovitch E, et al. High Photoluminescence Quantum Yield in Band Gap Tunable Bromide Containing Mixed Halide Perovskites. Nano Lett. 2016 Jan 13;16(1):800–6.

46. Savenije TJ, Ponseca CS, Kunneman L, Abdellah M, Zheng K, Tian Y, et al. Thermally Activated Exciton Dissociation and Recombination Control the Carrier Dynamics in Organometal Halide Perovskite. J Phys Chem Lett. 2014 Jul 3;5(13):2189–94.

47. Khenkin MV, Amasev DV, Kozyukhin SA, Sadovnikov AV, Katz EA, Kazanskii AG. Temperature and spectral dependence of CH 3 NH 3 PbI 3 films photoconductivity. Appl Phys Lett. 2017;110(22):222107–222107.

48. Zheng H, Dai J. Temperature-dependent photoluminescence properties of [HC(NH 2 ) 2 ]PbI 3 perovskite nanorods. Mater Lett. 2017 Feb;188:232–4.

49. Jiang Q, Zhao Y, Zhang X, Yang X, Chen Y, Chu Z, et al. Surface passivation of perovskite film for efficient solar cells. Nat Photonics. 2019 Jul;13(7):460–6.

50. K H G. Advances in surface passivation of perovskites using organic halide salts for efficient and stable solar cells. Surf Interfaces. 2021 Oct;26:101420.

51. Kang DH, Kim SY, Lee JW, Park NG. Efficient surface passivation of perovskite films by a post-treatment method with a minimal dose. J Mater Chem A. 2021;9(6):3441–50.

52. deQuilettes DW, Zhang W, Burlakov VM, Graham DJ, Leijtens T, Osherov A, et al. Photo-induced halide redistribution in organic–inorganic perovskite films. Nat Commun. 2016 Sep;7(1):11683.

53. Deng X, Wen X, Zheng J, Young T, Lau CFJ, Kim J, et al. Dynamic study of the light soaking effect on perovskite solar cells by in-situ photoluminescence microscopy. Nano Energy. 2018 Apr;46:356–64.

54. Merdasa A, Tian Y, Camacho R, Dobrovolsky A, Debroye E, Unger E, et al. "Super-trap" at Work: Extremely Efficient non-Radiative Recombination Channels in MAPbI3 Revealed by Luminescence Super-Resolution Imaging and Spectroscopy. ACS Nano. 2017;in revision-in revision.

55. Tian Y, Merdasa A, Peter M, Abdellah M, Zheng K, Ponseca CS, et al. Giant photoluminescence blinking of perovskite nanocrystals reveals single-trap control of luminescence. Nano Lett. 2015;15(3):1603–8.

56. Yuan H, Debroye E, Caliandro G, Janssen KPF, Loon JV, Kirschhock CEA, et al. Photoluminescence Blinking of Single-Crystal Methylammonium Lead Iodide Perovskite Nanorods Induced by Surface Traps. 2016;

57. Wen X, Ho-Baillie A, Huang S, Sheng R, Chen S, Ko H chen, et al. Mobile Charge-Induced Fluorescence Intermittency in Methylammonium Lead Bromide Perovskite. Nano Lett. 2015 Jul;15(7):4644–9.

58. Seth S, Mondal N, Patra S, Samanta A. Fluorescence Blinking and Photoactivation of All-Inorganic Perovskite Nanocrystals CsPbBr 3 and CsPbBr 2 I. J Phys Chem Lett. 2016 Jan;7(2):266–71.

59. Pathoor N, Halder A, Mukherjee A, Mahato J, Sarkar SK, Chowdhury A. Fluorescence Blinking Beyond Nanoconfinement: Spatially Synchronous Intermittency of Entire Perovskite Microcrystals. Angew Chem Int Ed. 2018 Sep 3;57(36):11603–7.

60. Sergé A, Bertaux N, Rigneault H, Marguet D. Dynamic multiple-target tracing to probe spatiotemporal cartography of cell membranes. Nat Methods. 2008 Aug;5(8):687–94.

61. Servalli M, Schlüter AD. Synthetic Two-Dimensional Polymers. Annu Rev Mater Res. 2017 Jul 3;47(1):361–89.

62. Wang W, Schlüter AD. Synthetic 2D Polymers: A Critical Perspective and a Look into the Future. Macromol Rapid Commun. 2019 Jan;40(1):1800719.

63. Das TK, Prusty S. Review on Conducting Polymers and Their Applications. Polym-Plast Technol Eng. 2012 Oct;51(14):1487–500.

64. Namazi H. Polymers in our daily life. BioImpacts. 2017 Jun 16;7(2):73–4.

65. Pillai O, Panchagnula R. Polymers in drug delivery. Curr Opin Chem Biol. 2001 Aug;5(4):447–51.

66. Sung YK, Kim SW. Recent advances in polymeric drug delivery systems. Biomater Res. 2020 Dec;24(1):12.

67. Facchetti A. π-Conjugated polymers for organic electronics and photovoltaic cell applications. Chem Mater. 2011;23(3):733–58.

68. Rossi G, Chance RR, Silbey R. Conformational disorder in conjugated polymers. J Chem Phys. 1989 Jun 15;90(12):7594–601.

69. Pullerits T, Mirzov O, Scheblykin IG. Conformational Fluctuations and Large Fluorescence Spectral Diffusion in Conjugated Polymer Single Chains at Low Temperatures. J Phys Chem B. 2005 Oct;109(41):19099–107.

70. Yaliraki SN, Silbey RJ. Conformational disorder of conjugated polymers: Implications for optical properties. J Chem Phys. 1996;104(4):1245–53.

71. Vacha M, Habuchi S. Conformation and physics of polymer chains: a single-molecule perspective. NPG Asia Mater. 2010 Oct;2(4):134–42.

72. Qin T, Troisi A. Relation between structure and electronic properties of amorphous MEH-PPV polymers. J Am Chem Soc. 2013;135(30):11247–56.

73. Kobayashi H, Onda S, Furumaki S, Habuchi S, Vacha M. A single-molecule approach to conformation and photophysics of conjugated polymers. Chem Phys Lett. 2012 Mar;528:1–6.

74. Mirzov O, Scheblykin IG. Photoluminescence spectra of a conjugated polymer: from films and solutions to single molecules. Phys Chem Chem Phys. 2006;8(47):5569–76.

75. Huser T, Yan M, Rothberg LJ. Single chain spectroscopy of conformational dependence of conjugated polymer photophysics. Proc Natl Acad Sci. 2000 Oct 10;97(21):11187–91.

76. Bin H, Zhang ZG, Gao L, Chen S, Zhong L, Xue L, et al. Non-Fullerene Polymer Solar Cells Based on Alkylthio and Fluorine Substituted 2D-Conjugated Polymers Reach 9.5% Efficiency. J Am Chem Soc. 2016 Apr;138(13):4657–64.

77. Menon A, Dong H, Niazimbetova ZI, Rothberg LJ, Galvin ME. Polydispersity Effects on Conjugated Polymer Light-Emitting Diodes. Chem Mater. 2002 Sep 1;14(9):3668–75.

78. Bounos G, Ghosh S, Lee AK, Plunkett KN, DuBay KH, Bolinger JC, et al. Controlling Chain Conformation in Conjugated Polymers Using Defect Inclusion Strategies. J Am Chem Soc. 2011 Jul 6;133(26):10155–60.

79. Mallada B, Chen Q, Chutora T, Sánchez-Grande A, Cirera B, Santos J, et al. Resolving Atomic-Scale Defects in Conjugated Polymers On-Surfaces. Chem – Eur J [Internet]. 2022 Jul 6 [cited 2022 Aug 12]; Available from: https://onlinelibrary.wiley.com/doi/10.1002/chem.202200944

80. Beenken WJD, Pullerits T. Spectroscopic Units in Conjugated Polymers: A Quantum Chemically Founded Concept? J Phys Chem B. 2004;108(20):6164–9.

81. Kuzmany H, Kürti J. The physical meaning of the conjugation length in polymers. Synth Met. 1987 Aug;21(1–3):95–102.

82. Kishino S, Ueno Y, Ochiai K, Rikukawa M, Sanui K, Kobayashi T, et al. Estimate of the effective conjugation length of polythiophene from its $|\chi(3)(\omega;$ Phys Rev B. 1998;58(20):R13430–3.

83. Schwartz BJ. Conjugated polymers: what makes a chromophore? Nat Mater. 2008;7(6):427–8.

84. Becker K, Da Como E, Feldmann J, Scheliga F, Thorn Csányi E, Tretiak S, et al. How Chromophore Shape Determines the Spectroscopy of Phenylene−Vinylenes: Origin of Spectral Broadening in the Absence of Aggregation. J Phys Chem B. 2008 Apr;112(16):4859–64.

85. Saini S, Bagchi B. Photophysics of conjugated polymers: interplay between Förster energy migration and defect concentration in shaping a photochemical funnel in PPV. Phys Chem Chem Phys. 2010;12(27):7427.

# Chapter 4:
# Multi-dimensional microscopy

This chapter treats the different multi-dimensional methods used, developed and or improved in this thesis. It dives into details about the different calibration measurements needed as well as some of the data analysis.

## 4.1   Multiplane Microscopy

As mentioned in Chapter II, the main driver behind multiplane imaging is to reduce the acquisition time for 3D images. This is achieved by acquiring multiple sample sections (=planes) in a single shot allowing for very fast 3D imaging.

The setup developed and used in this thesis is shown in Figure 4.1. It was developed over a few years at Prof. Hofkens's lab. It uses a prism which split the detected fluorescence into eight equivalent parts. The prism characteristics are such that these eight parts will travel a different path length through the prism thereby outputting a different focus on the detector. Note that the prism also shifts them in the x-y space so that 4 of them can be collected on a single camera (sCMOS). The 8 planes have 250 or 500 nm distance from each other depending on the camera configuration (Figure 4.1 a,b,c) leading to a total image volume of about 50x50x5um acquired in a single shot. This setup was largely inspired by the work of Prof. Lasser's group[1] initially done with three beam splitters and later improved using a prism.[2]

To study the 3D dynamics of nanoparticles, an optical trap was added to the system. The 1064 nm laser travels through a separate path from the excitation and is collimated toward the objective to obtain a sharp focal spot in the image plane. The focus of the laser can be adjusted by the collimation lens to be at the top, the centre or the bottom of the imaging volume depending on the needs of the experiment.
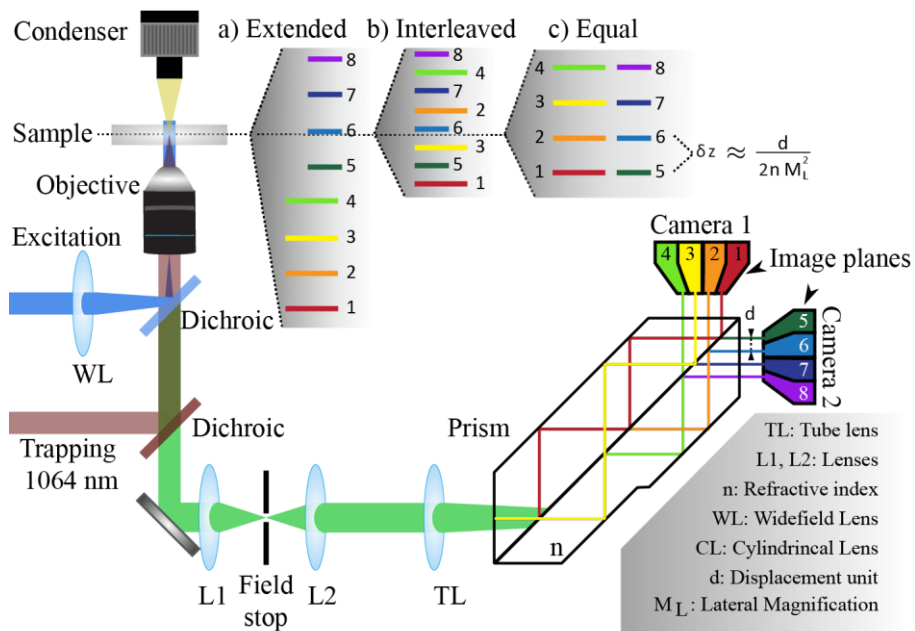
**Figure 4.1: Multiplane Microscope with an optical trap: The system is mostly similar to a standard fluorescence microscope except for two elements, the prism and the trapping laser. The prism split the detected fluorescence signal into 8 while giving each of the 8 parts a different path length through the prism effectively yielding a different focus on the detector. The camera can be aligned into 3 different configurations represented in a), b) and c). The optical trapping laser goes through a different path from the excitation where it is collimated to be focused by the objective on the imaging plane.**

## Calibration

Figure 4.2 shows an exemplary data set obtained on the multiplane setup described in Paper I where each camera collects 4 imaging planes. We can see from the shape of the particle circled in blue that it is captured in 3D in a single time frame. However, we do not directly obtain a 3D image, there are additional steps needed. These steps include image plane detection, ordering and registration. To ensure that these steps are performed in the best way possible, a calibration measurement is performed before the data acquisition.

The calibration measurement consists in measuring a sample of spin-casted fluorescent beads, at a concentration where individual beads can be distinguished. The sample is scanned along the axial direction with the motor so that it appears in

focus in each plane at some point along the scan. This will help with organizing the planes by their axial position and for the image registration.
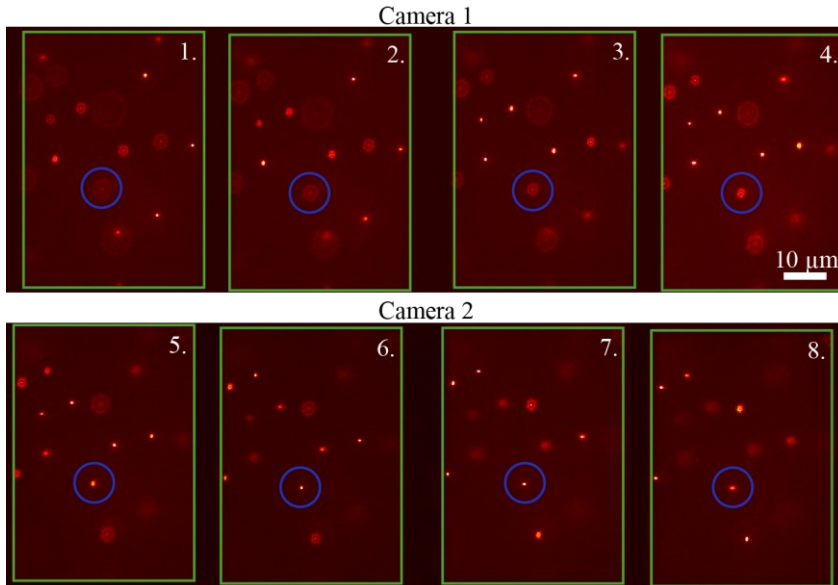


**Figure 4.2: Sample of fluorescent beads in glycerol. Each camera shows an image composed of 4 different image planes. The 8 images are acquired in a single shot. The green rectangle shows the results of the plane detection. The blue circle just highlight the same particle to show how it appears in and out of focus depending on the plane observed**

*Plane detection*

To be able to process the data, the first step is to find and crop the image planes out of the camera frame. Since the background inside the image is significantly higher than the camera shot noise, a simple intensity threshold-based segmentation can be used. The result is shown by the green frames around the images in Figure 4.2.

*Plane position determination*

After that, the next step is to determine the planes' axial positions and order them accordingly. To achieve this, we compute the image gradient for each plane for every frame in the calibration measurement. The image gradient is calculated by taking the difference between neighbouring pixels along x (Gx) and along y (Gy), the magnitude is then computed. The image gradient is maximum when the image is in sharp focus. By plotting it against the motor position we obtain Figure 4.3. The

curves can then be fitted with a Gaussian to get the relative distance between each plane with high accuracy.
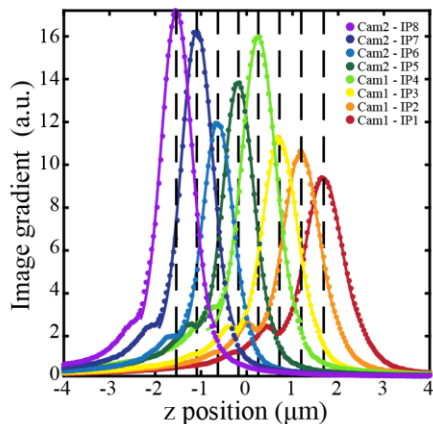


**Figure 4.3: Multiplane calibration. Image gradient of a spin caster fluorescent beads sample as a function of the motor position as it scans through the different image planes. The solid line represent the Gaussian fit used to obtain the position of the planes.**

*Image plane registration*

Since the planes are collected in different parts of the cameras and on two different cameras, we need to ensure that each image planes have the same number of pixels and that they correspond to one another. To achieve this, for each consecutive image plane pair (1-2, 2-3, 3-4…), we select the frame in which the sample is in between the two planes (where the image gradient crosses in Figure 4.3) and perform image correlation between the image from the plane (i) and image from the plane (i+1) to find whether there is a translational shift between them. If there is, the green frame can be adjusted accordingly. The procedure is repeated for every image plane.

*Calibration of new experimental data*

After calibration, we know exactly where the image planes are, what is the axial distance between them as well as the translational shifts. For every measurement performed on the same day, we can apply the same transformation to the data to calibrate it.

## 3D single particle tracking

In this thesis, the 3D images obtained with the multiplane microscope were mostly used to do 3D SPT. Papers I, II, III and IV all use 3D SPT to understand better optical trapping and optically formed nanoparticle assemblies.

As explained in Chapter 2, the image analysis of 3D data can be slow if one does not carefully choose the tools to be used. Hence, we used a phasor to determine the x and y coordinates which was demonstrated by Koens et al.[3] to be significantly faster while being as reliable as standard 2D Gaussian fitting. The phasor is obtained by taking the 2D FFT of the image of the particles (5x5 ROI centred on the detected particle). The first Fourier components are the coordinates of a phasor. From the phase, we can obtain the x (resp. y) shift from the centre of the ROI while the magnitude is proportional to the width of the pattern.[3]

Since an (x,y) pair of coordinates is obtained for each particle and image plane, we need to reduce this to a single coordinate per particle in 3D. We consider localization from different planes to belong to the same particles if they are within a radius of 2 pixels around the coordinates. After collecting all localizations that belong to the same particles, we kept the ones for which the particle focus was the sharpest.

The magnitude of the phasor was found to be quite sensitive to the signal-to-noise ratio as well as the width of the pattern. Since both these parameters change as a function of the axial position for a static emitter, we can use this dependence to extract the axial position of the emitter. Figure 4.4 shows a fit of the magnitude dependence on the plane position. This allows for 3D localization without the need for 3D fitting or calibration making the processing significantly easier and faster. The details can be found in Paper I.
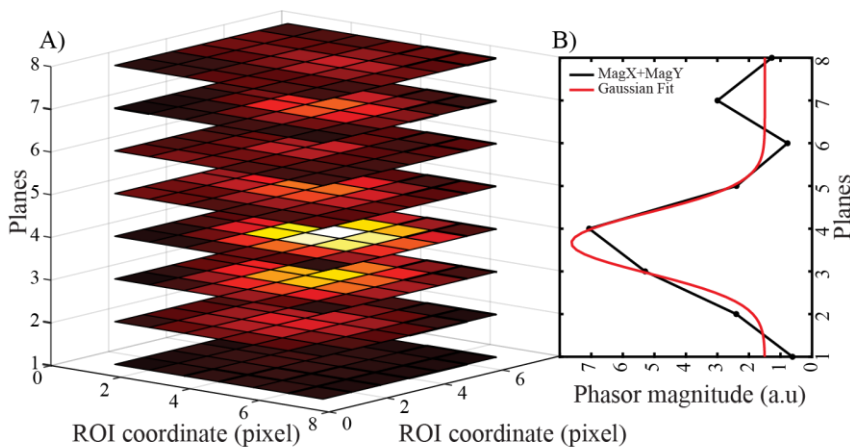


**Figure 4.4: Phasor for 3D localization: A) Detection of a particle in the 8 planes B) determination of the Z position by fitting the dependence of the phasor magnitude in X, Y on the Z position.**

Finally, once we have a single x,y,z coordinate triplet per particle per timeframe, single particle tracking can be performed. The SPT is achieved using a tolerance

radius which describes how far off its previous position the particle is reasonably expected to be. When more than one particle fits within the radius, a minimization of the square displacement is performed using the Munkres algorithm.[4]

### Hardware synchronization

Since multiplane setups often use two or more cameras, it is important to ensure that the cameras are perfectly synchronized. The best way to achieve this is by using transistor-transistor logic (TTL) trigger signal. Both cameras are triggered by external hardware which sends TTL pulses that are split into two equivalent channels each send to one of the cameras. In our case, we used a NI-Instrument board with home-built LabVIEW software for the TTL pulses. Frame rate up to 200/s and beyond are reachable with perfect camera synchronization.

## 4.2 Correlation imaging

The first spectroscopic imaging method uses the time correlation between neighbouring pixels as an additional dimension to segment the image into its different high-correlation regions. This allows us to obtain information beyond the ensemble average in samples where the emitters are too close to be distinguished. As shown in Paper V, the method also allows for generating a higher-resolution image and obtaining information about the local PL dynamic in a fluctuating perovskite film.

As seen in Chapter II, when analysing intensity fluctuations or blinking in fluorescence microscopy, the emitting objects are first detected on the image so that the signal can be studied. The advantage is of course that one knows for certain that the signal obtained comes from the object it was taken from. However, when the distance between these objects becomes small, it is not clear anymore where the objects start and where they end. This is the case for semiconductor films like metal halide perovskite which are composed of highly interconnected grains, for example. Direct detection becomes impossible because the spacing between the object of interest (e.g., grains) is smaller than the diffraction limit. The main idea of the correlation method developed here is to solve this issue by analysing the time correlation of individual pixels' intensity fluctuations with that of their neighbours. The pixels that show a strong correlation in their intensity fluctuations are grouped. Once we obtain groups of pixels that fluctuate similarly, we can compute the intensity trace of the group and thus get information on the PL dynamics.

The Pseudo-correlation clustering method (PcoClust) developed in this thesis is composed of a few steps, first, the correlation relationship between neighbouring

pixels needs to be calculated. Then, the correlated pixels are grouped based on correlation criteria that will be detailed later. Finally, a super-resolved map and intensity traces for the different regions were found via the methods.

The method is illustrated here using simulated images. The application of the method on experimental data is found in Paper V. Briefly, these simulations were achieved by simulating 100 intensity traces (Figure 4.5 A). At each time point, the intensity value had a certain probability to switch from a bright to a dark state and vice versa, 6000 frames were simulated in this way. The intensity traces were used to build a 10x10 array of point sources of light (1 pixel per source, see figure 4.5 C) whose intensity fluctuate in time independently. To obtain the final movie, the array of point sources was convoluted with a Gaussian PSF (Figure 4.5 B) to yield Figure 4.5 D. The emitters were placed close enough to each other so they couldn't be distinguished as single entities with standard methods. We can clearly see that the image is highly inhomogeneous and that it is not possible to distinguish individuals.
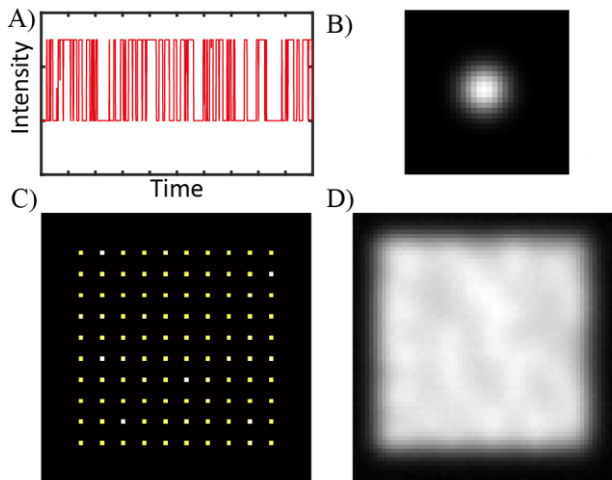


**Figure 4.5: Image simulation: A) Simulation of intensity switching with an equal probability for switching ON or OFF B) Normalized Gaussian PSF with a full width half maximum chosen to be unresolvable in combination with C). C) array of delta function with intensity modulated in time using A). D) Result of the convolution of B and C for a given time point.**

## Correlation extraction

Since the method is based on time correlation, the raw data needs to be of the form (x,y,t). To analyse the correlation between neighbouring pixels the image is scanned

with a 3x3 window for which the Pearson correlation coefficient for each pixel to the central pixel of the window is calculated.

Figure 4.6 illustrates the principle of scanning for correlation relationships. It shows two examples of 3x3 windows where each number represents a correlation value to the pixel at the centre. |CN| depicts the average correlation of the centre pixel to its neighbours and is later used to generate the correlation map. When the window is in an area of strong signal fluctuations, the correlation values are quite high. In a region with low fluctuations (background, non-fluctuating emitters) they are low.

After this step, we know the correlation relationship between each pixel and its neighbour. Moreover, we can compute the correlation map which is an image where the intensity values were replaced by the average correlation of the pixels to their neighbour (|CN| values). The correlation map visualization is important and will be treated in more detail later.
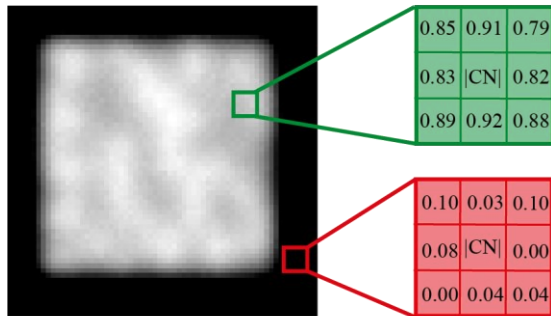


**Figure 4.6: Correlation extraction: The time correlation is extracted by sliding a 3x3 window and calculating the correlation between the pixels inside the window with the pixel at the centre of it. The window extracted at relevant signal position will show relatively strong correlation and will be saved for further analysis while the window extracted in weak signal position (e.g., background) will yield low correlation and will be removed from further considerations. |CN| represent the average correlation of the pixel centre pixel to its neighbour**

## Pseudo-correlation clustering (PCoClust)

*Pseudo Clustering*

Using the correlation relationship, PCoClust groups the pixels with their highly correlated neighbours. This procedure is similar to reconstructing a family tree. For instance, if we know that Bob is the father of Josh and that Josh is the brother of Hilda, then we know that Bob is also Hilda's father (considering simple family relationships only). If we do the parallel for pixels if pixel A is correlated to pixel B

and if pixel C is correlated to pixel B, then the odds are that pixel C and pixel A are correlated. In this way, can reconstruct groups of pixels that belong together based on their correlation in time.

At the start, all the pixels are individual, and no groups are created yet. The search always starts with the pixel that has the highest average correlation to its neighbour (|CN| value). It is used as a starting pixel for a new group (= cluster). After that, the neighbours of the starting pixel are added to the same group if their correlation to the starting pixel is above a certain threshold (more details in the dedicated subsection). Then, the latest added pixels are checked for correlation to their neighbours which are also added if their correlation is above the threshold. The procedure is repeated until there is no new neighbour found that is correlated to the pixels inside the current cluster, at which point the procedure initializes a new group and starts over. The procedure is repeated until all pixels are treated. Note that only the correlation between a pixel and its direct neighbour is calculated, henceforth, long-range correlations are not considered here.

*Enforcing cluster consistency*

The attentive reader will note from the explanation above that the procedure described is too simple and could run into some issues. Indeed, what happens when we treat a pixel that would be at the same distance from two entities that fluctuate differently? This pixel will exhibit a linear combination of the two fluctuations and therefore, present a decent degree of correlation to both. Following the simple logic described above, we could therefore end up including it in one of the clusters but also, start to include pixels from the other entity into the current group just because they are correlated to the pixels at the border. This situation occurs if pixel A is correlated to B, B is correlated to C, but A is not correlated to C. Since the correlation between A and C is never verified, the algorithm may fail.

To take this into account, a step we called enforcing cluster consistency was added to the procedure. Its role is to ensure that the cluster remains consistent, that is, that no uncorrelated pixel is added to it. To do this, the correlation between new pixel candidates (not added yet to the cluster) and a random subset of 10 pixels that are already in the cluster is calculated. The new pixel candidates are added to the cluster if and only if they correlate with at least 70% of the pixels in the random subset.

Figure 4.7 shows the single emitter simulated, the resulting PL image, and the results obtained from the PCoClust algorithm as a cluster map. Each colour in the cluster map represents a cluster of pixels that are correlated. It is worth noting that the algorithm has found a 10x10 array of clusters which is exactly what was in the simulation. The centres of the clusters were also found to match with the simulated emitters showing that the developed method works as intended in these simulations.
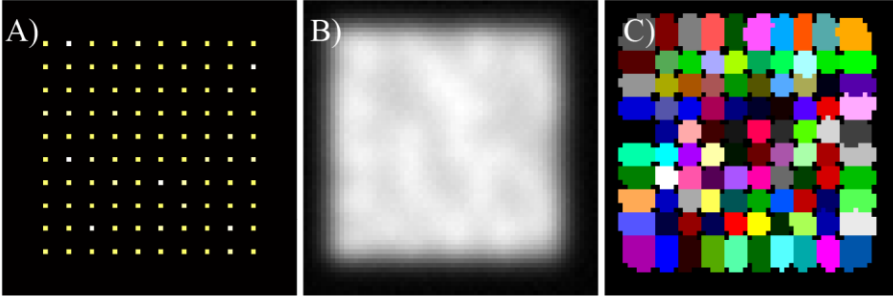
**Figure 4.7: Clustering map: A) Image of the simulated single emitters with intensity fluctuating over time B) Simulated PL image obtained from convoluting A) with a Gaussian function. C) Cluster map, group of pixels that are correlated are represented by the colour. Note that they are more clusters than color and thus some colors are repeated.**

With simulations, it is relatively easy to know whether the pseudo algorithm is performing as expected because the simulated conditions are known in advance. However, systematic evaluation criteria are needed to be able to evaluate the performances of PCoClust on experimental data.

*Evaluation of the clustering quality and threshold determination*

To evaluate the quality of the clusters, we first need to define precisely what is expected from the algorithm: to group pixels that have significant correlation together. Hence, one of the relevant criteria is the average correlation between pixels inside a cluster. However, we also want the clusters to be different from one another. Indeed, it is not because cluster A and cluster B present a high average correlation between their pixels that they are good clusters. If cluster A and cluster B present a high level of correlation with each other, they are not good clusters.

A metric that takes into account both the intra- and inter-cluster correlation is the silhouette[5], which is commonly used to evaluate clusters in machine learning. It considers both the affinity of an element of a cluster with its cluster (in this case the average correlation to other pixels inside the same cluster) and the affinity of the element for the cluster with which it correlates best outside of its own cluster (in this case the average correlation to the pixels inside the cluster that would fit the pixel best outside the one it is currently in). By comparing the two, the silhouette allows gauging how well each pixel fits in the cluster they were placed in. The mathematical definition is given by equation eq. 4.1, 4.2 and 4.3.

$$S(i) = \frac{b(i) - a(i)}{\max\{a(i), b(i)\}}$$

(Eq. 4.1)

Where:

$$a(i) = \frac{1}{C_i - 1} \sum_{j \in C_i, j \neq i} c(i,j) \qquad \text{(Eq. 4.2)}$$

$$b(i) = \frac{1}{C_k - 1} \sum_{k \in C_k,} c(i,j) \qquad \text{(Eq. 4.3)}$$

$C_i$ is the cluster to which pixel i belongs.

$C_k$ is the cluster for which pixel i has the best affinity (highest correlation) after the cluster to which it belongs.

Hence, from equation 4.1, it can be understood that if a pixel is misclassified, the silhouette will be negative, if it is poorly classified the silhouette will be close to 0 and if the classification is very good, the silhouette will be close to 1.

*Threshold determination*

To avoid user bias in choosing the threshold an automated procedure was designed. The procedure consists in running PCoClust on a small portion of the image and trying every threshold from 0.4 to 0.9 with a 0.05 step. For each pseudo clustering obtained, a quality metric was used which was crafted from the previously mentioned silhouette and the proportion of pixels in the image that were clustered. The reasoning behind the inclusion of the latter parameter is that improving the silhouette metric should not be made at the cost of the fraction of the image that is processed.

## Pseudo-clustering output and applications

There are two types of information that can be extracted with this method. The first one is linked to the correlation (e.g. correlation map, silhouette map, correlation relationships) and the second one is linked to the analysis of the fluctuations themselves.

*Correlation output*

Figure 4.8 shows a comparison between the PL image and the correlation image.

The correlation map is interesting as it shows the area of the image that presents a strongly correlated signal in time. In addition, it provides a contrasted image that brings to light features of the image that could not be seen in the raw fluorescence image. Indeed, the correlation map clearly shows an array of 10x10 emitters which

is exactly what was simulated but can not be seen from the PL image. Hence by combining information from multiple dimensions (x,y,t,r) we obtained additional spatial information.
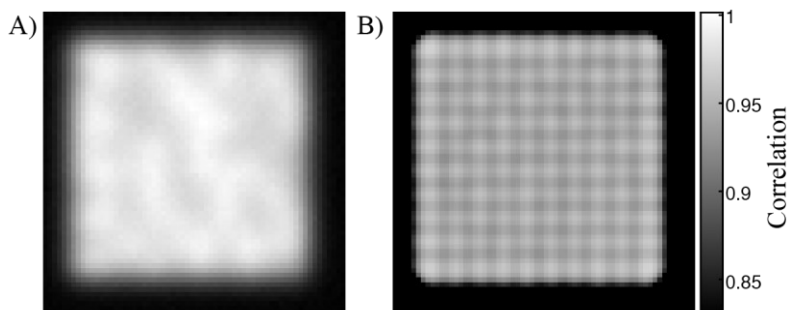


**Figure 4.8: Correlation Map: A) PL Image B) Correlation Map, represent the average correlation to neighbour for each pixel. The contrast in the image allows to distinguish the 10x10 array of fluctuating emitter simulated in the original image.**

*Fluctuations analysis*

Now that the pixels are clustered, the cluster map can be used to obtain information about the size and shape of the correlated area (see Figure 4.9), similar to the segmentation explained in Chapter 2. In addition, the time-dependent intensity from these regions can be extracted to study the fluctuations.
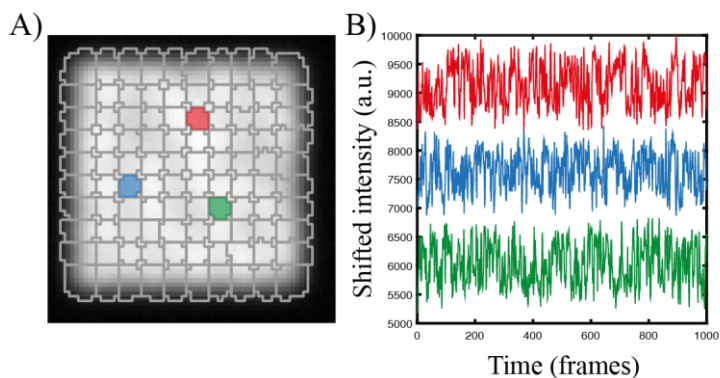


**Figure 4.9: Intensity extraction using clusters. A) Superimposition of the cluster map and the fluorescence image indicating three coloured regions from which intensity fluctuations were taken. B) Intensity traces from the regions highlighted in color in A).**

Once the intensity traces are obtained, the fluctuations can be analysed using any method one finds suited. The method to analyse fluctuation is beyond the scope of this thesis. The interested reader is referred to the following publications.[6–10]

Having information about the spatial distribution, spatial sizes and fluctuations allow us to study the interdependence of these parameters which can yield valuable information as shown in Paper V.

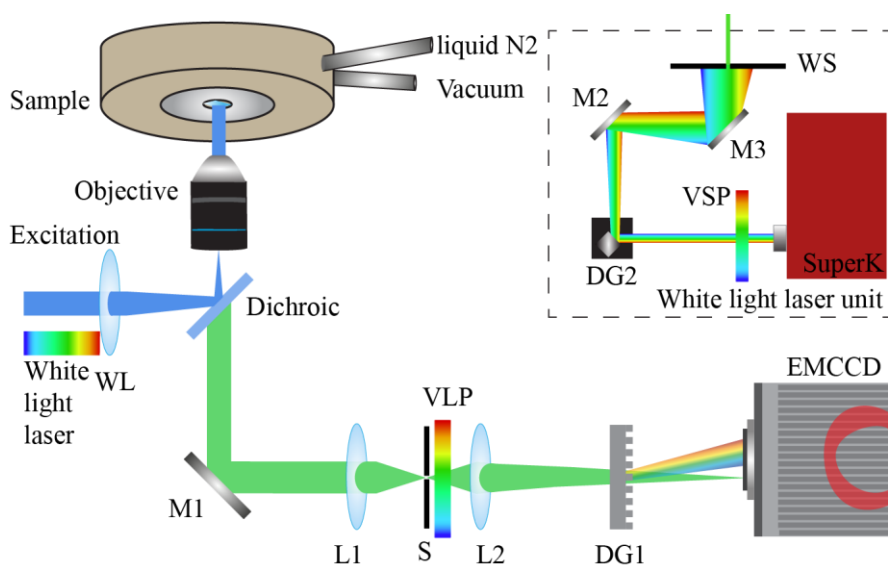## 4.3   Single-molecule excitation-emission spectroscopy



**Figure 4.10: Spectroscopic imaging microscope. Several excitation sources are available including CW laser, pulsed laser, and a white light laser. The white light laser unit is presented schematically. The white light exits the laser box and is directed to a home-made motorized diffraction grating (DG2). The diffraction grating split the white light into its different components and send it to the wavelength selector which is composed of two mirrors (M2, M3) and a diaphragm (WS) and allow to select which wavelength goes out of the white laser unit. The wide field lens (WL) focuses the excitation on the back focal aperture of the objective. A cryostat allows to perform temperature-controlled experiment if needed. L1 is a lens that generate an image plane where a slit (S) is placed to be able to select a ROI. F is a variable long pass filter. L2 is the tube lens. Finally, a diffraction grating DG1 allows to visualize the spectra of the emitted light on the camera.**

Excitation and excitation-emission spectroscopy are two examples of techniques that make use of excitation wavelength and/or emission wavelength as the additional dimensions allowing us to retrieve more information on the sample of interest by connecting the spatial context to the spectroscopic properties. These two types of measurement can be performed on a standard microscope after some modifications that are described below.

## Spectroscopic imaging microscope

Figure 4.10 shows a simplified schematic of the spectroscopic imaging microscope present in Prof. Scheblykin's group. There are a few components that are worth describing in a bit more detail as they are not so commonly found on microscopes designed for imaging only.

*Excitation sources*

A broad range of excitations is available which include wavelength covering the visible but also pulsed laser sources for lifetime measurements and a pulsed white light laser. The white light laser has a dedicated section as it is used both in excitation spectroscopy and excitation-emission spectroscopy.

*Super continuum wavelength selection*

The supercontinuum laser (NKT photonics, superK) contains a short pass that is moved together with the wavelength selection to remove unwanted far-red and near-IR emissions. After this clean-up, the laser light is sent to a diffraction grating monochromator (DG2 in Figure 4.10) which is mounted on a homemade motorized mount allowing control of the grating orientation via Arduino and Labview. The light is consequently split into its different wavelength components of which a single wavelength is selected via a diaphragm. Hence, by moving the diffraction grating, the different wavelengths can be selected. The system can output any wavelength between 450 and 800 nm with a spectral width of about 6 nm.

*Variable long pass*

The variable linear long pass (VLP in Figure 4.10) has a transmission edge that depends on the position in the horizontal direction. It is placed upon a linear motor which moves the filter along its axis across the detection path allowing it to control which wavelengths are filtered. This is mostly used for excitation-emission measurement and allows us to change the excitation wavelength without having to worry about laser leakage onto the detector.

*Diffraction grating*

The diffraction grating splits the emission light into its different wavelength components. The $0^{th}$-order diffraction corresponds to the image itself while the $1^{st}$-order shows a wavelength-dependent spatial dispersion. The grating is aligned such

that the image and the spectra appear on the same line horizontally (see Figure 4.13A). The spectra can then be determined based on the distance between the $0^{th}$ order and the $1^{st}$ order after calibration (see the excitation-emission section for more details on the calibration).

*Slit*

The slit is a field stop which controls the dimension of the image in the horizontal direction (x-axis), it is shown as dotted lines in Figure 4.13A. There are two main uses for it. If the objects of interest are larger than the diffraction limit, the slit needs to narrow the image down to a diffraction-limited width to ensure optimal spectral resolution. This is because each point of the image will be dispersed based on the wavelength it contains so the broader the object, the broader would be the spectra. If the objects of interest are diffraction limited, the slit is used to reduce the field of view such that the spectra do not overlap.

*Calibrations*

A significant part of the setup is motorized and is changed during the measurement automatically. Hence, we need to calibrate the system and ensure that it performs as expected.

First, the white light laser needs to be tuned, to ensure that the wavelength output is indeed the one selected on the homemade software. This is achieved by using an Ocean optics spectrometer placed above the objective and testing it for a few wavelengths in the range of the measurement to be performed.

After that, the power is calibrated such that the same amount of photon is sent to the sample for each wavelength. For this, the power meter is set above the objective and a reference wavelength/power combination is chosen. The software then adjusts the power of the other wavelength using a feedback loop with the power meter. A calibration file is then generated with the list of power for each wavelength which is then used during the measurements.

## Excitation Spectroscopy

In single-molecule excitation spectroscopy (SMES), the excitation wavelength is scanned, and an image of the sample is acquired for each wavelength. Our system can scan from 450 nm to 800 nm with a 5nm step size. In addition, software and hardware synchronization between the laser and the camera ensures the correct acquisition of the desired sequence. In our case, whenever the laser starts emitting, it sends a TTL pulse to the camera set to wait for a trigger to start the acquisition.

*Calibration of the illumination profile*

In this system, the illumination of the sample shows a broad Gaussian-like profile. The system is typically aligned such that the profile is as flat and broad as possible to obtain an even illumination. However, the alignment is never perfect, and optics often have wavelength dependence (grating moves, filters changed, etc), thus, the illumination profile can vary from wavelength to wavelength. This needs to be considered because if the shape is not constant for all wavelengths, then the number of photons received will also not be constant which leads to errors (Figure 4.11).
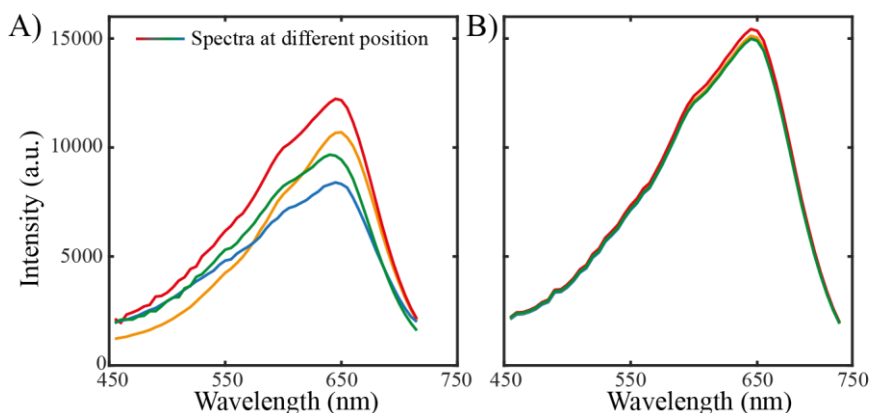


**Figure 4.11: Excitation spectra from different region of the sample before and after correction. A) Excitation spectra before correction for beam shape and beam movement for different region of a TQ1 film. The difference between spectra in intensity, and shape can clearly be seen. B) Same spectra extracted from the same region after correction, the spectra are now identical.**

To correct this, we typically use a calibration sample made of a thin film from either the material of interest or a material that covers the same spectral range. Running an excitation spectrum for the calibration sample allows us to visualize the change of intensity and beam shape as a function of the wavelength and thus compute a correction file. This is achieved by using background subtraction, smoothing and normalization of the illumination profile. The sample is then corrected by dividing the signal by the correction file. The result of the correction can be seen in Figure 4.11 where the spectra are collected at different positions on the sample and yield quite different results before correction.

*Extraction of the spectrum*

For films, the spectrum is obtained by integrating the chosen area of the sample or the entire image. When the sample is composed of multiple objects (e.g. microcrystals, single molecules) we need a different approach. First, simple object detection[11] is performed to detect the individual emitters. The area around the emitter is considered background if it does not overlap with other emitters detected. The intensity of the emitter is then integrated for each frame (one frame = one wavelength) and the background is subsequently subtracted from the region around the emitter. Figure 4.12 A shows an example of an image of TQ1 single molecules in which we scanned the wavelength from 450 to 700 nm. Figure 4.12B shows the resulting spectra obtained.
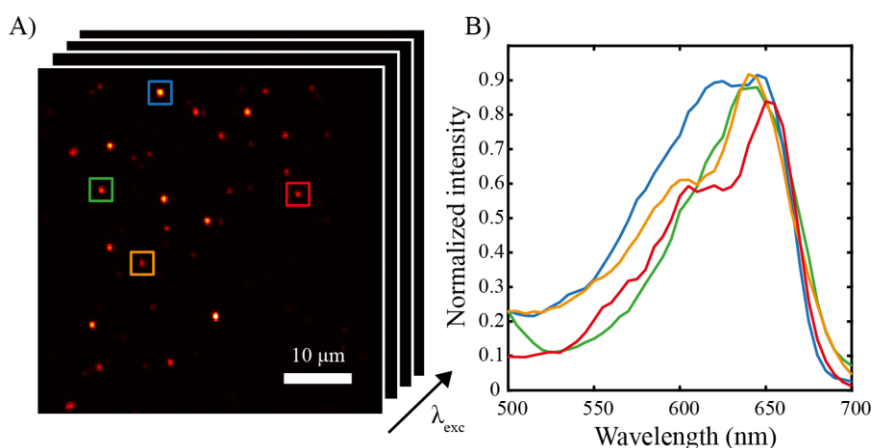


**Figure 4.12: Excitation spectroscopy: By scanning the excitation wavelength while imaging the sample, we obtain a multidimensional image in which the 3rd dimension is the excitation wavelength. Hence, by looking at the intensity of a region of interest in the image along the 3rd dimension we obtain an excitation spectrum for that specific region. B) Shows an example of excitation spectra obtained for different TQ1 single molecule extracted from A). This method was used in Paper VI.**

## Excitation-Emission Spectroscopy

Single-molecule excitation-emission spectroscopy (SMEES) is highly similar to SMES except that a diffraction grating is added in front of the camera to record the emission spectra at the same time (see DFG1 in Figure 4.10). Figure 4.13A shows how the camera record both an image of the emitter (left side) and its emission spectrum (right side).

The advantage of excitation-emission spectroscopy is that it allows for seeing the relationships between emission and excitation such as stoke-shift and correlation between peak position and or width of the spectra. However, this comes with the drawback of imaging a very narrow region in the x coordinate due to the slit. For film and non-diffraction limited objects we lose the x coordinate entirely.
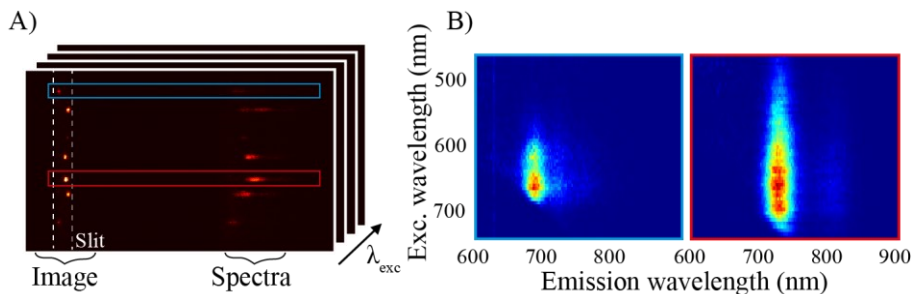


**Figure 4.13: Excitation-Emission spectroscopy A) Exemplary image showing on the left side shows the molecules (0$^{th}$ order of the diffraction grating) and on the right side their emission spectra (1$^{st}$ order of the diffraction grating). B) Resulting 2D spectra obtained by extracting the emission spectra for the different excitation wavelength scanned.**

The calibrations here are the same as in the excitation spectroscopy but there are two additional calibrations to be made. First, the diffraction grating (DG1, Figure 4.10) in front of the camera is calibrated by measuring the spectra of a Hg lamp. The different lines are assigned using literature data to determine the relationship between the distance from the 0$^{th}$ diffraction order to the 1$^{st}$ diffraction order and the wavelength.

Then, the variable long pass filter needs to be calibrated so that the transmission edge input in the software matches the transmission edge of the filter. For this, we used a white lamp and a diffraction grating (DG1, Figure 4.10). Different motor positions are scanned while acquiring an emission spectrum of the white lamp. The long pass edge can be visualized on the white lamp spectra thus, the relationship between the motor position and the transmission edge of the long pass can be determined.

Figure 4.13B shows the resulting fluorescence 2D spectra for the two selected molecules highlighted in figure 4.13A. One can observe how different the two molecules are. Indeed, the molecule circled in red has a much narrower excitation and emission while also being significantly redshifted from the molecule circled in blue. We can also observe that the emission does not depend on the excitation wavelength. SMEES is used in paper VI to study the spectroscopic unit and the influence of conformation in single TQ1 conjugated polymer chains.

# References

1.  Geissbuehler S, Sharipov A, Godinat A, Bocchio NL, Sandoz PA, Huss A, et al. Live-cell multiplane three-dimensional super-resolution optical fluctuation imaging. Nat Commun. 2014 Dec 18;5:5830.

2.  Descloux A, Grußmayer KS, Bostan E, Lukes T, Bouwens A, Sharipov A, et al. Combined multi-plane phase retrieval and super-resolution optical fluctuation imaging for 4D cell microscopy. Nat Photonics. 2018 Mar;12(3):165–72.

3.  Martens KJA, Bader AN, Baas S, Rieger B, Hohlbein J. Phasor based single-molecule localization microscopy in 3D (pSMLM-3D): An algorithm for MHz localization rates using standard CPUs. J Chem Phys. 2018 Mar 28;148(12):123311.

4.  Munkres J. Algorithms for the Assignment and Transportation Problems. J Soc Ind Appl Math. 1957;5(1):32–8.

5.  Rousseeuw PJ. Silhouettes: A graphical aid to the interpretation and validation of cluster analysis. J Comput Appl Math. 1987 Nov;20:53–65.

6.  Frantsuzov P, Kuno M, Jankó B, Marcus RA. Universal emission intermittency in quantum dots, nanorods and nanowires. Nat Phys. 2008;4(5):519–22.

7.  Haase M, Hübner CG, Reuther E, Herrmann A, Müllen K, Basché Th. Exponential and Power-Law Kinetics in Single-Molecule Fluorescence Intermittency. J Phys Chem B. 2004 Jul 1;108(29):10445–50.

8.  Cichos F, von Borczyskowski C, Orrit M. Power-law intermittency of single emitters. Curr Opin Colloid Interface Sci. 2007 Dec;12(6):272–84.

9.  Houel J, Doan QT, Cajgfinger T, Ledoux G, Amans D, Aubret A, et al. Autocorrelation analysis for the unbiased determination of power-law exponents in single-quantum-dot blinking. ACS Nano. 2015;9(1):886–93.

10. Seth S, Podshivaylov EA, Li J, Gerhard M, Kiligaridis A, Frantsuzov PA, et al. Presence of Maximal Characteristic Time in Photoluminescence Blinking of MAPbI $_3$ Perovskite. Adv Energy Mater. 2021 Nov;11(44):2102449.

11. Sergé A, Bertaux N, Rigneault H, Marguet D. Dynamic multiple-target tracing to probe spatiotemporal cartography of cell membranes. Nat Methods. 2008 Aug;5(8):687–94.

# Chapter 5
# Results and Discussion

In this chapter, I briefly summarize the main results and conclusions of each paper with references to the publications and manuscripts collected at the end of this thesis.

## 5.1 Paper I and II: Multiplane microscopy unravels the 3D dynamics of nanoparticles incoming to an optical trap

In papers I and II, we demonstrate the potential of multiplane microscopy to perform 3D particle tracking on fast-moving targets in large volumes. By combining a multiplane microscope and an optical trap we studied the 3D dynamics of the incoming of 200 nm fluorescent nanoparticles (NP) to the optical trap. We also investigate the influence of several parameters (polarization, laser power, numerical aperture) on the observed 3D dynamics. The effects observed are rationalized by simulation of the 3D laser intensity profile.

Paper I focuses on the development of the multiplane microscope in combination with optical trapping. We also demonstrate an improvement of the phasor-based localization by Koens et al.[1] that allows us to obtain the z-position with a one-dimensional Gaussian fit and without the need for calibration. We show that we can localize in 3D with a precision of 10-20 nm in (x,y) and 20-40nm in z. Moreover, we demonstrate the tracking of NPs at 200 frames per second which allows us to follow their incoming pathways to the optical trap in three dimensions.

In paper II, we build upon paper I and studied the incoming of the same NPs (200 nm diameter) to the optical trap in greater detail. Figure 5.1 shows that we could follow the trajectory of the different particles. From the overlay of the traces where we can clearly see the cone shape from the laser-focused irradiation. We note that the NPs follow a Brownian motion outside the irradiated area, and then exhibit a directional motion once they enter the irradiation area.
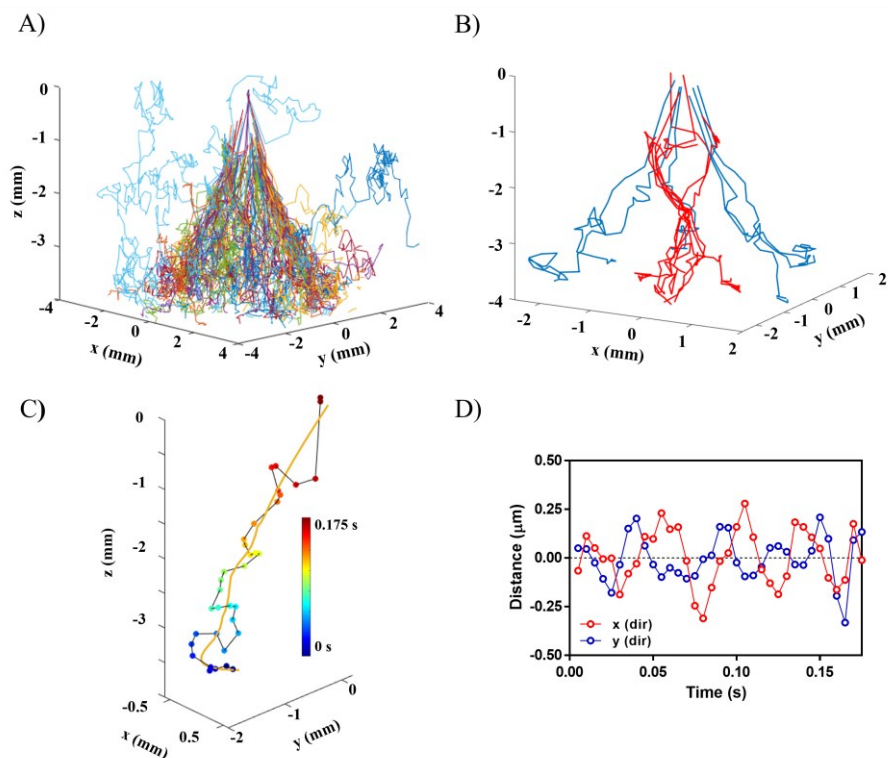
**Figure 5.1: Incorporation of individual fluorescent nanoparticles in the trapping site. A) Overlay of the 3D traces of all the trapping events acquired from 150 independent movies showing the cone shape of the irradiation area. The focal spot (i.e., trapping site) was localized approximately at z = 0 μm. B) Representative incorporation trajectories showing two distinct path to arrive to the trap, one via the inner part and one via the outer part of the irradiation (red and blue lines, respectively). C) Example of trace exhibiting a helicoidal motion as it is pushed toward the optical trap. As a visual aid (gold line), the trajectory is smoothed using a third order Savitzky-Golay filter. The color scale denotes the time scale. D) Relative distance between the previous trace and the smoothed trace in the x- and y-directions (red and blue lines, respectively) showing oscillation characteristics of a helicoidal trajectory.**

Figure 5.1B shows that not all the NPs take the same path toward the optical trap. Some NPs are trapped into a meta-stable position about 2 μm below the focus where they typically stay for a few tenths of milliseconds. Another peculiarity found in analysing the traces is shown in Figure 5.1 C where some NPs exhibit a helicoidal trajectory as they go to the optical traps. Figure 5.1D shows the variation of the x

and y position of the particle to a Savitzky-Golay smoothing filter exhibiting oscillations which confirm the helicoidal motion.

To understand these observed dynamics, the irradiation field of the laser was calculated for our experimental conditions. The calculations demonstrate that the observed phenomena are caused by the inhomogeneity of the laser irradiation field. Indeed, the irradiation field presents a periodically converging pattern made of concentric rings that induce a secondary focus 2 µm below the main focal point. This explains the metastable trapping position observed. Finally, the converging concentric rings create a periodic variation of the gradient force direction along the z-axis which likely causes the NPs to adopt a helicoidal trajectory.

In the rest of paper II, we apply the same strategy and analysis to investigate the influence of laser polarization, numerical aperture, and laser power. Briefly, the laser polarization induces a preferential path for NPs going to the trap in the direction perpendicular to the polarization. The numerical aperture changes the incorporation angle and the sharpness of the incorporation path. This is because the laser profile at lower NA is closer to a Gaussian distribution and therefore does not present the periodically converging pattern. Additionally, at low NA, the metastable trapping position is not there anymore. The laser power makes the incorporation channels significantly sharper. This is due to the optical driving force becoming significantly stronger than the random thermal motion. Finally, we show that the NP flux increases super linearly with the laser power which indicates that hydrodynamics interactions need to be considered. These results are discussed in more detail in Paper II at the end of this thesis.

To summarize, these two papers demonstrate the potential of multiplane microscopy to perform fast 3D imaging (200 fps and beyond) in large volume $(50x50x5(\mu m)^3)$ with high accuracy (10-20 nm in x,y  30-40 nm in z). Using this technique, we could follow 200 nm fluorescent NPs as they arrive at an optical trap. From the 3D traces, we observe the presence of a secondary metastable trapping site and that particles exhibit a helicoidal motion as they are pushed toward the optical trap. Using calculations, we show that the laser intensity field is very inhomogeneous in standard trapping conditions and composed of a series of concentric rings forming a periodically converging pattern. This pattern turned out to be the cause of both the metastable trapping position and the helicoidal trajectories, demonstrating the importance of the laser profile in optical trapping experiments.

# 5.2 Paper III: Tracking early stages of a gold nanoparticle assembly shows optical binding outside the laser focus

In Paper III, we use particle tracking to study the motion of gold nanoparticles (AuNPs) and interactions during the initial stage of the formation of an assembly of AuNPs made by optical trapping at a glass/water interface. When AuNPs are trapped, they first fill the laser irradiation spot and form a linear arrangement of 3 AuNPs (here referred to as 3LA) oriented perpendicular to the polarization. Optical binding, initially discovered by Burns et al.[2] was suggested to be the explanation for the 3LA periodic structure inside the irradiation area.[3]
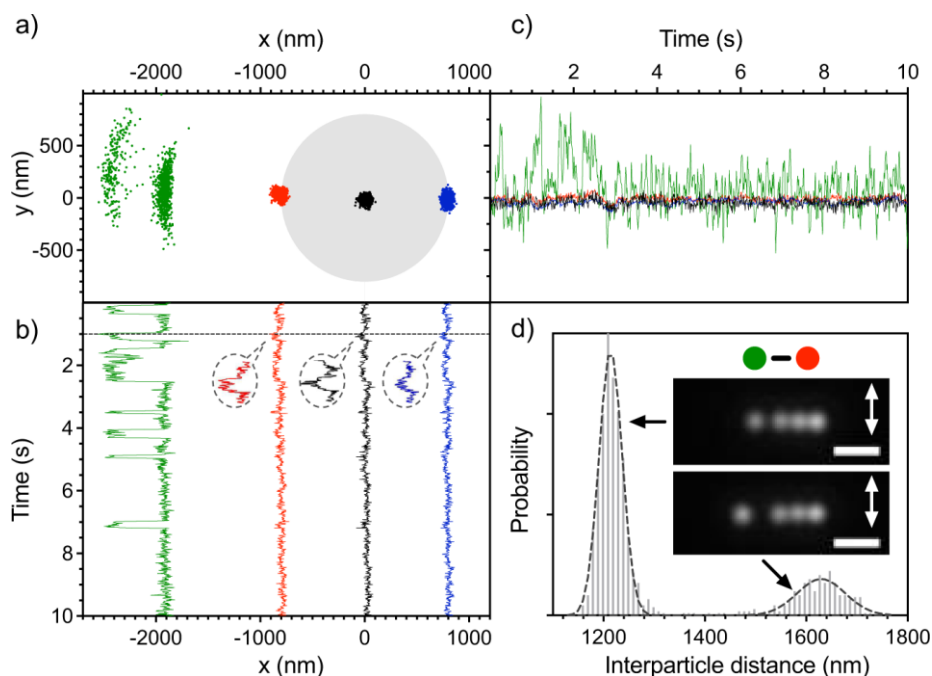


**Figure 5.2: Four nanoparticles case: a) The two-dimensional distribution in the x,y-focal plane, and the shadowed grey circle corresponds to the estimated diameter of laser focus (1.8 µm). b), c) Trajectories of NPs in x- and y-directions over time, and their colours (black, red, blue, and green) correspond to each NP in the two-dimensional distribution. The dashed-line bubbles show a magnification of the 3LA NP's motion to show how they are affected by the external NP hopping. d interparticle distance distribution between the external Au NP and the closest one inside the focus. The dashed lines are Gaussian fitting curves, which mean value approximately corresponds to 1.5 and 2 wavelength separations. Inset: Representative images when the external NP is localized at the first and second arc, respectively. The scale bar is 2 µm, and the arrows indicate the direction of the laser linear polarization.**

Upon increasing the number of particles, the structure of the assembly expands outside the focus, forming a dumbbell-shaped swarming assembly. While it was proposed that the trapping laser was efficiently scattered by the antenna-like

structure formed inside the focus of the laser toward the outside, the exact mechanism remains elusive.[3]

To understand this mechanism, we studied the initial stage of the assembly formation (1-6 AuNPs) using single particle tracking. When one or more particles are outside the laser focus area, the particles that do not fit will sit at the right and/ or at the left of the 3LA keeping the linear configuration. However, the particles sit at a different distance than the one between the particles within the 3LA. Figure 5.2 shows the four AuNPs case where the additional particle sits at the left of the 3LA. We note here that the particle sitting outside is much more mobile than the one inside the irradiation area. When looking at Figure 5.2, we see that the 4th particle localizes into two discrete stable positions along the x-axis with an arc distribution along y. The distance between this NP and the closest NP sitting inside the irradiation area is 1.2 and 1.6 µm for the first and second arcs respectively. These distances correspond to 1.5 and 2 times the laser wavelength in water ($\lambda_{H2O}$= 800 nm). Distances that are multiples of the wavelength indicate that the fourth particle is also optically bound to the 3LA.

Another evidence for optical binding is the fact that the motion in the x-direction of the NP sitting outside the 3LA shows a high correlation to the 3LA, particularly when inside the first arc ($r_{11}$=0.66 for the first arc, $r_{21}$ = 0.05 for the second). We also observe that the correlation decreases from the first particle in the 3LA to the last one ($r_{11}$ = 0.66, $r_{12}$=0.6, $r_{13}$ = 0.52). Because of this strong correlation, the 3LA shifts slightly when the particle hops from one arc to the other (see Figure 5.2b, particularly enlarge portion). This implies that the four AuNPs are bound as a single system, and therefore, the external NP movement affects the movement of the 3LA and vice versa. This is, to our knowledge, the first report of optical binding outside the irradiation area.

The external NP hopping between arcs indicates that there exists a potential barrier between them (see the green line in Fig. 5.2a–c), which is low enough to be overcome by random thermal fluctuations. Besides, a larger potential barrier exists on the right side of the first arc, translating into a sharper borderline (see Figure. 5.2a). Rarely, the external NP collides with the 3LA through a channel, which circumvents the potential barrier. In that case, the NP sitting at the edge on the other side of the 3LA is pushed out from the irradiation area like Newton's cradle system.

When the number of particles reaches 6, the motion of each NPs becomes much more complex and the number of possible arrangements increases drastically (e.g. 3:2:1,2:3:1,2:2:2…). The number of arcs also increases up to 4 when at least 3 particles are on the same side of the 3LA. This is crucial since it indicates that the particle outside of the focus expands the optical potential. Hence, it is likely that the addition of new particles expands the optical potential allowing to gather of more particles thereby progressively growing the assembly.

To summarize, paper III demonstrates for the first time, optical binding outside of the irradiated area. Moreover, optical binding is shown to be the main factor contributing to the extension of an assembly of AuNPs outside the trapping focus. When the number of NPs increases, the number of arcs where they can move also augments indicating that the laser potential is extended. The NPs' motion becomes more erratic facilitating the hopping between arcs. Hence with the increasing number of particles, the optical potential gradually smoothens to become a continuum, which explains well the previously observed dumbbell-shaped swarming assembly.[3]

# 5.3 Paper IV: 3D tracking of pistol-like ejections from a polystyrene microparticles assembly

Paper IV investigates the formation and 3D dynamics of an assembly formed by optical trapping of 1 μm polystyrene beads at a water/air interface using multiplane microscopy. Such assembly is a model system to understand the crystallization of amino acids by optical trapping.[4,5] The crystal formed were shown to extend up to tenths of micrometres beyond the focus. The mechanism for such growth, however, remains unclear. Since individual amino acids cannot be observed at such high density, replacing them with large beads can shine a light on some of the crystallization mechanisms.

We show that polystyrene microparticles (MPs) when trapped at a water/air interface form an assembly which extends beyond the focal spot of the trapping laser, not unlike the crystallization of amino acids. Initially, the assembly formed shows a concentric circular (CC)-like structure which stochastically rearranges to either a similar (CC)-like assembly or a hexagonal close-packing (HCP) structure.

The rearrangements of the assembly often trigger a pistol-like ejection of some MPs. We refer to the phenomenon as pistol-like ejection because a few MPs are ejected with high speed and directionality similar to a pistol. The phenomenon is illustrated with a cartoon in Figure 5.3A. Figure 5.3 C shows an image of the assembly before the ejection occurs at z = 0 μm. The two pairs of particles circled in red are about to be ejected. Figure 5.3D shows the assembly after the ejection, at z=-2.8 μm. The two pairs of particles circled in red are now far away from the assembly and in focus 2.8 μm below their starting point. This shows that the pistol-like ejection occurs in three dimensions.

Using 3D SPT we could obtain the traces of these ejections (see Figure 5.3 B). The colour indicates the axial position confirming that, as the particles are ejected out of the assembly, they are also ejected downward.
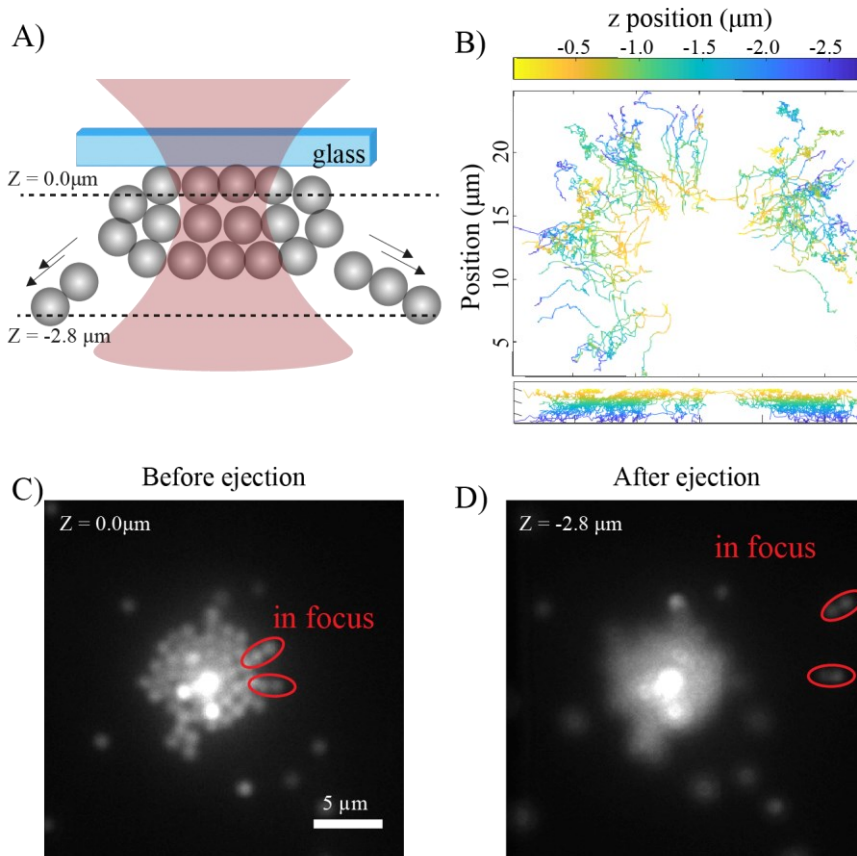
**Figure 5.3. 3D motion analysis of the pistol-like ejection using a fluorescent dye-doped MP. Laser power is 0.36 W. A) Schematic of the pistol-like ejection. The dotted lines represent the planes where the image in C and D were taken from. B) 3D tracking traces of the detected pistol-like ejections for x−y and radius-z projections. C) Image of the assembly before the ejection, the axial position is 0.0 µm. The two pairs of particles circled in red are the ones that will be ejected. D) Image of the assembly after the ejection, the axial position is -2.8 µm. The two pair of particles circled in red have been ejected from the assembly and are now in focus 2.8 µm below it.**

Using radial coordinates and localization density we determined the ejection angle to be around 13 degrees to the glass surface. Since the trapping laser illuminates a 45-135 degrees cone to the glass surface, the ejection occurs within a small angle outside the irradiation cone. However, it is not clear why we did not observe ejection at an angle comprised between 15 and 45 degrees.

To summarize, paper IV demonstrates the formation of a large concentric circular assembly by optical manipulation of 1 μm PS MPs. We also report highly directional ejection of MP from the assembly (pistol-like ejections) which are triggered by the rearrangements of the assembly and seem to follow the scattering pattern of the laser. After some time, the assembly rearranges to a hexagonal close packing where it stably grows without any ejection occurring. The assembling, rearrangements and pistol-like ejections are all driven by optical forces.

## 5.4 Paper V: Correlation imaging allows for analysis of fluorescence blinking in semiconductor films

Fluorescence blinking is a common phenomenon in single molecular systems[7,8] as well as in semiconductor nanocrystals.[9–11] While the exact mechanism depends on the system, it occurs when the system turns into a dark state from which it cannot emit. This explanation works well for quantum systems, however, blinking has been observed in larger-size crystals of semiconductors and even in films where a single state for a few micrometre object can simply not be assumed. [12,13] In these larger systems, blinking is usually explained with multiple recombination centres (MRC) or "super-trap". They are highly efficient traps which cause a large number of charges to recombine non-radiatively.[12] Blinking has also been observed in the film, however, there is no detailed study on it, likely due to the challenge posed by the analysis.

Paper V shows the development and application of a pseudo-correlation clustering algorithm (PCoClust) which uses the time-correlation between pixels in a movie of a blinking film to group the ones that blink in the same way together. The method is described in detail in Chapter IV.

Figure 5.4 shows the results of the PCoClust method for a MAPbI$_3$ perovskite film. For each sample, a movie of 6000 frames with 50 ms was acquired using a wide-field microscope. An exemplary PL image taken from one of these movies is shown in Figure 5.4A. It can be seen that the grains are not resolvable, however, the entire film displays local fluorescence blinking.

After applying the PCoClust algorithm to the MAPbI$_3$ film data, we obtain the cluster map and the correlation map (Figure 5.4 B, C). The cluster map shows numerous spots, a few micrometres radius each. They represent the area that the algorithm found to be correlated. The correlation map shows that a high correlation is found at the centre of these clusters and that they are separated by borders where the correlation is lower.

Figure 5.4 E, F, shows an example of a blinking trace extracted from one of the clusters. One can see that the frequency of the fluctuations is quite high and that the

amplitude is lower than what is typically observed in nanoconfined systems. Here the film parts never completely turn off.
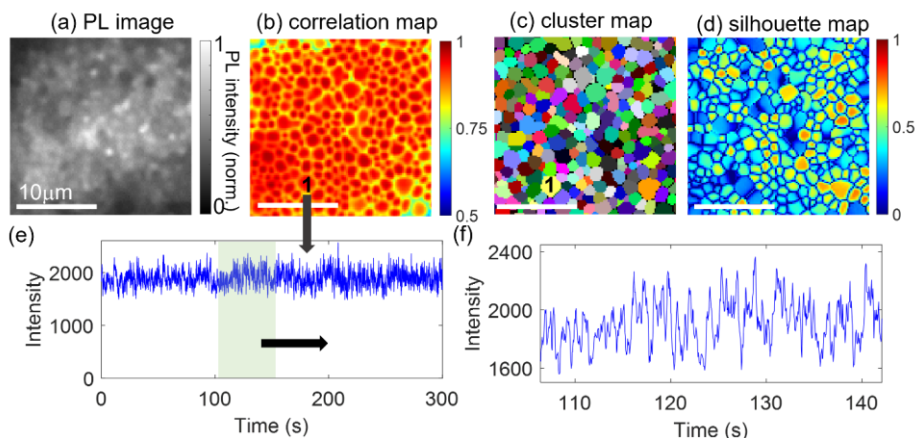


**Figure 5.4. Pseudo-correlation clustering of large grain MAPI film. (a) PL image, (b) correlation map shows microscale domains of high correlation separated by low correlation boundaries. (c) cluster map obtained at 0.7 optimum threshold. Here, each random false color designates an individual cluster. Two or more spatially isolated clusters can have the same colors but represent separate clusters. (d) Silhouette map demonstrates significant heterogeneity among the clusters meaning some areas present more independent fluctuations (high Silhouette value). (e) Exemplary PL trace showing time-dependent emission behavior of a cluster (marked 1) and (f) magnified view of the same trace. Scale bar = 10 μm.**

To get a better understanding of what these regions correspond to, we compared the cluster map with SEM images of the same region. We performed this comparative experiment on samples with different grain sizes. The results are summarized in Figure 5.5.

Figure 5.5A shows the SEM image for the different grain sizes, ranging from ≤1 μm for the sample with the smallest grains (MAPI-SG) to 4-5 μm for the sample with the largest grains (MAPI-POR). From the SEM image, we can see that these films are of very high quality since their surface is quite smooth, their shape regular and the individual grains do not seem polycrystalline.

Figure 5.5B and C show an almost perfect matching between the SEM images and both the correlation maps and the cluster maps. Indeed, in most cases, the cluster describes a single grain, and a maximum correlation is observed at the centre of the grain. This is quite important as not only the method allows for analysis of blinking in the film but in addition, we get a grasp of the structural arrangement of the grain in the film with a resolution close to SEM.

To summarize, paper V demonstrates the use of a correlation-based method (PCoClust) that allows the mapping of the regions of MAPbI$_3$ semiconductor films that blink differently. We showed the areas mapped to correspond to the individual grains by comparing PCoClust with SEM images of the same region. Hence, not only PCoClust allows for studying the intensity fluctuations in dense samples but it can also provide a high-resolution image and information on the structural arrangement of the grains in the film. This method paves the way to study the relationship between the grain structure and the device's properties in semiconductor films.
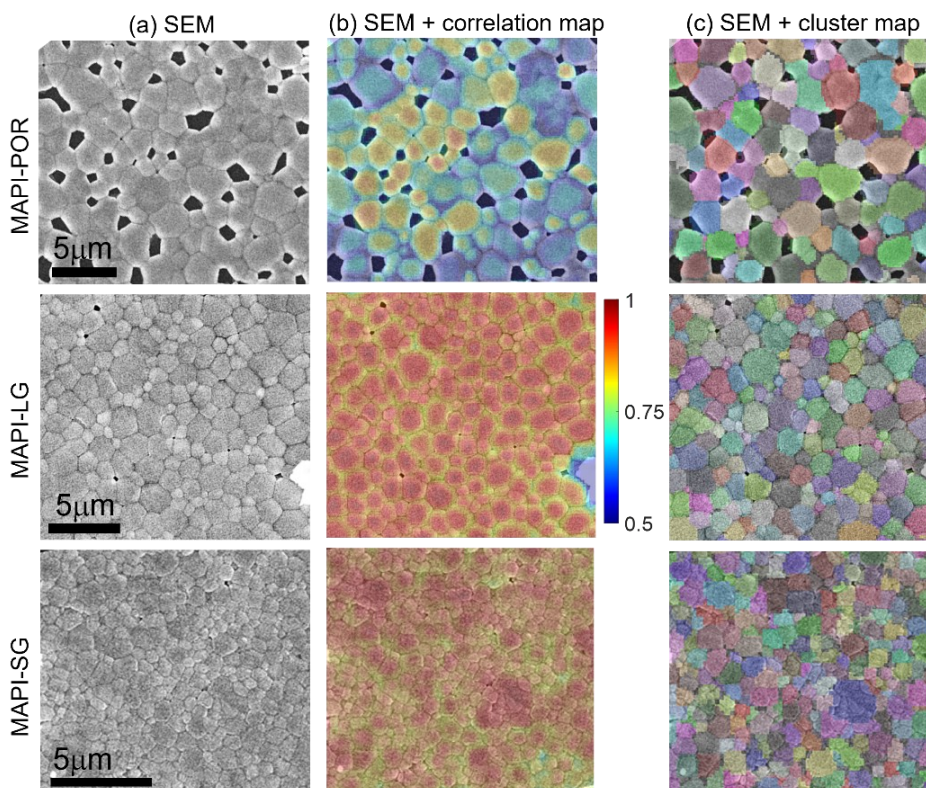


**Figure 5.5. Comparison of pseudo-correlation clustering maps and SEM for MAPI films of different grain sizes. (a) SEM for MAPI-POR, MAPI-LG, and MAPI-SG, (b) overlayed SEM and correlation map demonstrating distribution of high correlation at the center of the grains, (c) overlayed SEM and cluster map showing excellent matching of each grain with individual clusters**

# 5.5 Paper VI: Single-molecule excitation-emission spectroscopic imaging of TQ1 conjugated polymers

As explained in Chapter III, the relationship between the properties and the structure/conformation of the chain in conjugated polymer remain quite elusive. A conjugated polymer chain is a multi-chromophoric system with efficient energy transfer to the lowest unit, a large amount of information is lost in the emission spectrum. This is because while each chromophore absorbs only a single or a few units are responsible for the emission. [14–16]

To extract information about the multiple chromophores, absorption spectroscopy would be ideal. However, even though some single-molecule absorption has been reported [17–19], it remains virtually impossible to measure in most cases. Here, single-molecule excitation-emission spectroscopy (SMEES) is to study TQ1 conjugated polymers a commonly used polymer in photovoltaics.

To influence the set of conformation available to the individual chains we prepared different single molecule samples using different solvents (Toluene, Chlorobenzene), different matrices (PMMA, Polystyrene), and even chemical modifications (TQ1 vs TQp8). Figure 5.6 shows a summary of the different samples studied as well as the difference in chemical structure between TQ1 and TQp8 where the side chain sits in meta and para position respectively.



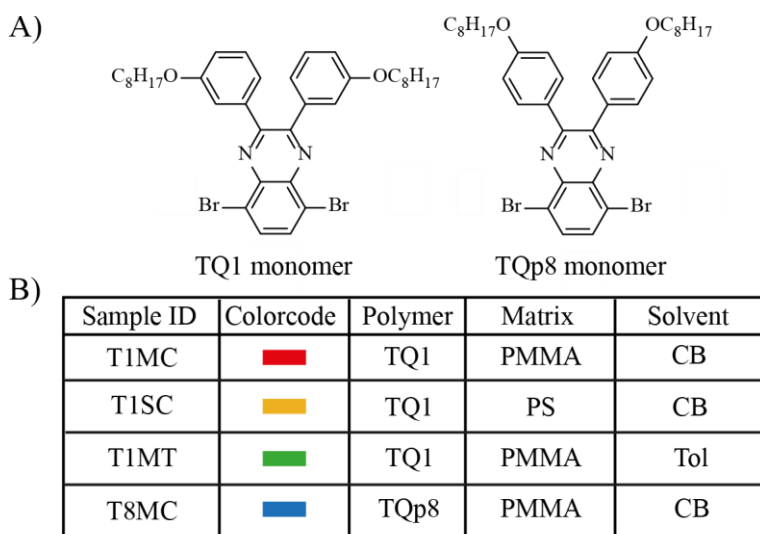| Sample ID | Colorcode | Polymer | Matrix | Solvent |
|-----------|-----------|---------|--------|---------|
| T1MC | 🟥 | TQ1 | PMMA | CB |
| T1SC | 🟧 | TQ1 | PS | CB |
| T1MT | 🟩 | TQ1 | PMMA | Tol |
| T8MC | 🟦 | TQp8 | PMMA | CB |

**Figure 5.6: TQ1 samples: A) Chemical structure of TQ1 and TQp8 showing that the side chains are in para instead of meta position on the TQp8 monomer. B) Table showing the different types of samples that are used in this study**

Figure 5.7 shows the spectra obtained via SMEES for the different samples. The film spectra of the corresponding samples are shown in the left column, the other spectra represent individual molecules. To the best of our knowledge, it is the first time that such measurement has been performed at the single molecule levels considering the range of wavelength studied here (450-710 excitation, full range of emission).
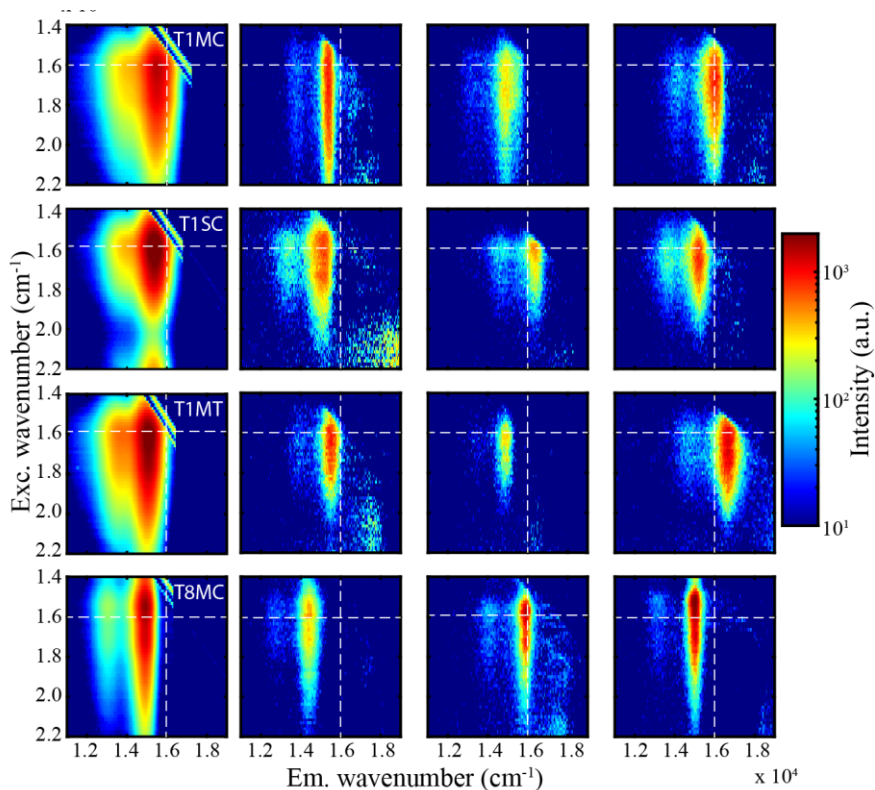


**Figure 5.7: 2D excitation-emission spectra of single TQ1 molecules: Each lines correspond to one sample (S1, S2, S3 and S4) and shows 3 (a,b,c) examples of 2D excitation spectra, extracted from different molecules. Excitation-emission spectra shows a true fingerprint of the molecule. Indeed, each of these spectra is vastly different, some have narrower emission, some narrower excitations, some are more or less blue shifted, etc…**

In general, all molecules present a significantly broader excitation spectrum than their emission. We can also see that the width of the excitation spectra of some of the single molecules is almost as broad as the film while the emission width is always significantly narrower. These results corroborate the current model of single-conjugated polymer molecules. Indeed, the spectroscopic units have different absorption spectra yielding a broad excitation spectrum for the molecule. However,

due to efficient intrachain energy transfer to the lowest energy units, only a single or very few chromophores emit the photons absorbed by the entire chains leading to a significantly narrower emission.[14,16,20,21]

Another fact that goes in the direction of this model is that the emission spectra appear to be independent of the excitation wavelength. If each spectroscopic unit having its own absorption spectrum, would emit individually, the emission spectrum would be wavelength dependent which is not the case here.

From the SMEES spectra, we can extract the width and the peak position and study the relationship between emission and excitation spectra. Paper VI shows the statistics of emission and excitation peaks, widths, and the stoke shifts for all the molecules measured (40-50 molecules per condition).

For the excitation and emission peaks, we observe that most of the data points sit below the diagonal which indicates that a shift in excitation does not result in an equivalent shift in emission. This is corroborated by the low correlation between the two variables for each population (r<0.2). This lack of correlation is also due to the disconnection existing between the absorbing chromophore population and the emitting one.

To conclude, Paper VI presents the measurements of single-molecule excitation-emission spectroscopy (SMEES) on TQ1 conjugated polymer individual molecules. SMEES is a two-dimensional fluorescence technique in which the emission spectrum is measured as a function of the excitation wavelength. We show that individual molecules display a significantly broader excitation spectrum than emission. This result supports the idea that all the spectroscopic units of a conjugated polymer chain contribute to absorption while only one, or a few spectroscopic units contribute to excitation. In addition, we found that the emission spectra of single molecules were excitation wavelength-independent which further supports this idea. We believe that SMEES has a great potential to unravel the structure-properties relationship in conjugated polymers and could help understand better the relationship between the conformation of the chain and the photophysical properties.

# References

1.  Martens KJA, Bader AN, Baas S, Rieger B, Hohlbein J. Phasor based single-molecule localization microscopy in 3D (pSMLM-3D): An algorithm for MHz localization rates using standard CPUs. J Chem Phys. 2018 Mar 28;148(12):123311.

2.  Burns MM, Fournier JM, Golovchenko JA. Optical binding. Phys Rev Lett. 1989 Sep 18;63(12):1233–6.

3.  Kudo T, Yang SJ, Masuhara H. A Single Large Assembly with Dynamically Fluctuating Swarms of Gold Nanoparticles Formed by Trapping Laser. Nano Lett. 2018 Sep 12;18(9):5846–53.

4.  Sugiyama T, Adachi T, Masuhara H. Crystallization of Glycine by Photon Pressure of a Focused CW Laser Beam. Chem Lett. 2007 Dec 5;36(12):1480–1.

5.  Yuyama KI, Sugiyama T, Masuhara H. Laser Trapping and Crystallization Dynamics of l-Phenylalanine at Solution Surface. J Phys Chem Lett. 2013 Aug 1;4(15):2436–40.

6.  Kudo T, Wang SF, Yuyama K ichi, Masuhara H. Optical Trapping-Formed Colloidal Assembly with Horns Extended to the Outside of a Focus through Light Propagation. Nano Lett. 2016 May 11;16(5):3058–62.

7.  Dickson RM, Cubitt AB, Tsien RY, Moerner WE. On/off blinking and switching behaviour of single molecules of green fluorescent protein. Nature. 1997 Jul;388(6640):355–8.

8.  Mirzov O, Cichos F, von Borczyskowski C, Scheblykin I. Fluorescence blinking in MEH-PPV single molecules at low temperature. J Lumin. 2005 Apr;112(1–4):353–6.

9.  Banin U, Bruchez M, Alivisatos AP, Ha T, Weiss S, Chemla DS. Evidence for a thermal contribution to emission intermittency in single CdSe/CdS core/shell nanocrystals. J Chem Phys. 1999;110(2):1195–201.

10. Frantsuzov P, Kuno M, Jankó B, Marcus RA. Universal emission intermittency in quantum dots, nanorods and nanowires. Nat Phys. 2008;4(5):519–22.

11. Efros AL, Nesbitt DJ. Origin and control of blinking in quantum dots. Nat Nanotechnol. 2016;11(8):661–71.

12. Merdasa A, Tian Y, Camacho R, Dobrovolsky A, Debroye E, Unger E, et al. "Super-trap" at Work: Extremely Efficient non-Radiative Recombination Channels in MAPbI3 Revealed by Luminescence Super-Resolution Imaging and Spectroscopy. ACS Nano. 2017;in revision-in revision.

13. Pathoor N, Halder A, Mukherjee A, Mahato J, Sarkar SK, Chowdhury A. Fluorescence Blinking Beyond Nanoconfinement: Spatially Synchronous Intermittency of Entire Perovskite Microcrystals. Angew Chem Int Ed. 2018 Sep 3;57(36):11603–7.

14. Yu J, Hu D, Barbara PF. Unmasking Electronic Energy Transfer of Conjugated Polymers by Suppression of O$_2$ Quenching. Science. 2000 Aug 25;289(5483):1327–30.

15. Becker K, Da Como E, Feldmann J, Scheliga F, Thorn Csányi E, Tretiak S, et al. How Chromophore Shape Determines the Spectroscopy of Phenylene−Vinylenes: Origin of Spectral Broadening in the Absence of Aggregation. J Phys Chem B. 2008 Apr;112(16):4859–64.

16. Schindler F, Lupton JM, Feldmann J, Scherf U. A universal picture of chromophores in -conjugated polymers derived from single-molecule spectroscopy. Proc Natl Acad Sci. 2004 Oct 12;101(41):14695–700.

17. Gaiduk A, Yorulmaz M, Ruijgrok PV, Orrit M. Room-Temperature Detection of a Single Molecule's Absorption by Photothermal Contrast. Science. 2010 Oct 15;330(6002):353–6.

18. Chong S, Min W, Xie XS. Ground-State Depletion Microscopy: Detection Sensitivity of Single-Molecule Optical Absorption at Room Temperature. J Phys Chem Lett. 2010 Dec 2;1(23):3316–22.

19. Celebrano M, Kukura P, Renn A, Sandoghdar V. Single-molecule imaging by optical absorption. Nat Photonics. 2011 Feb;5(2):95–8.

20. Collini E, Scholes GD. Coherent Intrachain Energy Migration in a Conjugated Polymer at Room Temperature. Science. 2009 Jan 16;323(5912):369–73.

21. Bout DAV, Yip WT, Hu D, Fu DK, Swager TM, Barbara PF. Discrete Intensity Jumps and Intramolecular Electronic Energy Transfer in the Spectroscopy of Single Conjugated Polymer Molecules. Science. 1997 Aug 22;277(5329):1074–7.

# Chapter 6
# Conclusions

In this thesis, we presented the development and improvement of multi-dimensional imaging methods and demonstrated their application in relevant areas of materials sciences. First, we showed the potential of multiplane microscopy (x,y,z,t) to unravel nanoparticle dynamics in optical trapping and optically formed assemblies. Second, we developed a time-correlation imaging method (x,y,t,r), PCoClust, to investigate the blinking of MAPbI$_3$ semiconductor films. Finally, we employed single-molecule excitation-emission spectroscopy (SMEES) to study the spectroscopic units of TQ1 conjugated polymer at the single-molecule level.
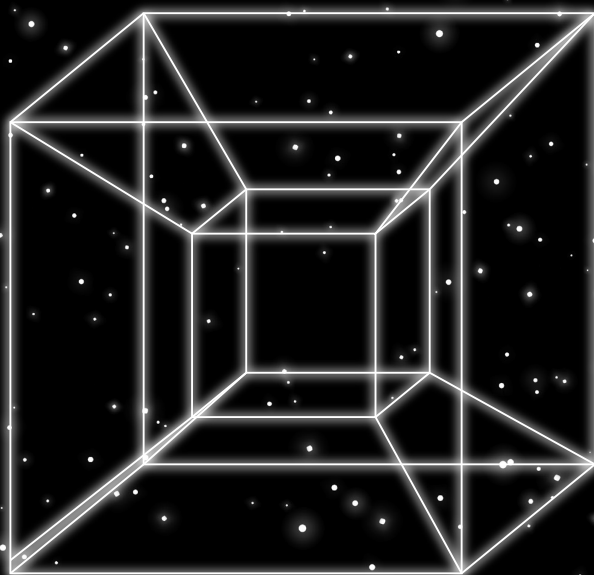
Using multiplane microscopy, for the first time, we tracked nanoparticles as they arrive at an optical trap. We showed that the nanoparticles presented a helicoidal motion as they went to the optical trap. Moreover, we demonstrated the existence of a metastable trapping site below the main focal spot. In a separate study, we presented a three-dimensional view of an optically formed assembly of polystyrene microparticles. We reported pistol-like ejections from the assembly that were induced by the rearrangements of the assembly and the scattering of the laser. These new phenomena could not have been unravelled without the use of three-dimensional imaging.

In our study of the initial stages of a gold nanoparticle assembly at a glass/water interface, we reported, for the first time, the observation of optical binding outside the irradiated area of the trapping laser. We also showed that optical binding was key to the formation and growth of the gold nanoparticle assembly.

With PCoClust, we showed that correlation clustering enabled the investigation of the blinking phenomenon in MAPbI$_3$ perovskite films. We were able to separate the different parts of the film that blink differently. Moreover, we showed that the regions obtained using PCoClust correspond to individual grains in the film by comparing them with electron microscopy images of the same region. Hence, not only PCoClust allows the study of intensity fluctuations in very dense samples but it can also provide a high-resolution image and information on the structural arrangement of the grains in the film. These results could not have been obtained without the use of the time correlation as an additional dimension in the measurements.

Using SMEES, we presented the first single-molecule excitation-emission spectra of TQ1 conjugated polymer on a wide range of wavelengths. We observed that individual molecules had very different spectra in terms of widths and peak positions. Moreover, the excitation spectra were always significantly broader than the emission spectra which were observed to be independent of the excitation wavelength. These results match the current model of conjugated polymer chains where the entire chain can absorb but most of the emission is done by one or few spectroscopic units. We believe that SMEES has a great potential to unravel structure-properties relationships in conjugated polymer and in particular the relation between the conformation of the chain and its photophysics.

All in all, this thesis demonstrated the power and versatility of combining multiple dimensions in a single measurement. With minimal modifications to a standard fluorescence microscope, almost any parameters can be coupled to the imaging increasing both the amount of information obtained from a single measurement and the spectrum of materials/systems that can be studied with the technique. It is only up to the experimenter's creativity to craft new multi-dimensional techniques making it an extremely powerful tool.

LUND
UNIVERSITY